
Characterization of Pressure Sensitive Adhesive Systems for Transdermal Patches

**Dissertation
zur Erlangung des Doktorgrades
der Naturwissenschaften (Dr. rer. nat.)**

an der Fakultät für
Mathematik, Informatik und Naturwissenschaften
Fachbereich Chemie
der Universität Hamburg

vorgelegt von

Marc Michaelis
aus Hannover

Hamburg 2015

Reviewer of the dissertation: Professor Dr. Claudia S. Leopold

Professor Dr. Patrick Théato

Reviewer of the disputation: Professor Dr. Claudia S. Leopold

Professor Dr. Hans-Ulrich Moritz

Dr. Birgit Fischer

Date of the disputation: 20.03.2015

"Die Grenzen meiner Sprache bedeuten die Grenzen meiner Welt."

Ludwig Wittgenstein

Danksagung

Diese Dissertation wurde an der Universität Hamburg am Fachbereich Chemie in der Abteilung Pharmazeutische Technologie auf Anregung und unter der Leitung von Frau Prof. Dr. Claudia S. Leopold verfasst.

Ich möchte mich an dieser Stelle bei vielen Personen bedanken, die mich bei der Erstellung dieser Arbeit sehr unterstützt haben.

An erster Stelle möchte ich Frau Prof. Dr. Claudia S. Leopold für die freundliche Überlassung des hochinteressanten Themas und die Bereitstellung des Arbeitsplatzes danken. Ich verdanke ihr darüber hinaus hilfreiche Unterstützung und viele anregende Diskussionen. Jede Phase dieser Arbeit wurde von ihr intensiv und warmherzig begleitet. Besonders bedanken will ich mich auch für die Freiheit, die sie mir während des gesamten Forschungsprojektes gewährte.

Herrn Dr. Albrecht Sakmann sei herzlich gedankt für die hilfreichen Tipps bei der Einführung in das Praktikum sowie die freundliche Aufnahme in den Arbeitskreis.

Herrn Prof. Dr. Patrick Théato gilt mein besonderer Dank für die freundliche Übernahme des Gutachtens der vorliegenden Dissertation. Herrn Prof. Dr. Hans-Ulrich Moritz und Frau Dr. Birgit Fischer danke ich für ihre Bereitschaft, als Begutachtende in der Prüfungskommission mitzuwirken.

Für die professionelle Einführung in die Rheologie der Haftklebstoffe danke ich Herrn Rüdiger Brummer der Firma Beiersdorf. Ebenfalls Herrn Frank Hetzel und Herrn Martin Griebenow der Firma Beiersdorf möchte ich für die stets hilfsbereite und sachkundige Unterstützung bei den rheometrischen Messungen im Hause Beiersdorf danken.

Großer Dank gebührt meinen Kollegen der Pharmazeutischen Technologie und der Pharmazeutischen Chemie. Vielen Dank für eure Unterstützung, die vielen konstruktiven Gespräche und schönen sowie in jeder Lebenslage humorvollen Momente. Besonders möchte ich dabei Frau Dr. Ines Saniocki und Herrn Dr. Sebastian Kruggel für das gewissenhafte Korrekturlesen danken.

Frau Petra Borbe danke ich für die ausgezeichnete und tatkräftige Unterstützung während meiner Arbeit am Lehrstuhl.

Den Mitarbeitern der TMC-Werkstatt möchte ich für ihre Geduld und ihre professionelle Umsetzung meiner zahlreichen Spezialanfertigungen danken.

Der Firma Henkel, sowie im Besonderen Dr. Paul B. Foreman und Mr. Nigel Brown möchte ich für die sofortige und immerwährende Unterstützung meiner Arbeit, zum einen durch Materialien zum anderen durch konstruktive Gespräche, meinen Dank aussprechen.

Bedanken möchte ich mich auch bei Herrn Prof. Dr. Ullrich. Schäfer, Herrn Dr. Harald Heßberger sowie Herrn Leslie Chao, die mir in entscheidenden Momenten meiner Arbeit die richtige Richtung gewiesen haben.

Weiterhin danke ich den Firmen Dow Corning, Epurex Films und 3M für die kostenlose Bereitstellung von Materialien für die Pflasterherstellung, sowie der Firma Stat-Ease für das Recht, Ergebnisse der Demo-Version von Design-Expert® 8.0.6 zu veröffentlichen.

Darüber hinaus möchte ich mich bei den Firmen Acino und Chemsultans für die Bereitstellung von Bildmaterial und das Recht für deren Veröffentlichung bedanken.

Meinen Eltern, meiner Schwester Nora, meiner Oma und meinen Freunden danke ich für ihr Verständnis, ihre Rücksichtnahme und ihren Beistand in jeder Phase der Promotion.

Zu guter Letzt möchte ich meiner Frau Heidi und meinen Kindern Finley, Emil und Bruno aus ganzem Herzen für Ihre Unterstützung danken, die nicht in Worte zu fassen ist und maßgeblich zum Gelingen dieser Arbeit beigetragen hat.

Summary

In general, transdermal patch development is a very straight forward, however non-systematic and not goal-oriented approach. Lack of methods for screening and collecting systematically data, even at the early stage of development, lead to the situation that most studies are performed via trial and error based on the personal experience of the developer.

The scope of the present work was to evaluate statistically designed methods for formulation development and to systematically investigate analytical methods as claimed in the international guidances.

Although many studies have been performed to investigate either the adhesion properties or the viscoelastic properties of plain pressure sensitive adhesives (PSAs), still little is known on the interaction of these properties if a low molecular weight substance is added. Most of the adhesion performance tests are influenced by the viscoelastic properties of the sample and should be described already in the development phase. Therefore, DMA/DMTA was used to investigate possible API-PSA interactions and to compare these measurements with standard adhesion performance tests. For this purpose patch-like samples as well as samples with sufficient thickness for rheometrical measurements were prepared. A method was developed to prepare patches of varying thicknesses and sizes comprising of a release liner, the adhesive matrix, the API and a backing membrane. Subsequently, the method was further modified to achieve samples of about 1200 μm thickness for rheometrical measurements. Special emphasis was laid on reproducibility and high quality of the samples (absence of air bubbles or coating defects). Therefore, the process was standardized and automatized as much as possible.

The crosslinked acrylic PSA DuroTak[®] 87-4287 was mixed with increasing amounts of ibuprofen as a model drug, and the adhesion performance was measured as rolling ball tack, probe tack and shear adhesion in dependence of the ibuprofen concentration. These results were compared with data from frequency sweeps and temperature sweeps from DMA/DMTA measurements. It could be shown that DMA/DMTA was a suitable method to detect the influence of ibuprofen on DuroTak[®] 87-4287 in dependence of its concentration. Furthermore, DMA/DMTA was able to significantly reveal the phenomenon of antiplasticization for the investigated drug-loaded matrices, and based on the data the term “antiplasticization space” was introduced.

The probe tack test proved itself as a fast method, applicable to the final pharmaceutical product and may be used as a process control sensor e.g. process analytical technology (PAT). In a second study it was decided to evaluate a systematic approach for a measurement system analysis (MSA) of the probe tack test. The strength of the introduced approach is on the one hand the possibility to identify significant parameters and their interactions with influence on the analytical test result. On the other hand the transferability of this methodology to other analytical methods is given. With the method of design of experiments (DoE), the effect of detachment speed, dwell time, contact force, adhesive matrix thickness and API content on the tack measurement of a pressure sensitive adhesive was investigated. The results implied that all investigated factors have a significant influence on the test parameters. Furthermore, interactions between dwell time, contact force, adhesive matrix thickness and API content could be identified. Remarkably, it was observed that with decreasing adhesive matrix thickness the PSA showed unexpectedly high tack values. This phenomenon could be explained by increased mechanical strength of thin PSA films caused by orientation of hydrophilic polymer chains of the PSA.

In a final study, the method “Mixture Design” was evaluated as a Quality by Design (QbD) approach to develop a multiple polymer drug-in-adhesive system. Only few studies have been performed to investigate multiple polymer adhesive systems to be applied in transdermal patches, and information on the influence of the components on the performance of these systems is rare. This may be a result of the complexity of these systems rather than the various possible interactions of the components. As a model drug ibuprofen was chosen and blended with varying amounts of silicone adhesive, acrylic adhesive and oleyl alcohol. Drug-in-adhesive samples were prepared at different levels of the components according to the mixture design. Response surfaces of tack, shear adhesion, extent of creaming, crystallization, droplet size and droplet distribution range were obtained as contour plots. The results implied that the levels of the components had a significant effect on the performance of the patch. In all cases adhesion properties were decreased when compared to the plain adhesives. Remarkably, it could be observed that crystallization was decreased at all component levels and correlated well with the droplet size of the mixtures, whereas lowest crystallization was observed at smallest droplet sizes. No beneficial effect of oleyl alcohol on the performance of the patch was observed at any level and interestingly, its addition had a negative effect on all responses. Based on these results an optimized mixture of a multiple polymer adhesive system as transdermal patch was calculated with a numeric optimization and experimentally verified.

Zusammenfassung

Die Entwicklung von transdermalen Pflastern basiert im Allgemeinen auf wenig systematischen, zielorientierten Methoden. Der Mangel an systematischen Methoden, die dem Screening und Sammeln von wissenschaftlichen Daten dienen könnten, führt dazu, dass die meisten Ergebnisse durch einfaches Ausprobieren erzielt werden. Demnach richten sich der Aufwand sowie letztendlich auch der Erfolg nach der Erfahrung des Entwicklers. Das Ziel der vorliegenden Arbeit war die Erprobung von statistischen Methoden für die Formulierungsentwicklung und die systematische Untersuchung analytischer Methoden, so wie es in den internationalen Richtlinien gefordert wird.

Obwohl bisher viele Untersuchungen durchgeführt wurden, um entweder die Klebeigenschaften oder die viskoelastischen Eigenschaften von reinen Haftklebstoffen zu bestimmen, ist wenig über die Änderung dieser Eigenschaften bekannt, wenn eine niedermolekulare Substanz hinzugefügt wird. Die meisten Tests zur Messung der Klebeigenschaften werden durch die viskoelastischen Eigenschaften der Probe beeinflusst und sollten bereits in der Entwicklungsphase bekannt sein. Daher wurde DMA/DMTA verwendet, um mögliche Arzneistoff/Haftklebstoff-Interaktionen zu untersuchen und die erhaltenen Ergebnisse mit denen von klassischen Klebkraft-Tests zu vergleichen.

Für diesen Zweck mussten zum einen pflasterähnliche Proben hergestellt werden, um die Klebkraft zu messen; zum anderen wurden jedoch auch Proben mit ausreichender Dicke für rheometrische Messungen benötigt. Es konnte eine Methode entwickelt werden, die es erlaubte, Pflaster bestehend aus Schutzfolie, Haftklebstoffmatrix, Arzneistoff und einer Abziehfolie in unterschiedlicher Dicke und Größe herzustellen. Diese wurde dann weiter entwickelt, so dass Proben mit einer Dicke von ca. 1200 µm für rheometrische Messungen erhalten werden konnten. Besondere Aufmerksamkeit wurde dabei auf eine gute Reproduzierbarkeit und hohe Qualität (Abwesenheit von Luftblasen und Beschichtungsdefekten) gelegt. Aus diesem Grunde wurde der Prozess weitestgehend standardisiert und automatisiert.

Der quervernetzte Acrylat-Haftklebstoff DuroTak® 87-4287 wurde mit steigendem Anteil an Ibuprofen als Modellarzneistoff gemischt und die Klebeigenschaften als Rolling Ball Tack, Probe Tack und Scherfestigkeit in Abhängigkeit von der Ibuprofen-Konzentration gemessen. Die Ergebnisse wurden mit Daten von Frequenz- und Temperaturversuchen aus DMA/DMTA-Messungen verglichen. Es konnte gezeigt werden, dass DMA/DMTA geeignet ist, um den Einfluss von Ibuprofen auf

DuroTak® 87-4287 in Abhängigkeit von seiner Konzentration zu bestimmen. Weiterhin konnte die Methode das Phänomen der Antiweichmachung für das untersuchte System signifikant nachweisen und der Begriff „antiplasticization space“ eingeführt werden.

Im Rahmen dieser Untersuchungen erwies sich der Probe Tack-Test als eine schnelle Methode, mit dem Potenzial als Sensor für die Inprozesskontrolle eingesetzt zu werden, wie z.B. als Process Analytical Technology (PAT). Im zweiten Teil der Arbeit wurde ein systematischer Ansatz zur Untersuchung dieser analytischen Methode im Sinne einer Messsystemanalyse (MSA) entwickelt. Die Bedeutung der vorgeschlagenen Methode besteht zum einen in der Möglichkeit, signifikante Testparameter sowie deren Interaktionen mit Einfluss auf das Messergebnis zu bestimmen, zum anderen in der Übertragbarkeit auf weitere analytische Methoden. Unter Verwendung von statistischer Versuchsplanung konnte der Einfluss von Abzugsgeschwindigkeit, Druckhaltezeit, Anpresskraft, Klebschichtdicke und Arzneistoffgehalt auf das Messergebnis der Probe Tack-Messung eines Haftklebstoffes untersucht werden. Die Ergebnisse zeigten, dass alle untersuchten Faktoren einen signifikanten Einfluss auf das Messergebnis haben. Weiterhin konnten eindeutige Interaktionen zwischen Druckhaltezeit, Anpresskraft, Klebschichtdicke und Arzneistoffgehalt identifiziert werden. Bemerkenswerterweise konnten mit abnehmender Schichtdicke unerwartet hohe Messergebnisse des Probe Tack-Tests erhalten werden. Dieses Phänomen konnte durch Zunahme der mechanischen Festigkeit bei dünnen Haftklebstoffschichten mittels Orientierung von hydrophilen Polymerketten des Haftklebstoffes erklärt werden.

Schließlich wurde im letzten Teil der Arbeit die Versuchsplanungsmethode „Mixture Design“ als ein Quality by Design (QbD) Ansatz zur Entwicklung von transdermalen Pflastern des Typs „drug-in-adhesive“ (DIA) mit einem multiplen Haftklebstoffsystem angewandt.

Bisher haben sich nur wenige Studien mit der Verwendung von multiplen Haftklebstoffsystemen für transdermale Pflaster befasst, und nur wenige Informationen über den Einfluss der Komponenten auf die Klebleistung dieser Systeme liegen vor. Dies mag zum einen der Komplexität dieser Systeme, zum anderen den vielfältigen Interaktionsmöglichkeiten der Komponenten geschuldet sein.

Ibuprofen wurde als Modellarzneistoff gewählt und Pflaster mit variierenden Mengen von Silikon-Haftklebstoff, Acrylat-Haftklebstoff und Oleylalkohol gemäß dem zuvor erstellten Mischungsplan hergestellt. Die erhaltenen „response surfaces“ von Tack, Scherfestigkeit, Phasentrennung,

Kristallisierung des Arzneistoffes, Größe und Spannweite der Tröpfchen wurden als Kontur-Diagramme dargestellt. Die Ergebnisse zeigten, dass die Mischungsverhältnisse der Komponenten einen signifikanten Einfluss auf die Klebleistung des Pflasters hatten. Bei allen Mischungen war die Klebleistung im Vergleich zu Proben mit reinen Klebstoffen schwächer. Bemerkenswerterweise konnte eine Reduktion der Kristallisation des Arzneistoffes bei allen hergestellten Pflastern beobachtet werden. Diese war mit der Größe der Tröpfchen in den Haftklebstoffmischungen insofern korreliert, dass die geringste Arzneistoffkristallisation bei den Mischungen mit den kleinsten Tröpfchen beobachtet wurde. In Bezug auf die gemessenen Eigenschaften konnte hingegen durch die Zugabe von Oleylalkohol kein positiver Effekt beobachtet werden. Basierend auf diesen Resultaten konnte eine optimierte Mischung eines multiplen Haftklebstoffsystems für die Anwendung als transdermales Pflaster über eine numerische Optimierung berechnet und anschließend experimentell bestätigt werden.

Contents

Danksagung	I
Summary	III
Zusammenfassung.....	V
Contents	VIII
1. Introduction.....	1
1.1. Transdermal patches.....	2
1.1.1. Overview of transdermal patches	2
1.1.2. Components of a transdermal DIA patch.....	4
1.1.2.1. Pressure sensitive adhesives (PSAs).....	4
1.1.2.1.1. Acrylate adhesives.....	5
1.1.2.1.2. Silicone adhesives	9
1.1.2.1.3. Polyisobutylene adhesives	12
1.1.2.2. Backing membranes and release liners.....	13
1.1.2.3. Active pharmaceutical ingredients.....	14
1.1.2.4. Additives.....	14
1.1.3. Manufacturing of DIA patches	15
1.2. Adhesion in transdermal drug delivery	17
1.2.1. Measurement of adhesion performance	18
1.2.1.1. Tack	18
1.2.1.2. Peel resistance	19
1.2.1.3. Shear adhesion.....	20
1.2.2. Rheology of pressure sensitive adhesives.....	21
1.2.3. Factors influencing adhesion.....	26
1.3. Design of Experiments (DoE).....	30

1.4. Objectives of this work.....	36
2. Materials and methods	38
2.1. Materials	39
2.2. Methods of “Evaluation of DMA/DMTA for transdermal patch development”	40
2.2.1. Determination of the NVC.....	40
2.2.2. Preparation of the wet mixes.....	40
2.2.3. Preparation of the dry adhesive matrices.....	40
2.2.3.1. Laminates for rheological characterization.....	41
2.2.3.2. Test specimens for probe tack experiments	41
2.2.3.3. Test specimens for rolling ball tack and shear adhesion experiments	41
2.2.4. Monitoring of ibuprofen crystal formation.....	42
2.2.5. Dynamic Mechanical Analysis (DMA) / Dynamic Mechanical Thermal Analysis (DMTA)	42
2.2.5.1. Strain sweeps	43
2.2.5.2. Frequency sweeps.....	43
2.2.5.3. Temperature sweeps.....	44
2.2.6. Adhesion performance.....	44
2.2.6.1. Probe tack test	44
2.2.6.2. Rolling ball tack test (PSTC-6).....	45
2.2.6.3. Shear adhesion test (PSTC-107 A)	46
2.2.7. Differential Scanning Calorimetry (DSC)	46
2.3. Methods of “Systematic investigation of the probe tack test”	47
2.3.1. Design of Experiments: IV-optimal design	47
2.3.2. Preparation of the wet mixes.....	49
2.3.3. Preparation of the dry adhesive matrices.....	49
2.3.4. DMA Measurements	49

2.3.5. Probe tack test	49
2.3.6. Statistical data analysis	51
2.4. Methods of “Formulation development of a multiple polymer adhesive patch”	53
2.4.1. Mixture design	53
2.4.2. Preparation of the wet mixes.....	56
2.4.3. Preparation of the dry adhesive matrices.....	57
2.4.4. Responses.....	57
2.4.4.1. Tack	57
2.4.4.2. Shear adhesion.....	57
2.4.4.3. Crystal growth	57
2.3.4.4. Extent of creaming (phase separation)	58
2.4.4.5. Droplet size.....	58
2.4.4.6. Droplet distribution range.....	58
2.4.5. Statistical data analysis	58
3. Results and discussion.....	59
3.1. Results and discussion of “Evaluation of DMA/DMTA for transdermal patch development” ...	60
3.1.1. Monitoring ibuprofen crystal formation	60
3.1.2. Dynamic Mechanical Analysis (DMA)/Dynamic Mechanical Thermal Analysis (DMTA)	60
3.1.2.1. Strain sweeps	62
3.1.2.2. Frequency sweeps.....	62
3.1.2.3. Temperature sweeps.....	70
3.1.3. Differential Scanning Calorimetry (DSC)	72
3.1.4. Adhesion performance.....	73
3.1.4.1. Probe tack	75
3.1.4.2. Rolling ball tack	76

3.1.4.3. Shear adhesion	77
3.1.5. Suggested model of plasticization and antiplasticization	79
3.1.6. Conclusion	80
3.2. Results and discussions of “Systematic investigation of the probe tack test”	82
3.2.1. DMA Measurements	82
3.2.2. ANOVA of the results of the probe tack test.....	83
3.2.3. Evaluation of the main effect plots	86
3.2.3.1. Factor A: Detachment Speed	86
3.2.3.2. Factor B: Dwell time	87
3.2.3.3. Factor C: Contact force.....	88
3.2.3.4. Factor D: Adhesive matrix thickness	89
3.2.3.5. Factor E: API Content	92
3.2.4. Interaction plots	92
3.2.4.1. Interaction between Factors B and D.....	93
3.2.4.2. Interaction between Factors C and D.....	93
3.2.4.3. Interaction between Factors D and E.....	94
3.2.5. Interpretation of the data	95
3.2.6. Conclusion	97
3.3. Results and discussions of “Formulation development of a multiple polymer adhesive patch”	99
3.3.1. Tack	102
3.3.2. Shear adhesion.....	107
3.3.3. Crystal growth	109
3.3.4. Extent of creaming	111
3.3.5. Droplet size.....	111
3.3.6. Droplet distribution range.....	112

3.3.7. Multi response optimization and validation	113
3.3.8. Interpretation of the data	113
3.3.9. Conclusion	114
3.4. Final discussion.....	115
4. References.....	118
5. Appendix	138
5.1 Appendix – Curriculum Vitae	139
5.2 Appendix – Publication List	140
5.3 Appendix – Hazardous Materials	144
6. Eidesstattliche Versicherung	146

1. Introduction

1. Introduction

1.1. Transdermal patches

1.1.1. Overview of transdermal patches

In 1979 Alza corporation obtained the approval for the first transdermal patch in the United States for delivery of scopolamine to treat motion sickness (1, 2). A decade later, nicotine patches became the first transdermal blockbuster. Today, patches of 17 different active pharmaceutical ingredients (APIs) such as fentanyl, estradiol and rivastigmin along with numerous generic products are on the market (3, 4). It is estimated that more than one billion transdermal patches are currently manufactured each year (2). In 2014 around 81 ongoing clinical trials were reported, ranging from applications in vaccines, drug delivery, to biofeedback loops. Transdermal delivery is estimated to generate a turnover of up to \$6 billion within the next 10 years (5).

Transdermal drug delivery has a variety of advantages compared to the oral or the parenteral drug delivery. The avoidance of the first-pass metabolism leads to a better bioavailability and may result in fewer side effects. Transdermal patches are non-invasive and can be administered by the patients themselves. Furthermore, transdermal patches can provide drug release for periods of up to one week and improve patient compliance (2, 6, 7, 8, 14).

The European Pharmacopeia defines transdermal patches as flexible pharmaceutical preparations of varying sizes, containing one or more APIs. Transdermal patches are intended to be applied to the intact skin in order to deliver the API to the systemic circulation after passing through the skin barrier (10, 11).

For successful transdermal administration the API should have a molecular mass of less than about 350 Daltons (2, 12, 13). Furthermore, to achieve a therapeutic effect at low blood concentrations

doses of only a few milligrams per day or less are necessary. The substances must exhibit octanol-water partition coefficients that show lipophilic properties to be able to penetrate the skin but at the same time hydrophilic properties to permeate subsequently into the bloodstream (2, 14, 15).

The earliest transdermal patches were membrane-type devices that used membranes to control the rate of drug release (6, 16–19). Membrane-type patches consist of three major components: the drug reservoir, the rate-controlling membrane and the adhesive (Fig 1a). Typically, the drug reservoir contains the API and excipients. The API permeates through the membrane and the adhesive to penetrate the skin (3). Today, in transdermal patches a drug is more commonly dispersed or dissolved in a pressure sensitive adhesive (PSA) matrix (6, 16–18). In so-called “drug-in-adhesive” (DIA) patches the active ingredient is homogeneously embedded in the adhesive which performs the role of matrix and adhesive (Fig 1b). In both categories, the API can be dispersed or dissolved (3, 11, 16, 18, 20, 21).

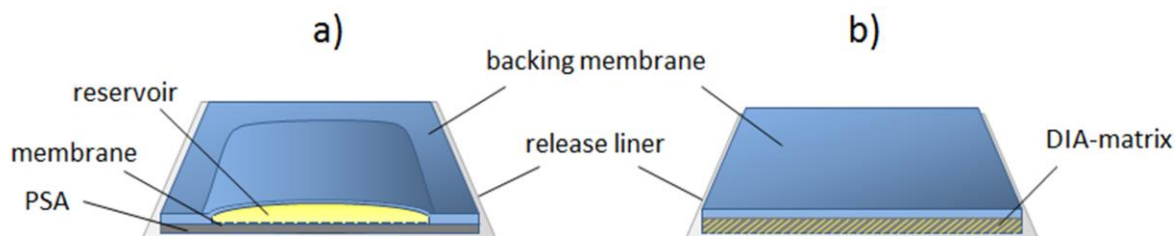


Fig. 1: Transdermal patches with (a) Membrane-type and (b) Drug-in-adhesive (DIA) design.

Transdermal patches are designed to slowly deliver the API through the intact skin, resulting in a prolonged and adequately constant systemic absorption rate. In membrane and matrix types, the rate of release is generally not constant: At the beginning of the application, there is a high concentration gradient between patch and skin leading to a rapid drug release. However, this gradient decreases

with time and the drug release is reduced. Therefore, transdermal patches often have to be replaced before the full amount of API is released. Despite the different dissolution profiles of the membrane and the matrix system, the rate limiting step for systemic absorption of the drug substance is usually the absorption through the skin (11, 22, 23).

Transdermal patches are composed of the API, the pressure sensitive adhesive (PSA) that assures the adhesion of the patch to the skin, the backing membrane which protects the patch from the outer environment and the release liner which protects the patch during storage (Fig. 1). To adjust adhesion performance, flexibility or stability of the patch, or to increase solubility or permeability of the API, additives such as penetration enhancers, tackifiers, plasticizers, fillers or solubilizers may be added to the formulation (24, 25).

1.1.2. Components of a transdermal DIA patch

1.1.2.1. Pressure sensitive adhesives (PSAs)

Pressure sensitive adhesives for the application in transdermal patches must allow as much contact as possible with the surface of the skin. To obtain this extent of contact, the material must be able to deform under slight pressure overcoming the roughness of the skin. Adhesion involves a liquid-like flow of the PSA resulting in wetting of the skin surface upon the bonding phase and the ability to resist shear and debonding forces when the patch is worn for an extended period of time (26). The interfacial adhesion and resistance to progressive debonding dominate the applicability of transdermal patches (27).

An ideal PSA for a transdermal patch is non-sensitizing to the skin, has good initial and long-term adhesion properties to individual skin phenotypes, is easily removable without skin damage, leaves

no residue on the skin upon removal, is compatible with the API and the excipients, and is comfortable to wear (3, 6, 18, 28).

In the context of these requirements, the following types of polymers represent the majority of PSAs used since the beginning of transdermal patch development.

1.1.2.1.1. Acrylate adhesives

Acrylic polymers are prepared by emulsion or organic solution polymerization of alkyl esters of acrylic acid (17, 29). Their general structure is displayed in Fig. 2. In the case of an acrylic ester, R_1 represents an H-atom in the case of a methacrylic ester, R_1 represents $-\text{CH}_3$, and R is an alkyl group usually in the range of $\text{C}_4 - \text{C}_8$.

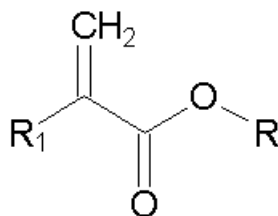


Fig. 2: General chemical structure of alkyl esters of acrylic acid with $R_1 = \text{H}$ for acrylic acid esters or $-\text{CH}_3$ for methacrylic acid esters and R = alkyl group.

Acrylic homopolymers are inherently poor adhesives, as they provide either good tack and low shear adhesion or good shear adhesion and low tack. Thus, it is absolutely necessary to design copolymers by mixtures of soft segments with a low homopolymer glass transition temperature T_g responsible for bonding (primary monomer) and hard segments with a higher homopolymer T_g for resistance to

debonding (secondary monomer). Such copolymers could be prepared either by a mixture of different acrylic esters or by the addition of vinyl monomers (6, 18, 29–31).

Primary monomers are responsible for good tack and sufficient peel resistance. As primary monomers, the patent literature recommends either n-butyl acrylate (BA) with a homopolymer T_g of $-43\text{ }^\circ\text{C}$ (32) or 2-ethyl hexyl acrylate (EHA) with a homopolymer T_g of $-58\text{ }^\circ\text{C}$ (32) with about 50 % to about 98 % by weight of the PSA (29, 33).

As already discussed, a good PSA also requires secondary monomers, also called modifying monomers. Commonly used monomers are methyl methacrylate (MMA) and vinyl acetate (VAc) which both provide sufficient cohesive strength usually in the range between 10 and 35 % by weight of the PSA. Their presence ensures clean removal and resistance to shear forces to prevent cold flow or oozing and dark rings (29).

In some cases, monomers with polar functional groups have to be added to adjust the amount of dipole-dipole interactions due to adjustment of adhesion or to change the pH of the polymer (33). This may be necessary if the API or excipients act as plasticizers or if a special environment for pH-sensitive drugs is needed. Also, the solubility of the API in the polymer can be adjusted by introduction of functional groups in the PSA. For this purpose, usually carboxylic acids such as acrylic acid or methacrylic acid are used. If acid base reactions between the API and the polymer are expected, 2-hydroxyethyl acrylate is a preferred alternative monomer (34). Normally, it is used up to a fraction of 5 %. However, proportions of up to 30 % have been reported to increase API solubility (16).

The molecular weight M_w of acrylic PSAs is directly proportional to the storage modulus G' (35). A high molecular weight is responsible for good shear adhesion and good debonding properties; a low

molecular weight is beneficial for good bonding properties and flexibility. Therefore, the molecular weight has to be adjusted to the intended use.

Additionally, the molecular weight between entanglements M_e plays an important role with respect to the mechanical behavior of acrylic PSAs. The storage modulus G' is inversely proportional to M_e , whereas the mechanical strength improves if M_e decreases and the number of entanglements increases (36, 37). Entanglements can be increased either by physical or chemical crosslinking (29, 35). Physical crosslinks can be formed by microphase separation due to hydrogen, electrostatic or ionic bonding between functional groups among themselves or between functional groups and additives. Chemical crosslinking can be achieved by chain transfer or by internal crosslinking of functional groups of monomers such as 2,3-epoxypropyl methacrylate and 2-hydroxyethyl acrylate. An alternative approach is external crosslinking, where organometallics are used to crosslink these groups.

Compounding of acrylic PSAs with tackifiers is not as common because acrylic PSAs can be manufactured with tailored adhesion properties (29).

In the following studies DuroTak® 387-2287 and DuroTak® 87-4287 from Henkel were used as acrylic adhesives. The chemical name of DuroTak® 387-2287 is poly (2-ethylhexyl acrylate-co-vinyl acetate-co-2-hydroxyethyl acrylate-co-2,3-epoxypropyl methacrylate) with a ratio of the components of 67:28:5:0.15 by weight (38) (Fig. 3b). It is a lipophilic molecule with hydrophilic pockets (carbonyl groups) and hydrophilic anchors (hydroxyl groups) (Fig. 3c). Personal communication with Henkel confirmed that DuroTak® 87-4287 has a similar chemical composition but differs in the degree of crosslinking.

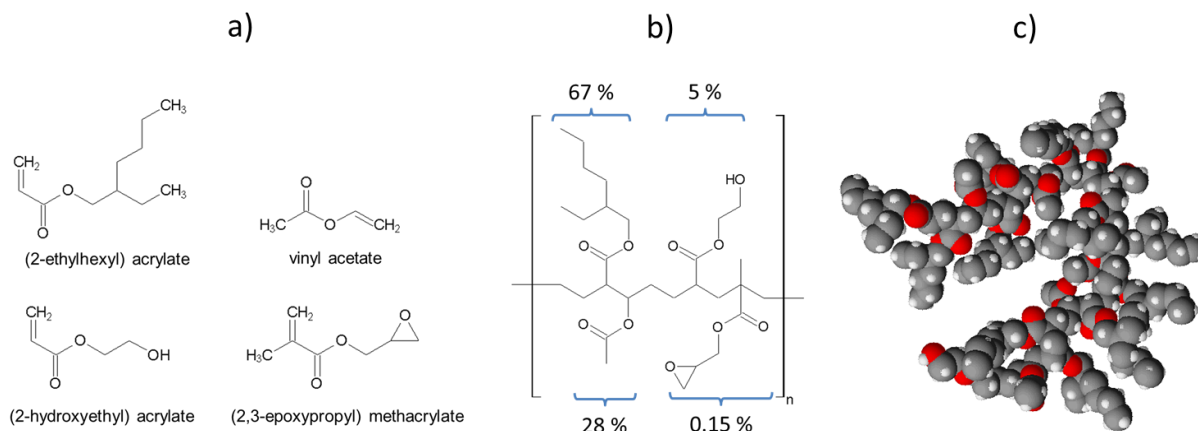


Fig. 3: (a) Monomers of DuroTak® 387-2287, (b) Ratio of monomers, (c) 3D-structure of DuroTak® 387-2287 (n = 20 monomers), generated with ACD/ChemSketch 12.01 software. Grey spheres represent carbon, red spheres oxygen and white spheres hydrogen atoms.

1.1.2.1.2. Silicone adhesives

Silicone adhesives are composed of linear silicone polymers and siloxane resins (6, 18, 39, 40).

Linear silicone polymers are high molecular weight poly dimethyl siloxane (PDMS) polymers with the general structure of $M^{OH}D_nM^{OH}$ as illustrated in Fig. 4a, b. Siloxane resins are composed of M units and Q units (Fig. 4b, c). It is believed that MQ siloxane resins build a highly branched three dimensional network where a core of Q-units is surrounded by a shell of M-units (39) (Fig. 4c, d).

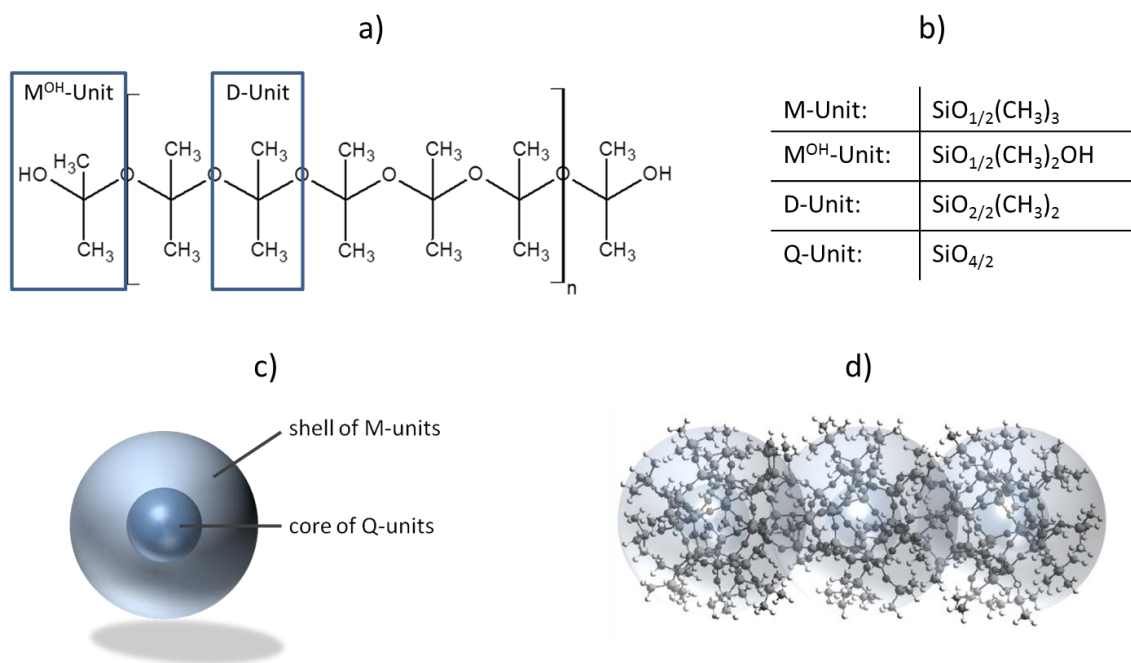


Fig. 4: (a) Chemical structure of linear silicone with M^{OH} - and D-Units, (b) Table of silicone units, (c) Scheme of MQ siloxane resin with core of Q-units and shell of M-units, (d) Computer model of a MQ siloxane resin, modified from: (39).

To achieve improved cohesive strength of the PSA, both components (i.e. PDMS and MQ siloxane resin) are crosslinked by a condensation reaction through the silanol functionalities. The reaction

product is often referred to as “bodied” silicone PSA (41–43) (Fig. 5). This standard silicone product contains a relatively high amount of silanol functionality. These silanol groups will readily react with the amine functionalities of many drugs, thereby limiting their use in transdermal patches. Therefore, the adhesive can be endcapped with an inert terminal trimethylsilyl functionality to yield an amine-compatible silicone PSA (44, 45) (Fig. 5).

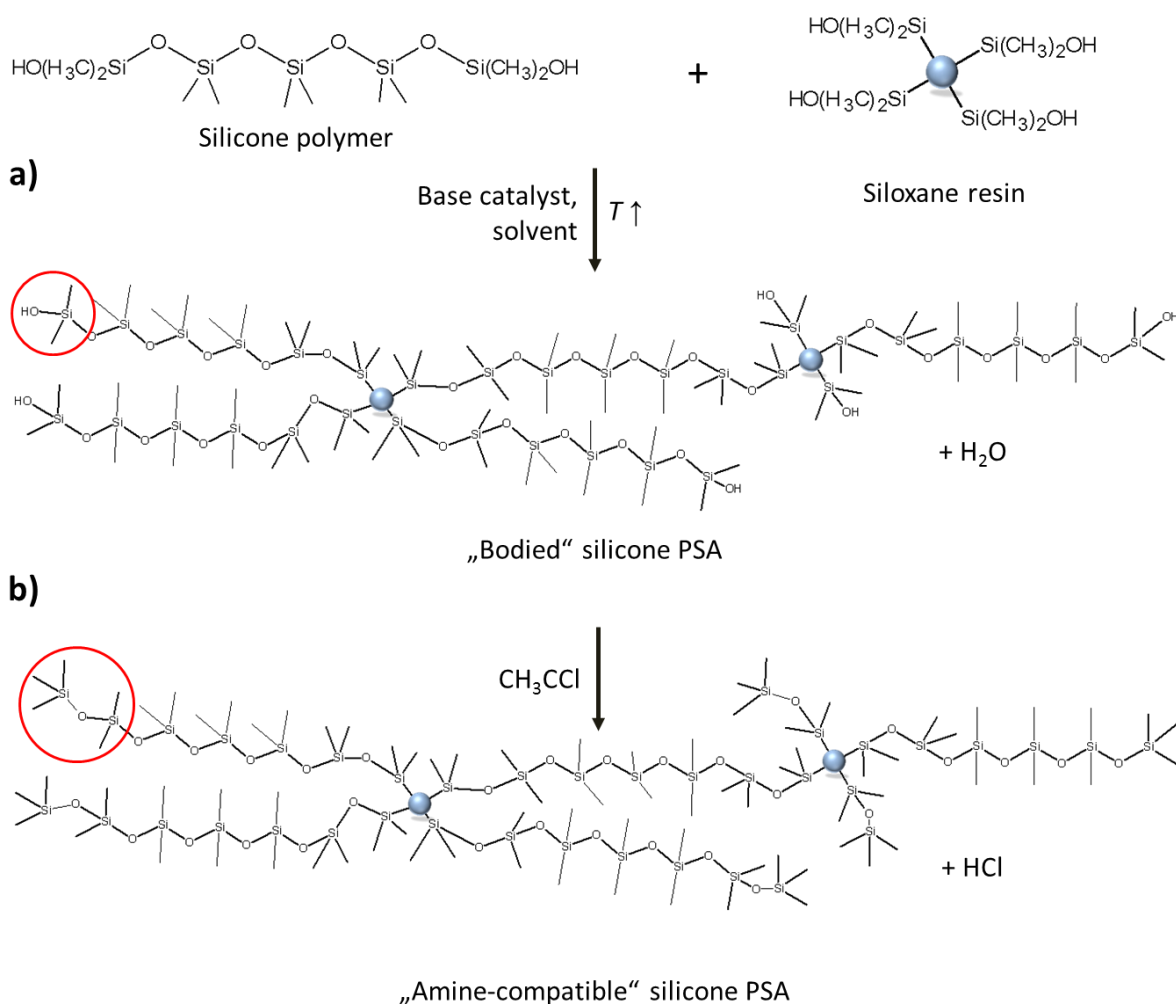


Fig. 5: (a) Preparation of a “bodied” silicone PSA via condensation reaction, (b) Preparation of amine-compatible silicone PSA, both modified from: (39).

Silicone PSAs show medium adhesive properties, which so far limits their application to short time wearing periods. The solubility and permeability for lipophilic APIs in silicone PSAs is very good, but is limited with hydrophilic APIs due to the lack of hydrophilic functionalities. Silicone adhesives have a good air and water permeability, which is an advantage, as no skin maceration takes place. However, their biggest drawbacks are currently the missing functionalization option and their high price (40, 46–50).

1.1.2.1.3. Polyisobutylene adhesives

Polyisobutylenes (PIBs) have been used as synthetic rubber adhesives since the early days of transdermal patch development. They are well known from the tape industry and consist of homopolymers of isobutylene and have a continuous structure of a hydrocarbon backbone with unsaturation only at the polymer chain ends (18, 51–56) (Fig. 6). Because PIB polymers are not supplied as ready-to-use adhesives, transdermal patch manufacturers have to formulate their own PIB–PSA formulations by combination of low and high molecular weight PIBs to achieve a balance of tack and cohesive strength (40, 57).

Ready-formulated PIBs show high initial tack, excellent peel resistance on skin and are inexpensive. Their stability, inertness, and broad acceptance in FDA-regulated applications rationalize why PIBs are still good adhesive candidates for the use in transdermal patches (40).

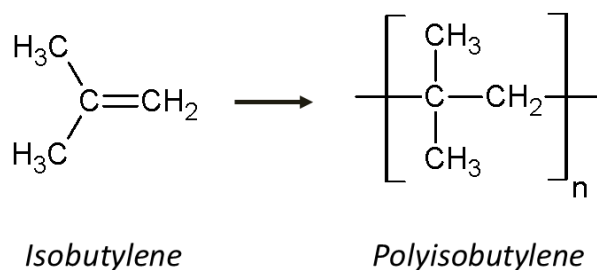


Fig. 6: Chemical structure of isobutylene and polyisobutylene (PIB)

The main disadvantages of PIB adhesives are related to their poor long-term cohesion at skin temperature. Another drawback is their low air and water vapor permeability. On the one hand, occlusion may be desired to enhance the drug flux through the skin. However, on the other hand, skin

maceration and irritation may occur, especially if the patch remains in the same position for a prolonged period of time.

1.1.2.2. Backing membranes and release liners

The **backing membrane** protects the matrix from the outer environment and is selected with regards to appearance, flexibility and need for occlusion (58). The material used for the backing membrane should be inert and incapable of absorbing drugs or other components of the formulation. Examples of polymers useful for the backing are polyesters, polyethylene, polypropylene and polyurethane (59–64). The thickness of the backing membrane is preferably in the range between 15 μm and 250 μm and may be pigmented or aluminum vapor coated. Metal layers often lead to stiffness and high occlusiveness with retention of moisture vapor and air, which cause the transdermal patch to peel-off and possibly irritate the skin during long-term wear (3, 65). The backings are tan or translucent and have in most cases a matte finish which may be printable (66). Corona treatment is avoided in backing membranes for pharmaceutical applications because of the possible reactive byproducts which may be formed during treatment (66).

During storage the patch is covered by a protective liner that is removed and discarded before application of the patch to the skin. As the **release liner** is in intimate contact with the transdermal patch, the liner should be chemically inert and impermeable to the drug. Release liners are typically made of polyesters or polypropylene treated with silicone or fluorocarbons (65, 67–69). The thickness of the liner has to be accurate to allow die cutting and is usually in the range between 50 and 150 μm (66).

1.1.2.3. Active pharmaceutical ingredients

Generally, a transdermal patch contains a sufficient amount of API to achieve therapeutic blood levels for up to 7 days. To provide a high API flux through the skin, the API should be dissolved close to its solubility limit in the matrix, but not significantly exceed this critical limit. With supersaturated systems there is a high risk of recrystallization of the API during storage (70). Several attempts have been undertaken to determine the solubility of an API in a PSA or in a polymer in general, but so far none of them could provide an accurate forecast of solubility making it difficult to determine the stability of transdermal patches over the minimum time scale of two years (71, 72).

1.1.2.4. Additives

Penetration enhancers can increase skin permeability, but their potential of irritation and toxicity to living cells in the deeper skin layers has constrained their application (2). Today's patches contain propylene glycol, ethyl oleate, lauric acid, oleic acid, N-methyl-pyrrolidone, Azone®, isopropyl myristate, or ethanol as penetration enhancer (73–79). Williams and Barry described the modes of action of penetration enhancers and proposed three main mechanisms (80): (1) disruption of the highly ordered structure of stratum corneum lipids, fluidization of the lipid layers and increase in the diffusion coefficient of the drug within the stratum corneum; (2) interaction with intracellular protein and provision of short polar transport pathways for the drug; and (3) improvement in partitioning of the drug, coenhancer, or cosolvent into the stratum corneum.

Pressure sensitive adhesives such as acrylics are designed to inherently have good tack properties and should be tailored for their end use without need for further modification. Silicone and polyisobutylene adhesives may be tackified with their own low molecular weight fractions (40, 57,

81). For styrene-butadiene adhesives, rosin ester resins, hydrocarbon resins and polyterpenes were found to efficiently increase the tack (40, 82–85). Generally, the addition of **tackifiers** should be avoided, as they may cause stability problems by syneresis or migration into the packaging material. Also, their potential for skin irritation and possible interactions with the API may constrain their use in transdermal patch development.

Plasticizers improve flexibility and removability from skin by reduction of polymer-polymer chain secondary bonds thus increasing the polymer free volume (86, 87). Small molecules such as paraffin oil (88–90), triacetin (91, 92), oleic acid (93), or triethyl citrate (TEC) (94) may be added to the PSA.

The main reason for application of **fillers** in transdermal patches is an increase of cohesiveness. Preferably substances such as fumed silica, silica gels or microcrystalline wax are used due to their transparent appearance in the matrix (25, 40, 95). Nevertheless, traditional fillers such as clay and microcrystalline cellulose are still found in some systems (40).

To achieve higher concentrations of the API in the matrix an association colloid can be added. The incorporation of a substance into or onto the micelles of an association colloid is called micellar solubilization or briefly solubilization (96, 97). Known **solubilizers** in transdermal patches are Tween 80[®] (98), Span80[®] (98), oleic acid dimer (65), neodecanonic acid (65), Kollidon 25[®] (99), Labrasol[®] (100) or a mixture of PVP and DMSO (101).

1.1.3. Manufacturing of DIA patches

Generally, the production of a DIA patch is carried out by coating, drying, laminating, cutting and packaging (20, 102, 103) (Fig. 7, 1-5). First, the process starts with mixing of the adhesive, the additives and the API. The so-called wet mix is applied to the release liner. To avoid skin building and

inclusion of bubbles in the adhesive film, it is dried along a temperature gradient. In the next step the dried adhesive film is laminated to the backing membrane and the bulk (mother) rolls are slit into final (daughter) rolls. From these rolls, patches are punched out via die cut and packaged into pouches. As for most coating technologies, clean room conditions are absolutely necessary to avoid coating defects.

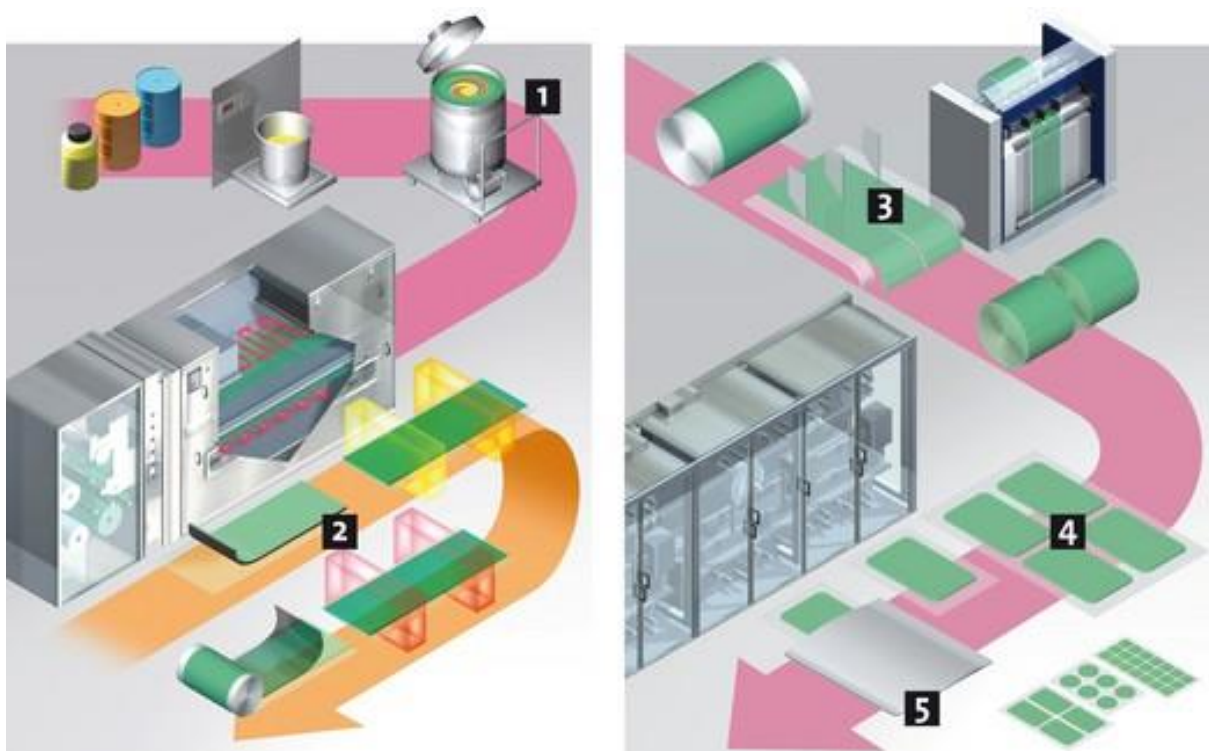


Fig. 7: Manufacturing method for drug-in-adhesive type matrix patches: (1) Weighing and mixing of all ingredients as wet mix, (2) Coating, drying and lamination resulting in a drug-in-adhesive layer, (3) Slitting of the laminate into daughter rolls, (4) Punching of the patch contours, (5) Single patches sealed into pouches. Printed with permission of Acino, Aesch, CH.

1.2. Adhesion in transdermal drug delivery

The therapeutic performance of a transdermal patch can be affected by the quality of the contact between patch and skin. Lack of adhesion and dark rings around the patch caused by cold flow of the adhesive alter the contact surface and result in improper dosing (3, 18, 104, 105). Therefore, good adhesion is required for transdermal patches. However, it is desired that the patch is removable without leaving residuals and with moderate force to prevent skin damage (18, 28).

Adhesion is a complex process. Given the variety of all factors, no single model or theory may meet the requirements of a universal description of the underlying mechanism. The thermodynamic model of adhesion which is believed to explain most of the reported effects is based on the assumption that the adhesive adheres to the substrate because of interatomic and intermolecular forces established at the interface. The most common interfacial forces result from van der Waals and Lewis acid–base interactions. Generally, for formation of a bond, close contact is achieved by spreading of the adhesive on the substrate. Therefore, the criteria for good adhesion essentially correspond to those for good wetting (26, 106). To ensure good wetting, the ideal adhesive should possess a slightly lower surface energy than that of the substrate and should be able to deform under low pressure.

However, the wetting ability is a necessary but not sufficient condition. According to this condition water would be a good adhesive. In addition, a PSA needs to be able to build a network structure that is able to resist debonding forces by high cohesion and energy dissipation (3, 37, 105, 106).

As indicated earlier, PSAs originate from a film-forming elastomer which has an ability to quickly wet the substrate and overcome the surface roughness to provide instant bonding at low pressure as a result of its flow characteristics. In addition, PSAs possess sufficient cohesiveness and elasticity, to resist debonding and to be removed from surfaces without leaving residues. Essentially, PSAs require

a balance between their viscous and elastic properties. It should be noted that PSAs have to satisfy these contradictory requirements under different strain rate conditions. Which means that at low strain rates they must flow (bonding) and at high strain rates (i.e. peeling) they have to respond elastically (debonding) (6, 37) (Fig. 8).



Fig. 8: Adhesion performance considering tack, peel resistance, shear adhesion and their relation to liquid- and solid-like behavior of bonding and debonding of a PSA.

1.2.1. Measurement of adhesion performance

The adhesive properties of a transdermal patch can only be fully and correctly characterized by measurement of the essential adhesion performance such as tack, peel resistance and shear adhesion. Generally, the first two properties, i.e. tack and peel resistance, are directly related to each other while both are inversely related to shear adhesion (6, 28, 37, 104).

1.2.1.1. Tack

Tack is the ability to form a bond of measurable strength by short contact with a surface. It is not a fundamental material property with mathematically exact correlations to other factors, however it is

strongly influenced by the viscoelastic and interfacial properties of the materials and by the type of measurement (82, 107–109).

The majority of methods for tack measurement of transdermal patches such as rolling ball, loop and probe tack are adapted from the tape industry (110). All measurements try to imitate the regular “thumb tack test” and include a bonding and a debonding step. During the bonding step, contact is made with the surface of the adhesive, and the contact area increases by wetting out and elastic deformation. For typical tack tests, the bonding time is between a few milliseconds and a few seconds (26, 111). During the debonding step the adhesive has to resist debonding forces by elastic deformation and energy dissipation (37).

The different tests mainly vary in the time frame of the bonding as well of the debonding step (83). The quickest and most simple test is the rolling ball tack test (112, 113) (Fig. 9a). However, it has a poor reproducibility and is therefore mostly used for in-process control during production. The loop tack test (Fig. 9b) is predominately used to test different types of substrates and the influence of the backing membrane on the test result. The probe tack test (Fig. 9c) has the advantage of applying a uniform stress and strain rate to the adhesive allowing the complete bonding and debonding process to be investigated (36, 114).

1.2.1.2. Peel resistance

Peel resistance is the force required to remove a pressure sensitive tape from a test surface at a controlled angle and at a specified peel rate (110). Two standard setups are used for peel resistance tests: peel resistance at 180° angle and at 90° angle. With both methods a sample is applied to the surface with controlled pressure. Then the tape is peeled off at the respective angle and a specified

peel rate and the peel force is measured throughout the test (26, 84, 115–120) (Fig. 9d). Peel resistance correlates with tack and is strongly influenced by the type of backing membrane and the mechanical behavior of the surface.

1.2.1.3. Shear adhesion

Shear adhesion is the ability to resist shear forces. It is the resistance of the matrix to flow and may be considered as a measure of the cohesiveness of the matrix itself (37, 84, 104, 121–124). Low cohesion manifests itself in patch oozing, dark rings on the skin around the patch or adhesive residues in the package (3, 8). To determine shear adhesion, the sample is applied to a standard steel panel under controlled pressure. The panel is mounted vertically, a standard mass is attached to the free end of the tape and the time to failure is determined (121) (Fig. 9e).

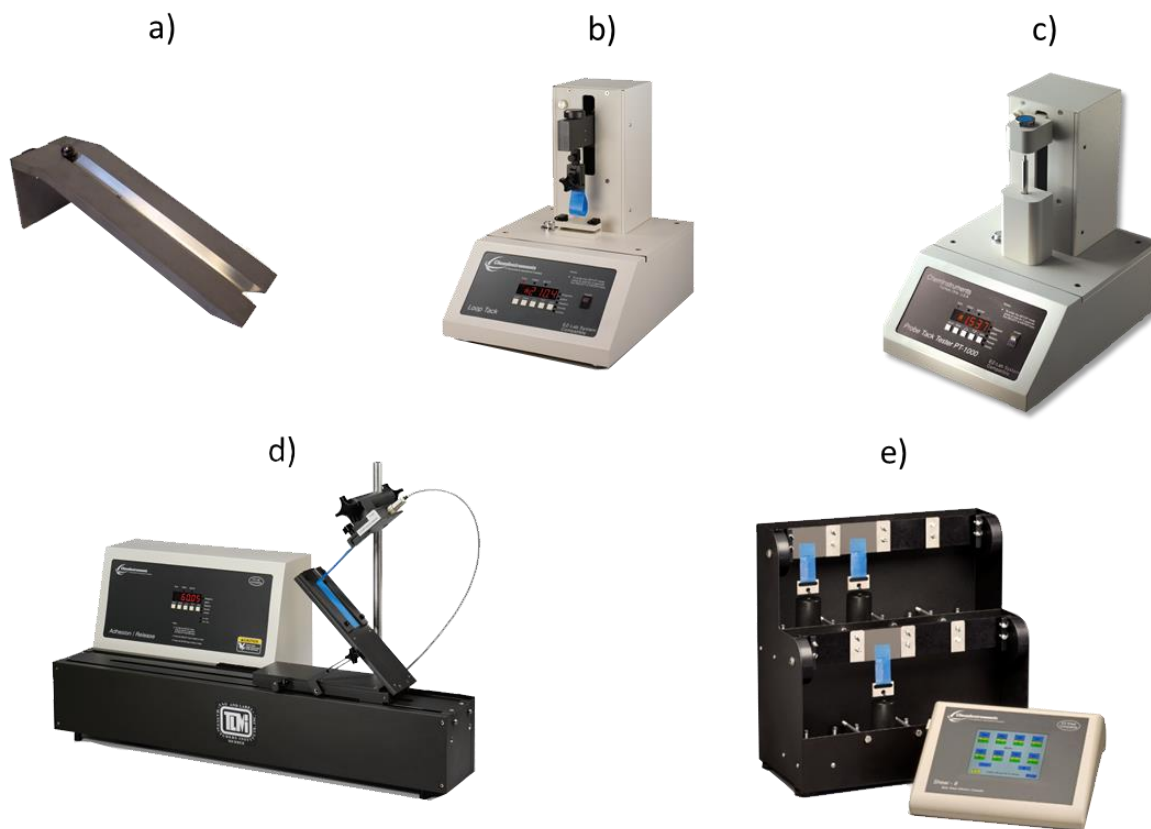


Fig. 9: Adhesion performance tests with (a) Rolling ball tack, (b) Loop tack, (c) Probe tack, (d) Peel resistance at 90° and 180°, (e) Shear adhesion. Printed with permission of Chemsultants International, Mentor/OH, USA.

1.2.2. Rheology of pressure sensitive adhesives

To determine the time- and temperature-dependent rheological parameters of a PSA, dynamic mechanical (thermal) analysis (DMA/DMTA) is known to be a versatile method (6, 18, 28, 37, 83, 84, 125–129). In stress controlled mode, DMTA supplies an oscillating force which causes a sinusoidal stress to a sample generating a sinusoidal strain (Fig. 10a, b). Measurement of the magnitude of deformation at the peak of the sine wave and the lag between the stress and strain waves, allows determination of the storage modulus G' , the loss modulus G'' and damping $\tan \delta$ (125) (Fig. 10b, c).

DMTA can also be performed in strain controlled mode, where an oscillating deformation is applied, generating a sinusoidal stress.

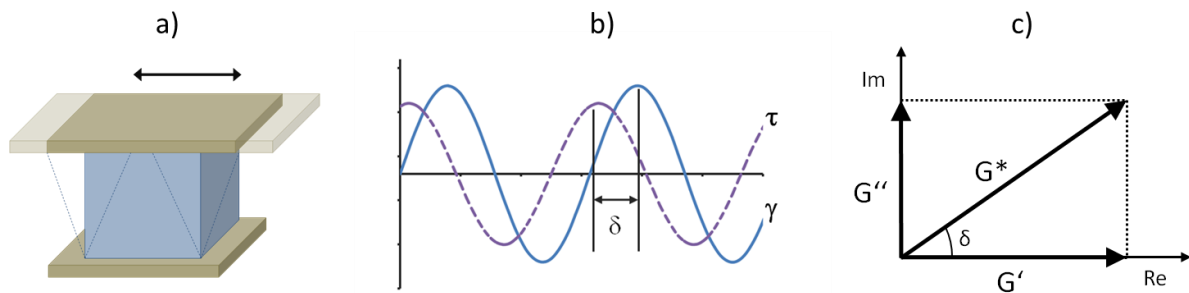


Fig. 10: (a) Oscillatory deformation, (b) Sine waves of stress τ and strain γ , and their phase angle δ , (c) Vectorial illustration of the complex modulus G^* , the storage G' and the loss modulus G'' .

Before starting oscillatory measurements, the linear viscoelastic region (LVR) must first be determined to assure that deformations are linearly reversible and rheological parameters can be calculated from the raw data. The LVR is determined by an amplitude sweep, during which the amplitude of the shear stress or alternatively the amplitude of the deformation is varied while the frequency is kept constant (Fig. 11a).

To allow assumptions about the time dependent mechanical behavior of the PSA, a frequency sweep can be performed. With a frequency sweep, the amplitude of the shear stress or alternatively the amplitude of the deformation is kept constant while the frequency is varied (Fig. 11b). The data at low frequencies describe the behavior of the samples at slow shear stress (or deformation) whereas the behavior at fast shear stress (or deformation) is expressed at high frequencies.

During a temperature sweep, the amplitude and the frequency are kept constant whereas the temperature is varied continuously or stepwise (Fig. 11c). With this method, the temperature dependent behavior as well as the dynamic glass transition temperature $T_{g \text{ dyn}}$ of the PSA may be determined.

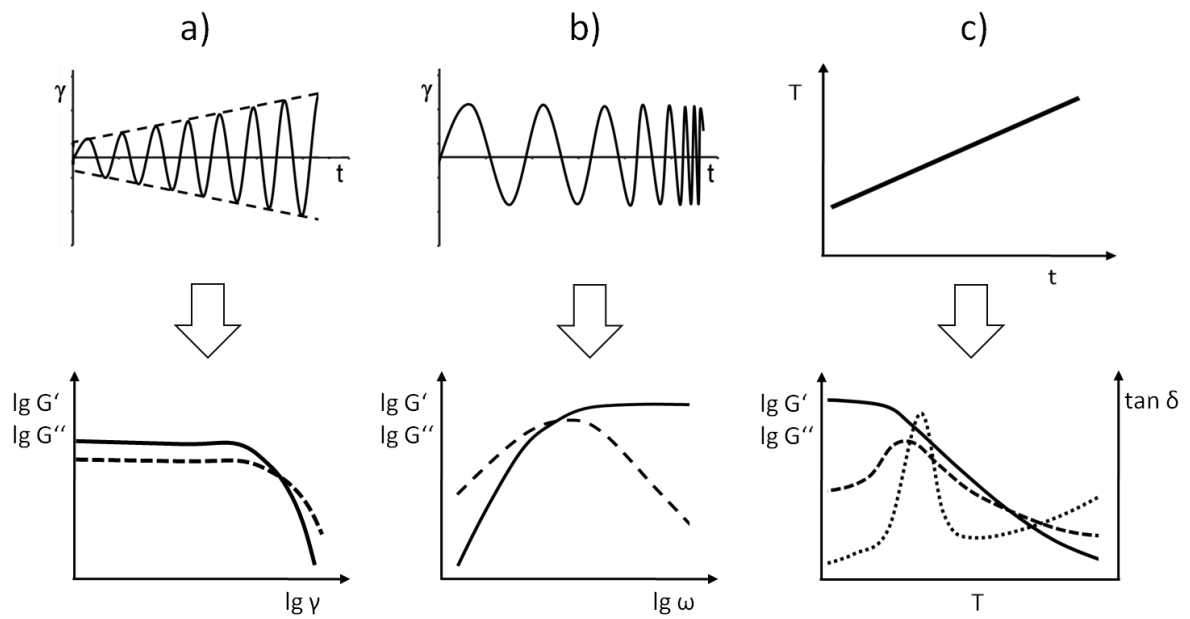


Fig. 11: Overview of DMA/DMTA methods: (a) Amplitude sweep, (b) Frequency sweep, (c) Temperature sweep.

A pressure sensitive adhesive requires properties of a liquid during bonding and properties of a solid during debonding (26). PSAs will not undergo a drying step or a chemical solidification reaction and have to remain flexible after application. To understand the principals of pressure sensitive adhesion it is absolutely necessary to consider their viscoelastic behavior.

The most important difference between bonding and debonding by far is the duration. The process of bonding in typical tack or peel tests for a PSA is longer than the process of debonding. A properly designed PSA will exhibit a strong gradient of the storage modulus G' between these two processes allowing it to bond quickly and to resist debonding (26, 130–132) (Fig. 12). Ideally, the value of the storage modulus should vary within the range of 20 and 300 kPa between bonding and debonding (37).

Adhesives with a modulus higher than the upper limit of 300 kPa display poor bonding, while adhesives with moduli below the lower limit of 20 kPa exhibit poor cohesive strength (i.e. low shear adhesion) (3, 37).

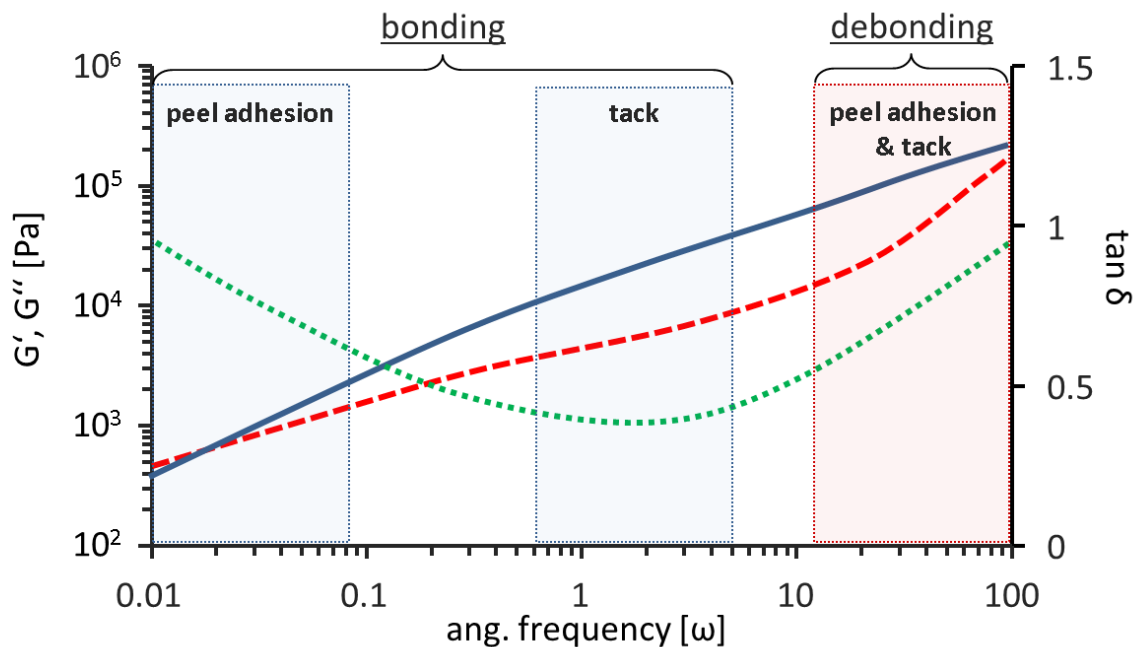


Fig. 12: Frequency sweep of a typical PSA, with storage modulus G' (blue), loss modulus G'' (red) and $\tan \delta$ (green) in dependence of the angular frequency ω . The bonding zones are displayed for tack tests and for peel tests.

In addition to the required behavior of the storage modulus, high energy dissipation at debonding promotes good adhesion. Dissipation can be expressed by the loss modulus G'' . It is proposed that the loss modulus peak temperature of PSAs for transdermal patches should be between $-20\text{ }^{\circ}\text{C}$ and $-30\text{ }^{\circ}\text{C}$, i.e. $50\text{ }^{\circ}\text{C}$ below the operating temperature (37). Furthermore, G'' should already be located in the so-called transition zone to dissipate the energy caused by deformation (Fig. 12) (105). The transition zone represents the onset of the glass transition. If the strain rate exceeds the movability of the polymer chains, they are no longer able to follow the applied strain and become brittle. It therefore can be stated that a typical pressure sensitive adhesive is in a rubbery-liquid like state at bonding and in a rubbery-glassy like state at debonding.

There have also been attempts to determine the adhesion properties using the damping factor $\tan \delta$ (37, 83). As the $\tan \delta$ peak correlates with the glass transition temperature T_g , it obviously should be located at sufficiently low temperatures to allow the PSA to wet the substrate during bonding (132). Also, shear adhesion and peel resistance properties may be correlated with $\tan \delta$ at low frequencies (37, 129). Although, it has been found that a change of $\tan \delta$ may lead to a change of adhesion behavior, the adhesion behavior can be modified without recognizing a change of $\tan \delta$ (37). Unfortunately, the damping factor $\tan \delta$ which is equivalent to the ratio between G'' and G' does not cover all necessary factors for determination of the adhesion performance. However, it can be helpful in conjunction with the other rheological parameters to determine small changes in adhesion performance, especially in the low shear region (129).

Finally, it has to be mentioned that in common tack, peel and shear adhesion tests, strains of up to 1000 % may occur (26). In addition, strain rates usually are non-constant during testing (37). Therefore, correlations of rheological and adhesion data sometimes are not easy to interpret.

1.2.3. Factors influencing adhesion

It can be assumed that the measured adhesive performance of a PSA may be expressed as a function of two main factors, namely interfacial molecular interactions and viscoelastic properties of the adhesive (26, 84). Factors influencing one of these main factors will consequently have an impact on the adhesion behavior. Apparently, adhesion is a good example for a multivariate and non-linear phenomenon. Factors can have similar or contrary effects on both main factors with varying impact. For example, elevated **temperatures** may soften the adhesive and therefore increase the bonding behavior, but at the same time decreases the cohesiveness and has a negative effect on the resistance to debonding (84, 124, 133). Prolonged **time** for bonding (dwell time) as well as high **pressure** may increase the adhesion up to a certain level due to more pronounced wetting whereas an excessive increase of both parameters will not necessarily further amplify the effect (3, 84, 85, 107, 109, 134). Also, an increase of **surface roughness** increases adhesion, initially up to a maximum and then decreases due to a reduced contact area (135–137).

Surface related factors such as surface energy are dependent on the **surface chemistry of the polymer and the substrate**. **Surface energy** cannot be considered as being an intrinsic property of a polymer as it can drastically change depending on the nature of the medium in contact and the polarity and mobility of the polymer chains. This phenomenon results from an **orientation** and organization of the macromolecules to minimize the interfacial energy between the polymer and the orienting substrate. These oriented structures exhibit a glassy-like behavior with increased moduli (e.g. G' , E') and thus, an increased mechanical strength (138–145). Interestingly, this phenomenon has not been studied well with PSAs. However, tack, peel resistance and shear adhesion may directly be correlated to G' and E' (6, 18, 26, 37, 84, 134, 146) and therefore, it is assumed that they are

affected by the mechanical strengthening. For example, higher values of shear adhesion were observed on stainless steel panels than on high density polyethylene (HDPE) panels (147).

As already mentioned, the temperature range in which the polymer changes from a rubber-like state into a glassy state, known as the **glass transition temperature T_g** , has a particular relevance in the characterization of PSAs (17, 33, 37, 84, 125, 134). Differences in the T_g can be directly related to the steric size of the side chains and the mobility of the polymer (37, 148–150). Because the T_g is not a thermodynamic phase transition but a dynamic phenomenon, it cannot be determined as an absolute value and depends on the mechanical history and the method of determination. Two major measuring principles are exploited in the determination of the T_g of a PSA. The first is based on a change of heat capacity at the T_g and can be determined by differential scanning calorimetry (DSC). The second principle directly measures a change in deformation behavior and can be determined by DMTA. A close and predictable relationship exists between the T_g measured by DSC and the dynamic $T_{g\ dyn}$ measured by DMTA (35, 37, 151). With regard to the tack of PSAs, a T_g in the range between 40 °C and 75 °C below the operating temperature was found to be optimal (33, 84, 134). Thus, factors influencing the T_g affect the adhesion behavior.

A **plasticizer** in the sense of external plasticization is defined as a low molecular weight compound that is added to polymers to reduce the T_g , improve polymer flexibility, decrease tensile strength, stiffness, and toughness, and to increase elongation and ductility (35, 89, 152–156). It is known that the addition of a plasticizer reduces the entanglements of a polymer and decreases the storage modulus G' (26, 87, 89). The efficiency of a plasticizer depends on its molecular size and its ability to interact with the polymer (157). For plasticization of PSAs, small molecular weight compounds as mentioned in chapter 1.1.2.4 are used. However, in most cases the addition of plasticizers to polymers in pharmaceutical applications is unintentional and may even occur with the incorporated

APIs as observed for ketoprofen and guaifenesin in polyethylene oxide (152), nitroglycerin and nicotine in PSAs (21), lidocaine and diphenhydramine in Eudragit® E100 (94), ibuprofen and metoprolol tartrate in Eudragit RS (157), chlorpheniramine maleate in Eudragit® RL PM and Eudragit® RS PM (158) and ibuprofen, chlorpheniramine maleate and theophylline in Eudragit® RS 30 D (155).

Antiplasticization can be observed, if only small amounts of plasticizer are added to a polymer. Except for the decrease in T_g , opposite effects such as an increase of the storage modulus as well as the mechanical strength and a decreased elongation were reported (35, 86, 153, 156, 159). Antiplasticization has been observed with traditional plasticizers (159, 160) as well as with non-traditional plasticizers such as APIs (161, 162). According to Anderson (160), the plasticizer molecules accumulate in the existing free volume voids of the polymer and interact with the polymer to build a network structure by physical crosslinking.

Generally, if a substance is added to a PSA, an unpredictable alteration of the adhesive properties can occur due to its plasticizing or antiplasticizing effect (6). The effect of non-traditional plasticization and antiplasticization is one of the major topics of the performed studies and will be discussed in more depth later on.

In Fig. 13 an overview is given of factors contributing to the two main factors of interfacial molecular interactions and the viscoelastic properties of the adhesive and therefore, to the adhesion performance. For in-vivo measurements the additional factor of individual skin properties has to be taken into account (8, 105).

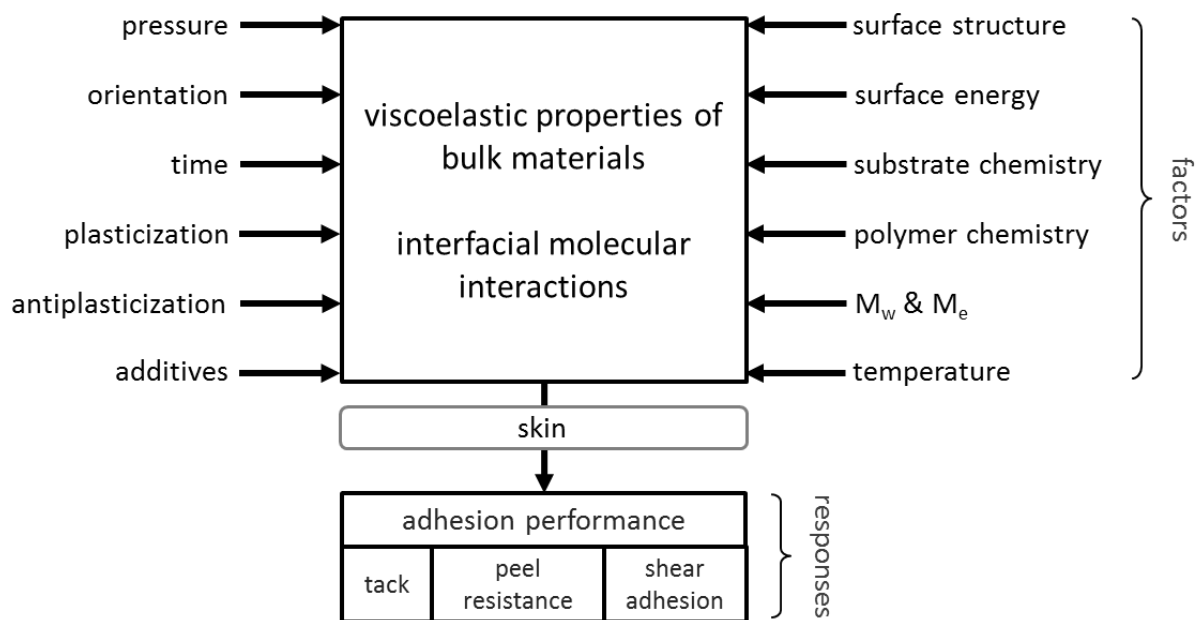


Fig. 13: Overview of factors contributing to the adhesion performance, measured as tack, peel resistance and shear adhesion.

1.3. Design of Experiments (DoE)

In general, with the implementation of the methodology of DoE detailed information on effects of factors significantly influencing the output of a process can be assessed by controlled experiments (163–169).

Every process can be described with controllable and uncontrollable factors as input variables and responses as output variables (170) (Fig. 14). To investigate the influence of a factor, its level is set between a minimum and a maximum value. Subsequently, the difference in the response is measured. All other factors must be kept constant or at least be monitored to be able to clearly differentiate between the effects of the respective factors. The controlled setting of each factor has to be performed in all possible combinations and will represent the design space.

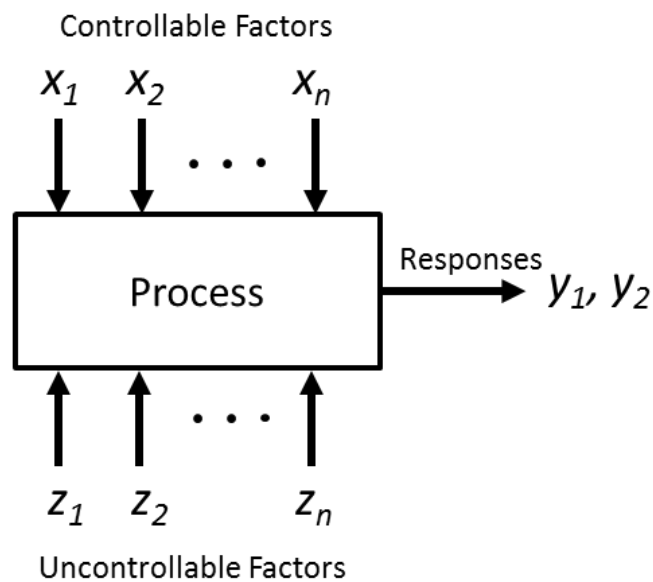


Fig. 14: Process with controllable and uncontrollable factors as input variables and responses as output variables.

In Fig. 15a, a one factorial design with two levels and three levels is displayed, respectively. If the experiment is augmented to two factors, the number of experiments increases with two levels to four experiments and with three levels to nine experiments (Fig. 15b). For three factors the number of experiments increases with two levels to eight and with three levels to 27 (Fig. 15c).

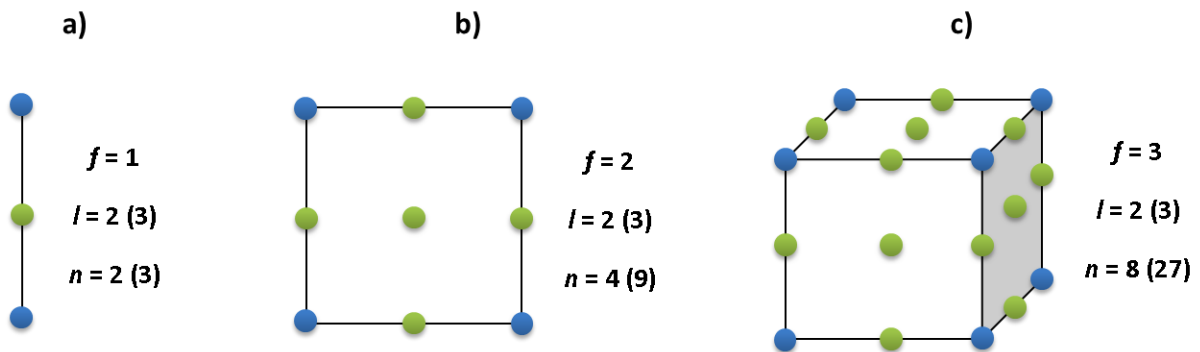


Fig. 15: (a) One factorial design, (b) Two factorial design, (c) Three factorial design. Blue spheres represent a two level design, blue and green spheres together represent a three level design. With f = number of factors, l = number of levels and n = number of experiments.

The number of factors f , the number of levels l and the number of experiments n are related as follows:

$$n = f^l \quad \text{Eq. 1}$$

With DoE a response surface which describes the influence of a factor on a response can be developed for every measured response in the design space. The advantage of developing a response surface is the possibility to detect interactions of factors or to reveal trends, minima, maxima or even more complex shapes of the response in the design space (Fig. 16). Also, the possibility of predictions

is given with a response surface. Predictions can help to control a process up to an optimum and allow assumptions on the expected response.

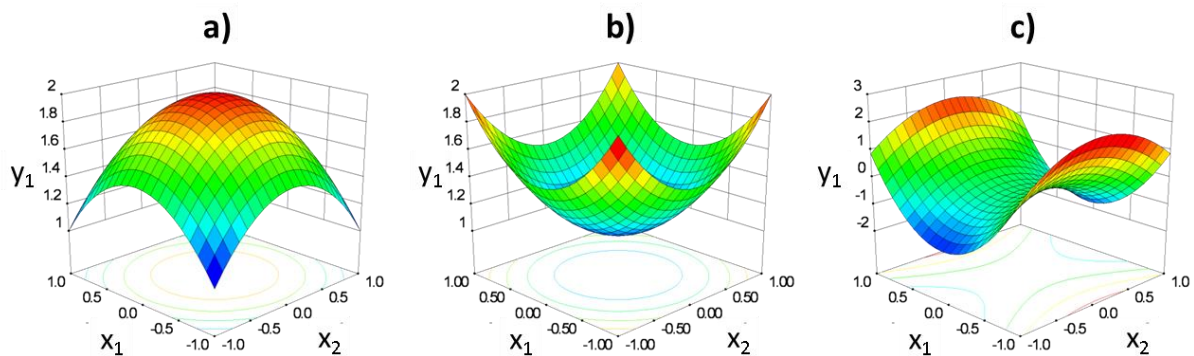


Fig. 16: Quadratic response surfaces with (a) Maximum, (b) Minimum, (c) Saddle-like structure; all created with the Design Expert® 8.0.6 software.

Generally, the expected polynomial of a response surface is unknown. Therefore, it is common to start with a two level design with an additional modification: Assuming that the levels of the design are set to the minimum (-1) and the maximum (+1) for all factors, a design point is added where all factors are balanced (0). This point is called center point, because it is located in the center of the design space with regard to all factors. In addition, the center point may be repeated to determine the standard deviation of the response surface. With the existence of a center point, a response surface can be tested for linearity. If the deviation of the center point from the response surface is larger than the standard deviation of the response surface, a lack of fit (LOF) is present. From this result it can be assumed that a linear response surface is insufficient to describe the influence of the factors on the selected response. Nevertheless, it is still unknown which polynomial may describe the

relationship exactly. In order to be able to further use the results of the performed experiments the design may be augmented, which means that additional design points are added to be able to determine a response surface with a higher polynomial. In most cases, a central composite design (CCD) is the preferred way to augment a two level design. So-called starpoints are added, either in a certain distance or face-centered in relation to the existing design (Fig. 17).

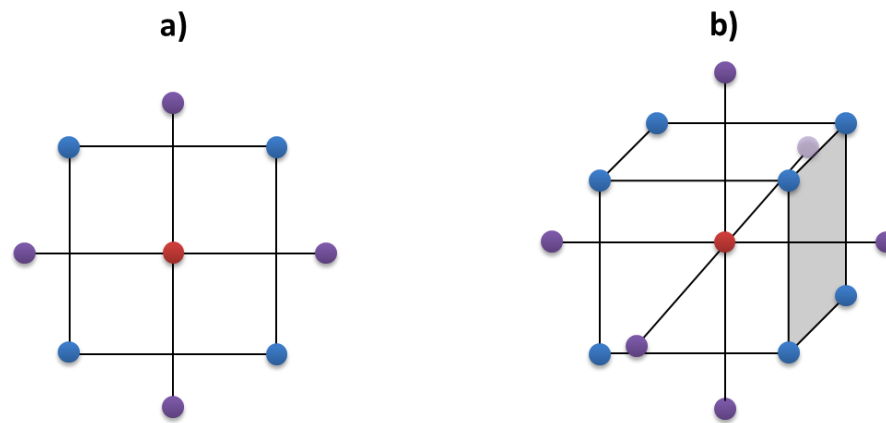


Fig. 17: Central composite design of (a) Two-level, two-factorial design, (b) Two-level, three-factorial design. Blue spheres represent the full factorial design, red spheres the centerpoints and purple spheres the starpoints of the CCD.

The discussed methods are known for decades and are well established but are limited to symmetric, non-constrained designs with limited factors involved. As computers can numerically calculate optimal design points within seconds, algorithms are able to create statistically optimized designs with a minimum of design points. These so-called optimal designs are created by algorithms which determine the optimal distribution of design points within the design space, either to optimize the estimates of the specified model coefficients (D-optimal) or to optimize the prediction variance

around the model (IV-optimal). One advantage is that augmentation of optimal designs can be performed stepwise to any polynomial and with any constraints of the factors.

A modification of DoE is the methodology of mixture designs (164, 165, 171, 172). Instead of factors, components are used and instead of levels, fractions. Mixture experiments differ from standard experiments, as a mixture experiment is an experiment in which the response is assumed to depend only on the relative proportions of the components but not on the amount of the components (171). The fractions of the components always have to sum up to 100 %. It is not possible to change one component without changing at least another. This fact has a profound effect on every aspect of experimentation with mixtures: the design space, the design properties, and the interpretation of the results (171).

The main differentiation between factorial experiments and mixture experiments is the construction of their design space. The design space of a factorial experiment is the set of possible combinations of its independent variables or components. The design space of a mixture experiment is the set of possible combinations of the relative proportion of each component, which usually add up to a value of 100 % (Fig. 18a). Mixture designs are often constrained, as the components may not be combined in any ratio without failing the targeted properties of the final product (Fig. 18b). Again, optimal designs can help to create an optimized experimental design space with a reasonable number of experiments.

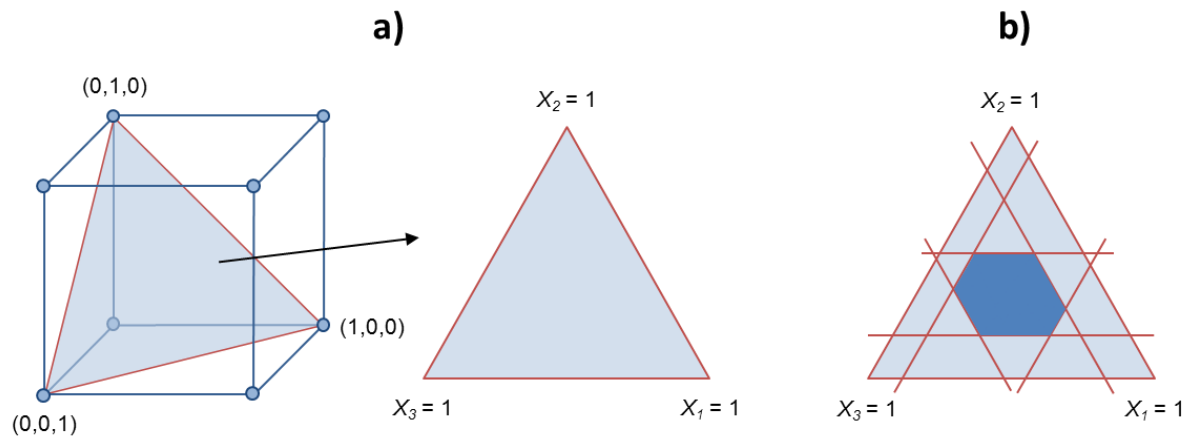


Fig. 18: (a) Design space of a three component mixture experiment, (b) Constrained design space of a three component mixture experiment.

Traditionally, design of experiments (DoE) has been used to evaluate the impact of the critical process parameters (CPPs) on the critical quality attributes (CQAs) in production and development processes (173–175). However, it may also be used as a tool for the evaluation of significant factors and their influence on an analytical result (176). Compared to a “one-factor-at-a-time” (OFAT) method, an experimental design method is able to detect possible interactions with a reasonable number of experiments.

1.4. Objectives of this work

Transdermal patches are known in the pharmaceutical community for decades but until now only few well established methods are available in the development and analysis of new patch formulations.

Currently, in many of the clinical trials placebo patches are used to determine the adhesion performance of new transdermal patch formulations (3). The use of placebo patches cannot be justified because the compatibility of the API with the patch components, especially the PSA, may have an effect on the adhesive properties of the final drug product. The addition of an API may alter the viscoelastic behavior and therefore also the adhesion performance of a transdermal patch (6).

The United States Food and Drug Administration (US-FDA) has received numerous reports of “adhesion lacking” for transdermal drug delivery systems (3, 177). In addition to the adhesive problems, there is the phenomenon of the so-called dark ring around the patch caused by cold flow resulting from low cohesive strength of the PSA (11, 105). Lack of adhesion and cold flow may result in improper dosing as the extent of contact between patch and skin directly affects drug delivery (3). Furthermore, problems during storage may occur because of oozing of the PSA into the pouch (8).

The main objective of this thesis is the attempt to introduce systematical methods in the development and analysis of transdermal patches as claimed by the draft “Guideline on quality of transdermal patches” (11) and the “ICH guidance Q8 Pharmaceutical Development” (167).

To gain a deeper insight into the adhesion performance of a transdermal patch, a reliable method to manufacture patches with different PSAs, varying API content and matrix thicknesses with emphasis on a reproducible quality is supposed to be established.

Currently, standard test methods from the tape industry are used to evaluate the adhesion performance of a patch (21, 28). Unfortunately, these methods were developed as quality control

tools for pressure sensitive products in general and show poor reproducibility and are not adjusted to pharmaceutical end points. Usually, single point measurements with a low degree of information are performed. Furthermore, these methods gather viscoelastic as well as interfacial properties of the patch. Because with DMA/DMTA the complete bonding and debonding behavior of a PSA can be examined, this method is investigated in the first part of the thesis with regard to its suitability to detect alterations in viscoelasticity and adhesion performance caused by an API.

In the second part of the thesis, the probe tack test which recently was demonstrated to be able to predict in-vivo adhesion performance of placebo patches (105) is investigated in depth. By introduction the method of design of experiments (DoE) in a measurement system analysis (MSA), the variation of the test result caused by interactions of the test parameters and the sample properties, can be discussed on a more consolidated background.

Finally, a novel method of formulation development for transdermal patches is established for a multiple polymer adhesive patch following the draft "Guideline on quality of transdermal patches" (11) and the "ICH guidance Q8 Pharmaceutical Development" (167).

2. Materials and methods

2. Materials and methods

2.1. Materials

Solvent based polyacrylic pressure sensitive adhesives DuroTak[®] 387-2287 and DuroTak[®] 87-4287 were kindly donated by Henkel, Bridgewater, USA. Solvent based silicone pressure sensitive adhesive BIO-PSA[®] 7-4302 was donated by Dow Corning, Seneffe, Belgium. Oleyl alcohol was purchased by Caesar & Loretz, Hilden, Germany. Ibuprofen was supplied by BASF, Ludwigshafen, Germany. Platilon[®] U073 100 Natural PE Backing Membrane was kindly donated by Epurex Films, Bomlitz, Germany. Fluoropolymer coated Scotchpak[®] 1020 Release Liner was purchased by 3M, Neuss, Germany. All other reagents used were of analytical grade.

2.2. Methods of “Evaluation of DMA/DMTA for transdermal patch development”¹

2.2.1. Determination of the NVC

The non-volatile content (NVC) of the adhesive was determined gravimetrically by drying accurately weighed amounts (2-3 g) of adhesive at 80.0 °C for 24 h. From five samples the average NVC was calculated.

2.2.2. Preparation of the wet mixes

Wet mixes were then prepared by addition of ibuprofen to the DuroTak[®] 87-4287 at concentrations of 1, 2, 4, 8 and 16 % (w/w) referring to the NVC. The samples were shaken in an overhead shaker (in-house development) at 30 rpm and room temperature (RT) for 24 h and then stored for additional 24 h to remove air bubbles. For plain, drug-free films the adhesive was used as supplied.

2.2.3. Preparation of the dry adhesive matrices

The wet mixes were cast on the release liner. To achieve the final thickness of dry films of 200 ± 10 μm for rheological and probe tack tests and of 55 ± 10 μm for rolling ball tack and shear adhesion tests, a CX 4 semiautomatic lab coater equipped with a bar film applicator (MTV Messtechnik, Cologne, Germany) was used.

Solvent evaporation was done by storage of the freshly prepared adhesive matrices for 15 min at RT and subsequently for 30 min at 80.0 °C in a drying oven (Heraeus T6060, Thermo Fisher Scientific,

¹ This chapter has been published as shown in Table 10, p. 141.

Waltham, USA). The thickness of the adhesive matrices was measured with a digimatic indicator (Mitutoyo Deutschland, Neuss, Germany).

All films were stored in an air-conditioned room at 21.0 °C and 50 % R.H. for 24 h.

2.2.3.1. Laminates for rheological characterization

Adhesive matrices for rheological analysis were prepared by lamination of multiple layers of the dry adhesive matrix with a lamination device (in-house development) to achieve a final matrix thickness of $1145 \pm 82 \mu\text{m}$ (Fig. 19a). The samples were stored in an air-conditioned room at 21.0 °C and 50 % R.H. for 1 week. For further investigation the samples were cut into discs of 25.0 mm diameter each with a cutter (Richard Hess MBV, Sonsbeck, Germany).

2.2.3.2. Test specimens for probe tack experiments

For probe tack experiments the dry adhesive matrices were cut into 12.0 mm x 150.0 mm specimens with a strip cutter (Emmeram Karg Industrietechnik, Krailling, Germany) (Fig. 19b). The samples were stored as described in chapter 2.2.3.1.

2.2.3.3. Test specimens for rolling ball tack and shear adhesion experiments

For rolling ball tack and shear adhesion experiments laminates consisting of backing membrane, release liner and adhesive matrix were prepared by lamination of the dry adhesive matrix with the polyester backing membrane (Fig. 19b). The laminates were further treated as mentioned in chapter 2.2.3.2.

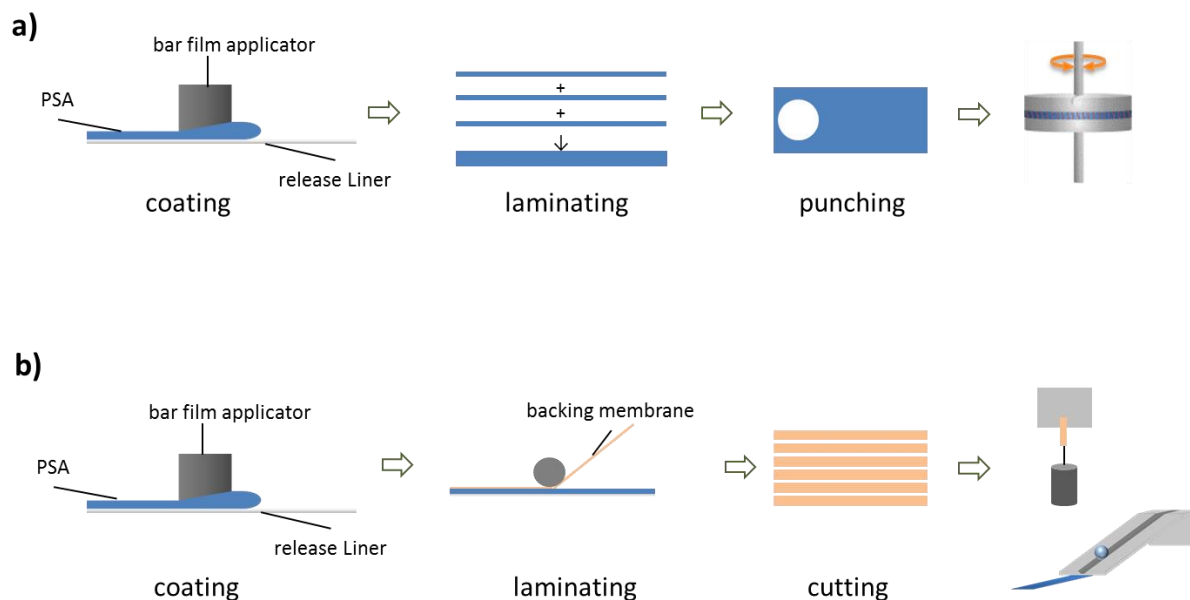


Fig. 19: (a) Preparation of laminates for rheological characterization, (b) Preparation of test specimens for rolling ball tack and shear adhesion experiments.

2.2.4. Monitoring of ibuprofen crystal formation

The absence of ibuprofen crystals was confirmed by polarization microscopy (Universal R Pol, Zeiss, Jena, Germany) at a 100x magnification over the whole area of all samples immediately after preparation, before testing and after 12 months.

2.2.5. Dynamic Mechanical Analysis (DMA) / Dynamic Mechanical Thermal Analysis (DMTA)

DMA/DMTA was performed with a strain controlled Rheometrics Dynamic Analyzer II (Rheometrics, Piscataway, USA) equipped with a 25.0 mm disposable aluminum parallel plate geometry and a convection oven attached to a Chiller. For data acquisition and processing the Orchestrator® software

(TA Instruments, Eschborn, Germany) was used. The upper release liner of the samples was peeled off and each sample was pressed onto the parallel plate geometry. Thereafter, the lower release liner was removed. To bring the specimen in contact with the lower plate the gap between the plates was adjusted by instrument normal force control to 8.0 N for 10 s. For the conditioning steps the normal force control was set to 0.0 N. Frequency sweep and temperature sweep experiments were conducted after determination of the linear viscoelastic region (LVR) by strain sweeps. All tests were performed in triplicate. Strain sweeps and frequency sweeps were run at 21 and 32 °C, respectively.

2.2.5.1. Strain sweeps

All samples were conditioned at the respective test temperature for 30 min. The LVR was determined by strain tests from 0.1 % to 20 % strain at $\omega = 0.01$ rad/s and 100 rad/s, respectively. These experiments were performed with plain adhesive matrix as well as with an ibuprofen content of 8.0 %.

2.2.5.2. Frequency sweeps

All samples were conditioned as described above. Frequency sweeps were performed from $\omega = 0.01$ up to 500 rad/s and at a controlled strain of 5.0 %. G^* , G' , G'' and $\tan \delta$ were determined in dependence of the angular frequency ω .

2.2.5.3. Temperature sweeps

All samples were conditioned at -55.0 °C for 60 min. The gap between the plates was adjusted by instrument normal force control to 0.0 N with an autotension sensitivity of 0.2 N. Temperature sweeps were run from -55.0 °C to +100.0 °C in steps of 1.0 K at $\omega = 1.0$ rad/s and a controlled strain of 1.0 %. Conditioning time period at each temperature step was 5.0 min prior data acquisition. G^* , G' , G'' and $\tan \delta$ were determined in dependence of the temperature T .

2.2.6. Adhesion performance

Test specimens were analyzed by a probe tack test at 21.0 °C and by standard test methods of the Pressure sensitive Tape Council (PSTC) such as rolling ball tack (PSTC-6) and shear adhesion (PSTC-107 A) at 21.0 °C and 32.0 °C, respectively. Experiments at 21.0 °C were performed in an air-conditioned room. For rolling ball tack and shear adhesion experiments at 32.0 °C the equipment was transferred into a Heraeus B5050E drying oven (Heraeus, Hanau, Germany). 24 h prior to the experiments the equipment as well as the specimens were conditioned at the respective test temperature.

2.2.6.1. Probe tack test

With the probe tack test the complete debonding process can be observed. Stress strain curves, generated from force and displacement data were used to determine the tack as stress maximum (σ_{max}).

For probe tack experiments test specimens consisting of release liner and dry adhesive matrix were transferred to a slideable aluminum mounting (in-house development). Prior the probe tack experiments the release liner was peeled off. The probe tack test was performed with an universal testing machine (Inspect Mini, Hegewald & Peschke, Nossen, Germany) equipped with a 3 mm stainless steel probe and test parameters shown in Table 1. All measurements were repeated 5 times.

Table 1: Test parameters for probe tack test.

Parameter	Setting
Approaching speed	0.1 mm/s
Contact time	1.0 s
Contact force	0.4 N
Detachment speed	5.0 mm/s

2.2.6.2. Rolling ball tack test (PSTC-6)

The rolling ball tack test is one method of attempting to quantify the ability of an adhesive to adhere quickly to another surface (121). For the tack measurements the size of the test specimens was 12.0 mm x 150.0 mm instead of 24.0 mm x 300.0 mm. The specimen were positioned adhesive side up on the working surface and the raceway of the rolling ball tack test apparatus (RBT-100, Cheminstruments, Fairfield, USA) was aligned with the specimen. A 13.5 mm stainless steel ball was released and rolled until it was stopped by the adhesive. The distance was measured from the point where the ball initially was in contact with the adhesive to the position where the ball was stopped. All measurements were repeated 5 times, each with a fresh specimen.

2.2.6.3. Shear adhesion test (PSTC-107 A)

Shear adhesion is the ability of a tape to resist static forces applied in the same plane as the backing (121). According to PSTC-107 A the ability of a pressure sensitive tape to adhere to a standard steel panel under constant stress is measured. A 12.0 mm x 150.0 mm specimen was applied to a standard steel panel under controlled pressure with a rubber covered steel hand roller (Cheminstruments, Fairfield, USA) such that the effective contact area between specimen and steel panel was 12.0 x 12.0 mm. The panel was mounted vertically in an 8 bank shear tester (S-HT-8, Cheminstruments, Fairfield, USA). A standard mass of 500.0 g was attached to the free end of the tape with a clamp and the time to cohesive failure was determined. All samples were measured in triplicate.

2.2.7. Differential Scanning Calorimetry (DSC)

T_g values of the dry adhesive matrices were measured by DSC (PerkinElmer, Waltham, USA) from -130 °C to 100 °C at a heating rate of 10 K/min with nitrogen purge of 20 ml/min. Accurately weighed samples of about 10 mg were placed in pin-holed and sealed 30 μ l aluminum pans. The first heating run data were discarded and only the second heating runs were evaluated. The T_g values were determined as the midpoint of the inflection in the DSC thermograms. Before measurement the DSC was calibrated with 1-pentanol analytical standard (Fluka) and water LiChrosolv® (Merck Millipore). All samples were measured in triplicate.

2.3. Methods of “Systematic investigation of the probe tack test”

2.3.1. Design of Experiments: IV-optimal design

To examine the significance of potential influencing factors and the linearity of the probe tack test, five factors were chosen to be investigated: detachment speed (A), dwell time (B), contact force (C), adhesive matrix thickness (D) and API content (E).

To evaluate the main effects of these five factors, their interactions and quadratic effects a randomized response surface design with 38 runs was built (Table 2) with the Design-Expert® 8.0.6 software (Stat-Ease, Minneapolis, MN, USA). An “IV-optimal” algorithm with point exchange was used because the thickness of the adhesive matrices and the API content were adjusted to predefined levels.

The maximum of the stress strain curve of the probe tack test (σ_{\max} , Fig. 20d) was selected as response.

Table 2: Experimental design of the probe tack test with the five investigated factors detachment speed (A), dwell time (B), contact force (C), adhesive matrix thickness (D) and API content (E).

		factor A	factor B	factor C	factor D	factor E
Standard	Run	detachment speed	dwell time	contact force	adhesive matrix thickness	API content
		mm/s	s	N	µm	% (w/w)
8	1	2.9	10.0	2.6	200	0
3	2	1.0	8.7	4.0	50	0
5	3	5.0	7.8	0.5	100	0
26	4	2.7	7.1	0.5	50	12
6	5	1.0	4.0	0.5	200	3
24	6	1.0	1.4	4.0	50	10
12	7	4.0	7.0	4.0	200	5
18	8	3.0	5.5	2.3	150	6
17	9	3.0	5.5	2.3	150	6
23	10	2.0	1.0	0.5	50	8
30	11	5.0	8.0	2.0	150	12
14	12	3.0	5.5	1.2	150	9
34	13	4.0	1.0	4.0	200	12
31	14	1.0	1.0	0.5	150	12
19	15	3.5	1.0	0.5	200	6
15	16	3.0	5.5	2.3	150	3
7	17	5.0	1.0	2.0	200	0
33	18	2.0	7.9	2.8	200	11
16	19	3.0	5.5	2.3	150	6
11	20	2.5	10.0	3.7	150	5
28	21	3.2	10.0	4.0	100	11
13	22	1.0	10.0	0.5	100	6
9	23	2.9	10.0	2.6	200	0
25	24	2.7	7.1	0.5	50	12
20	25	1.4	4.7	4.0	200	6
4	26	5.0	7.8	0.5	100	0
1	27	3.8	1.0	1.3	50	2
29	28	3.2	10	4.0	100	12
22	29	5.0	10	2.4	50	6
10	30	2.0	2.5	4.0	150	1
27	31	5.0	2.3	2.7	100	9
32	32	5.0	10	0.5	200	9
2	33	4.5	4.0	4.0	50	0
21	34	5.0	10	2.4	50	6
36	35	5.0	7.8	0.5	100	0
35	36	2.0	2.5	4.0	150	7
37	37	3.0	5.5	2.3	150	7
38	38	3.0	5.5	2.3	150	7

2.3.2. Preparation of the wet mixes

The NVC of DuroTak[®] 387-2287 was determined as described in chapter 2.2.1. The wet mixes were prepared as described in chapter 2.2.2. For drug-loaded matrices, ibuprofen was mixed with the adhesive at concentrations shown in Table 2 referring to the NVC.

2.3.3. Preparation of the dry adhesive matrices

For probe tack test experiments, adhesive matrices of DuroTak[®] 387-2287 with thicknesses shown in Table 2 were prepared as described in chapter 2.2.3. For DMA measurements, samples with 0 %, 6 % and 12 % (w/w) ibuprofen content were used.

2.3.4. DMA Measurements

DMA measurements were performed as described in chapters 2.2.5. and 2.2.5.2. at 21 °C. Strain sweeps were conducted for samples with 8 % ibuprofen content at 100 rad/s. Frequency sweeps were performed from 0.1 to 100 rad/s.

2.3.5. Probe tack test

The probe tack test was performed as described in chapter 2.2.6.1. however, equipped with an in-house developed 3 mm stainless steel probe (Fig. 20b). The probe was developed to apply constant stress to the test specimen during contact. Therefore, it was built in two parts: One part is a cylinder that is connected to the force transducer and holds the moveable probe. The probe was designed as a hollow piston that is able to move up and down inside the cylinder. The contact force was adjusted by

addition of small metal beads into the piston (Fig. 20c). If the probe is brought in contact with the specimen, the piston “stands” on the specimen without contact to the outer cylinder and the probe acts with its own gravity force. At the end of the dwell time the cylinder moves upwards and lifts the piston with the probe (Fig. 20e).

As test parameters, the settings shown in Table 2 with an approaching speed of 0.1 mm/s were used.

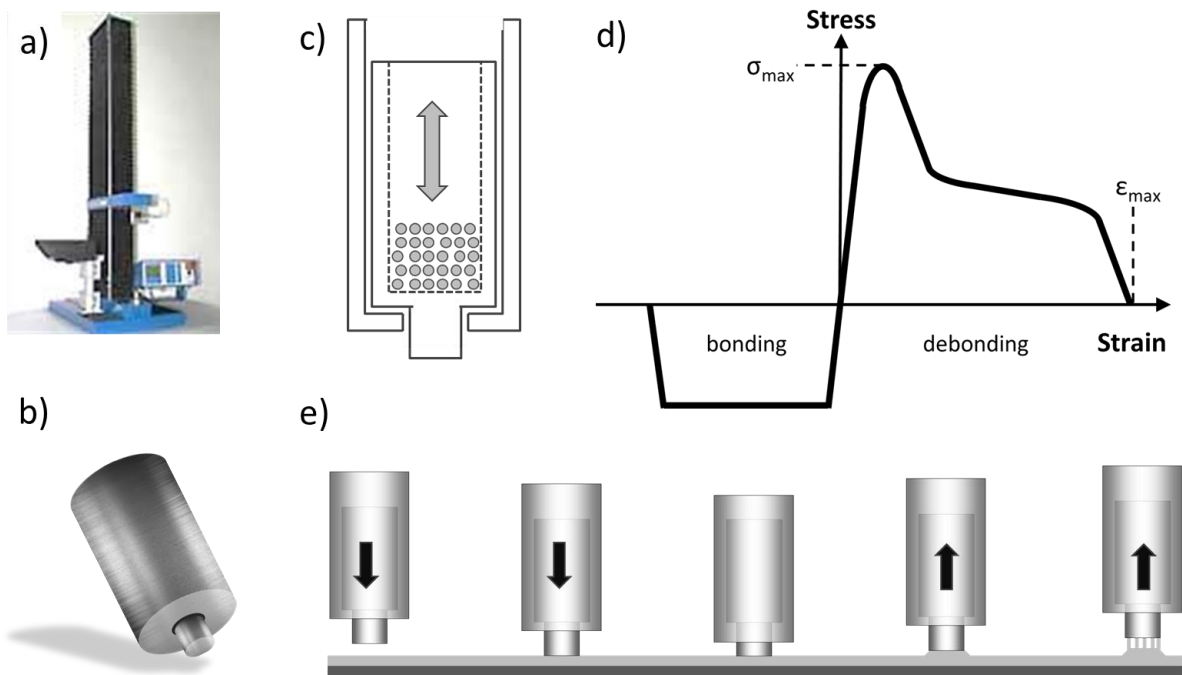


Fig. 20: Overview of the experimental setup of the probe tack test with (a) Material tester, (b) Tack probe (in-house developed), (c) Scheme of the probe, (d) Stress-strain curve, (e) Movement of the probe during bonding and debonding.

2.3.6. Statistical data analysis

Data analysis was performed by the scheme displayed in Fig. 21. At first, the “Fit Summary” of the design was checked. Then the model with the highest polynomial degree that was not aliased was chosen.

In the next step an ANOVA was evaluated for significance of the model, “Lack of Fit” (LOF) and adjusted R^2 as well as predicted R^2 . In case the predicted R^2 was too low a backward reduction of the model was performed.

For diagnostics the “Box-Cox” plot for power transformations was checked. If the “Box-Cox” plot recommended a data transformation, it was carried out and the scheme was repeated.

In the next step the “Normal Probability Plot of the Studentized Residuals” was investigated for normality of residuals. Then the “Internally Studentized Residuals vs. Predicted” plot was reviewed for constant error. Finally the “Externally Studentized Residuals” plot was investigated for outliers, i.e. influential values. Provided that the model statistics and diagnostic plots showed acceptable results, the procedure was finished up with the model graphs.

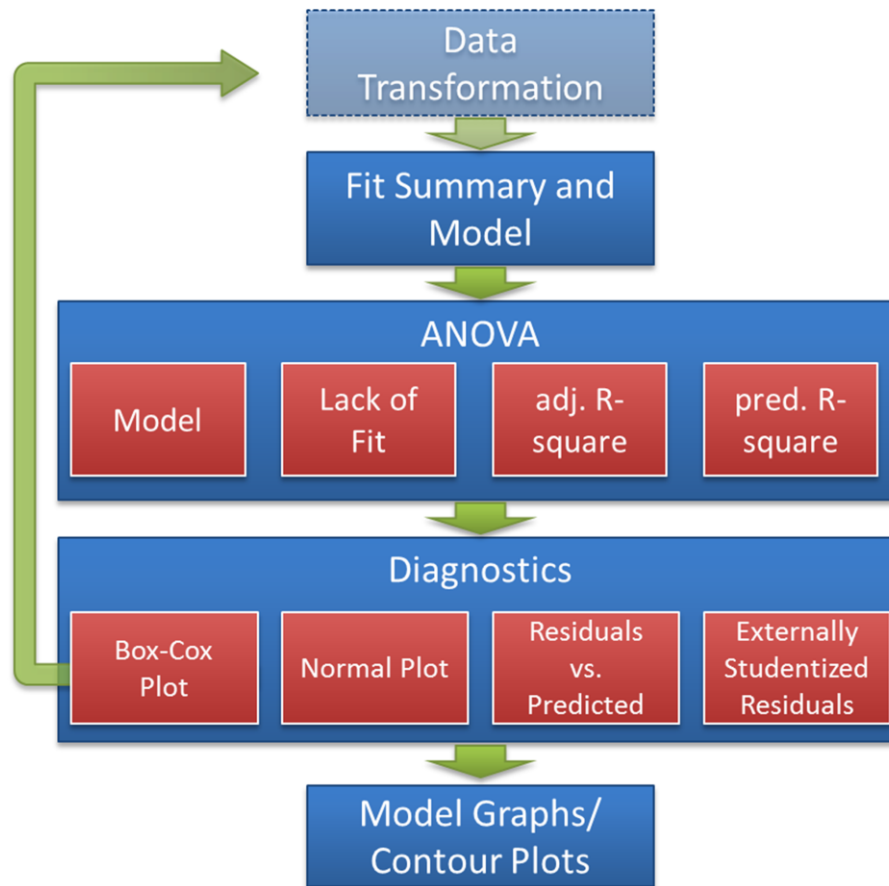


Fig. 21: Scheme of data analysis carried out with Design-Expert 8.0.6 software.

2.4. Methods of “Formulation development of a multiple polymer adhesive patch”²

2.4.1. Mixture design

To find an optimal mixture ratio of silicone adhesive BIO-PSA[®] 7-4302, polyacrylic adhesive DuroTak[®] 387-2287, oleyl alcohol and ibuprofen, the four components were considered to be combined within different constraints shown in Table 3.

Table 3: Constraints of the design space of the mixture components referring to the non-volatile content (NVC).

Components	Low [%]	High [%]
Acrylic Adhesive	20	70
Silicone Adhesive	10	60
Oleyl Alcohol	0	10
Ibuprofen	20	
Total	100	

The exact concentrations of the components were determined by an IV-optimal algorithm with Design-Expert[®] 8.0.6 software (Stat-Ease Inc., Minneapolis, MN). A randomized mixture design of 16 runs with 5 replicates and 5 runs to estimate the Lack of Fit (LOF) was compiled (Fig. 22, Table 4).

² This chapter has been published as shown in Table 10, p. 141.

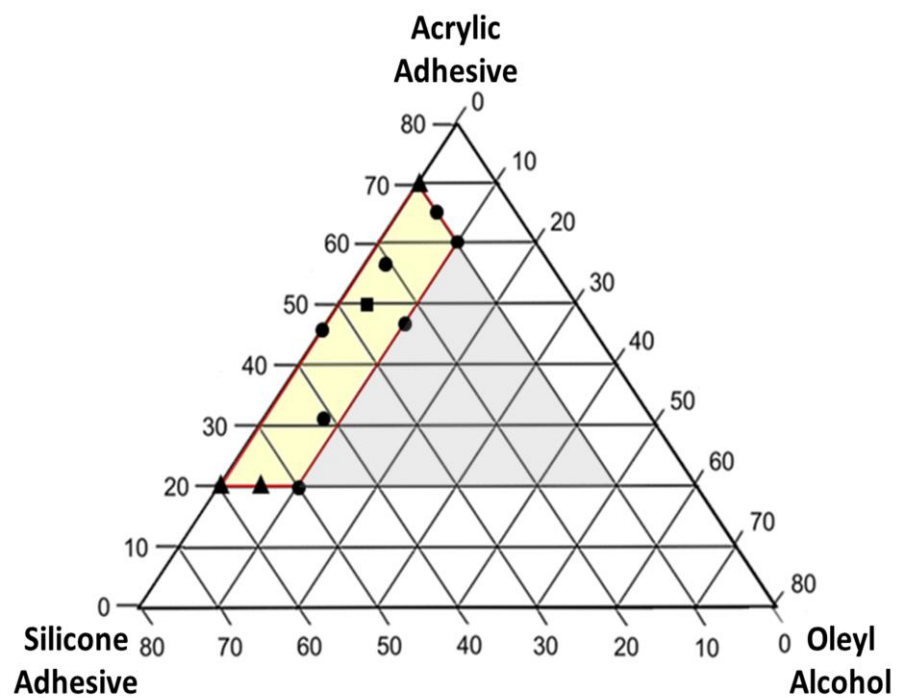


Fig. 22: Triplot of acrylic adhesive, silicone adhesive and oleyl alcohol. Mixture design space (yellow) with 16 runs comprising 7 single (●), 3 duplicate (▲) and 1 triplicate (■) run.

Table 4: The components of the design matrix and additional experiments (Ac = 100 % acrylic PSA, Si = 100 % silicone PSA, AcM = 80 % acrylic PSA + 20 % ibuprofen, SiM = 80 % silicone PSA + 20 % ibuprofen, Opt = Optimization, Val = Validation run).

Run	Components			
	A: Acrylic Adhesive	B: Silicone Adhesive	C: Oleyl Alcohol	D: Ibuprofen
	%	%	%	%
1	65.0	10.0	5.0	20.0
2	20.0	60.0	0.0	20.0
3	70.0	10.0	0.0	20.0
4	20.0	50.0	10.0	20.0
5	20.0	55.0	5.0	20.0
6	31.3	41.3	7.5	20.0
7	45.0	35.0	0.0	20.0
8	60.0	10.0	10.0	20.0
9	20.0	60.0	0.0	20.0
10	50.0	26.7	3.3	20.0
11	56.3	21.3	2.5	20.0
12	70.0	10.0	0.0	20.0
13	46.7	23.7	10.0	20.0
14	50.0	26.7	3.3	20.0
15	20.0	55.0	5.0	20.0
16	50.0	26.7	3.3	20.0
Ac	100.0	0.0	0.0	0.0
Si	0.0	100.0	0.0	0.0
Ac _M	80.0	0.0	0.0	20.0
Si _M	0.0	80.0	0.0	20.0
Opt	30.8	49.2	0.0	20.0
Val	31.0	49.0	0.0	20.0

As responses tack, shear adhesion, crystal growth, extent of creaming, droplet size and droplet distribution range were selected (Fig. 23).

Additionally, four reference samples with and without addition of ibuprofen were prepared for each adhesive.

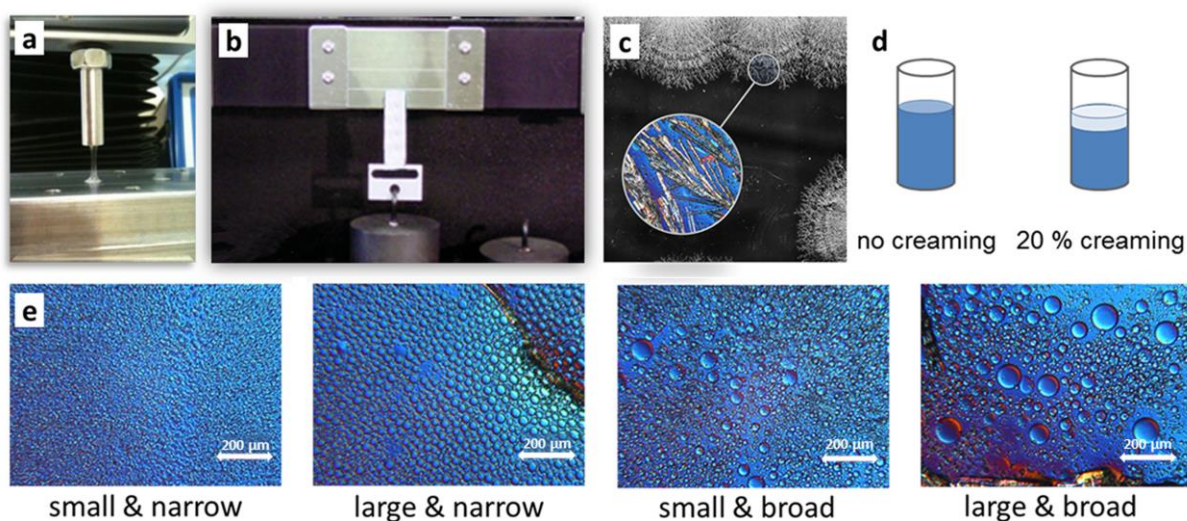


Fig. 23: Responses: a) Probe tack test, b) Shear adhesion, c) Crystallization of ibuprofen, d) Scheme of creaming, e) Examples for different droplet sizes and droplet distribution ranges.

2.4.2. Preparation of the wet mixes

The NVC of DuroTak[®] 387-2287 was determined as described in chapter 2.2.1. To eliminate effects caused by varying amounts of ethyl acetate all components were adjusted to a NVC of 40 %. Wet mixes of 20 g each were prepared in glass vials by addition of the components at concentrations shown in Table 4 referring to the NVC. After 15 min of shaking at 90 rpm in a MM 200 mixer mill (Retsch, Haan, Germany) the samples were stored for 24 h in a conditioned environment to determine the extent of creaming. For preparation of the adhesive matrix the samples required an

additional treatment at 90 rpm for 15 min and further intermediate storage for 60 s to remove air bubbles.

2.4.3. Preparation of the dry adhesive matrices

Dry adhesive matrices with a thickness of about 100 μm were prepared as described in chapter 2.2.3.

2.4.4. Responses

2.4.4.1. Tack

Probe tack experiments were performed as described in chapter 2.2.6.1 (Fig. 23 a).

2.4.4.2. Shear adhesion

For determination of the shear adhesion the test method from chapter 2.2.6.3 was applied with a standard mass of 250 g (Fig. 23b).

2.4.4.3. Crystal growth

An area of 100 cm^2 of the dry adhesive matrix was inspected with regard to crystallization of the API (Fig. 23c). As observed with all investigated samples crystallization proceeded homogeneously from the periphery of the adhesive matrix to the center of the adhesive matrix. Due to this fact, the area covered by crystals in % of the whole area was determined by cutting and weighing of the crystallized area after 24 h.

2.3.4.4. Extent of creaming (phase separation)

For determination of the extent of creaming, the height of the separated phase of the wet mixes compared to the total height in the vials after 24 h was measured using a digital caliper (Fig. 23d). From this measurement the percentage of separated phase to mixed phase was calculated.

2.4.4.5. Droplet size

As all blends of the mixture design exhibited two-phase dispersions the matrices were transferred to a glass slide and investigated by polarization microscopy (Universal R Pol, Zeiss, Jena, Germany) at a 100x magnification 24 h after preparation (Fig. 23e). The mean droplet diameter of 30 droplets was determined.

2.4.4.6. Droplet distribution range

Samples from the determination of the droplet size were also used for the evaluation of the droplet distribution range (Fig. 23e). The droplet distribution range was calculated from the size of the largest and the smallest droplet.

2.4.5. Statistical data analysis

The statistical analysis of the results was performed as described in chapter 2.3.6.

3. Results and discussion

3. Results and discussion

3.1. Results and discussion of “Evaluation of DMA/DMTA for transdermal patch development”³

The aim of the first study was to investigate the suitability of DMA/DMTA to detect changes of the PSA properties by adding ibuprofen as a model drug to provide a better understanding of API/PSA interactions.

3.1.1. Monitoring ibuprofen crystal formation

Immediately after preparation of the adhesive matrices, no ibuprofen crystal formation could be observed at all investigated concentrations. After storage of the matrices for 1 week crystal formation was observed for samples with 16 % ibuprofen content. Because of these results, only samples with 1 %, 2 %, 4 %, and 8 % ibuprofen content were used for further experiments. Re-examinations after 12 months showed similar results.

3.1.2. Dynamic Mechanical Analysis (DMA)/Dynamic Mechanical Thermal Analysis (DMTA)

The viscoelastic behavior of a PSA can provide information on the mechanical properties and therefore the quality of a PSA product such as a transdermal patch. The balance of these properties affects the time- and temperature-dependent responses as well as the adhesion performance of a transdermal patch.

³ This chapter has been published as shown in Table 10, p. 141.

For frequency sweeps, a good correlation of the storage modulus G' and the damping factor $\tan \delta$ with the tack of a PSA was found. The frequency at which G' and $\tan \delta$ are determined depends on the type of tack test. Bonding of a PSA is found at lower frequencies, whereas debonding is related to higher frequencies. At the bonding step, the adhesive has to be more liquid-like, and at the debonding step, it has to be more solid-like and should exhibit a high damping behavior at both. Thus, G' has to be low at low frequencies and high at higher frequencies with a sufficiently high slope. Furthermore, $\tan \delta$ should be high at lower frequencies because of a reduction of G' , indicating flowability. At higher frequencies, it should also be high because of the increase in the loss modulus G'' , indicating the onset of the T_g which is associated with strain-hardening. This results in an increased energy dissipation which prevents breaking of the adhesive bonds (18, 84, 105, 146). Dahlquist suggested that adhesives with G' higher than a limit of 10^5 Pa at the bonding frequency of the tack test have poor adhesive strength (37). Adhesives with G' below an acceptable limit at the debonding frequency exhibit poor cohesive strength and large amounts of adhesive remain on the skin during patch removal (33). A good shear adhesion performance is associated with a high plateau modulus of G' and thus with low $\tan \delta$ values at lower frequencies. This is in contrast to the formerly discussed requirement of a low G' and a high $\tan \delta$ for a good tack. Consequently, adhesives with a low $\tan \delta$ value at low frequencies show high shear adhesion but low tack and vice versa. With placebo patches, low shear adhesion was correlated with good in-vivo adhesion performance (105). In addition to the aspects discussed above, PSAs should have a T_g at least about 40 °C below application temperature (33, 84).

3.1.2.1. Strain sweeps

Evaluation of the recorded data showed no deviation from the linear viscoelastic behavior. Hence, the LVR could be confirmed for the whole investigated range of strain, frequency, temperature, and API concentration.

3.1.2.2. Frequency sweeps

The moduli G^* , G' , G'' , and the damping factor $\tan \delta$ are plotted in dependence of the angular frequency ω for 21 °C (Fig. 24a–d) and 32 °C (Fig. 25a–d). All moduli show frequency dependence in a way that they increase with rising frequency at all ibuprofen concentrations and at both investigated temperatures. Depending on the API concentration, the shape of the $\tan \delta$ curves is characterized by a shift of the minimum from $\omega = 1$ to 5 rad/s at 21 °C and from $\omega = 8$ to 20 rad/s at 32 °C.

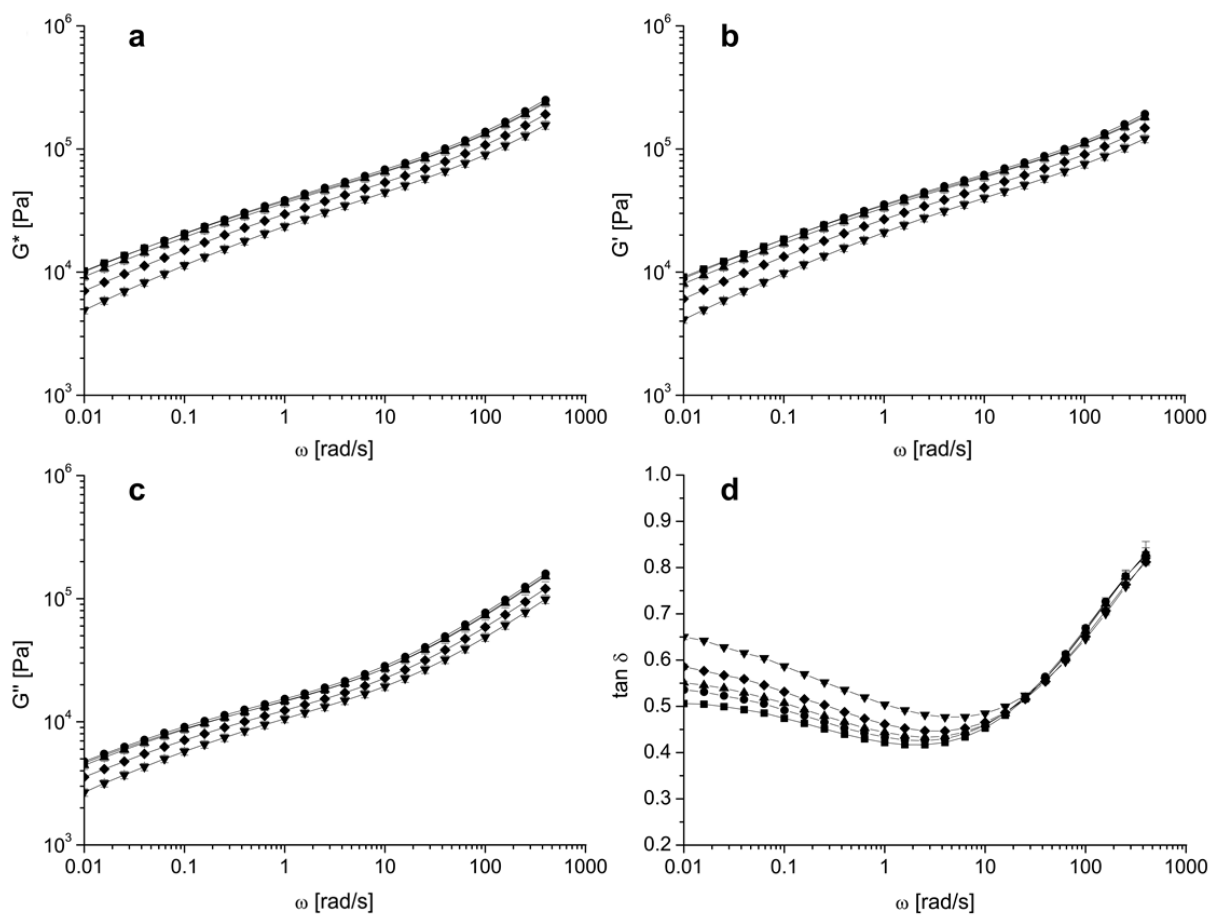


Fig. 24: Oscillation frequency sweep data of plain DuroTak® 87-4287 (—■—) and with ibuprofen concentrations of 1.0 % (—●—), 2.0 % (—▲—), 4.0 % (—◆—) and 8.0 % (—▼—), respectively, at 21 °C. The complex moduli G^* (a), the storage moduli G' (b), the loss moduli G'' (c), and the damping factors $\tan \delta$ (d) are plotted versus the angular frequency ω (means \pm SD; $n = 3$).

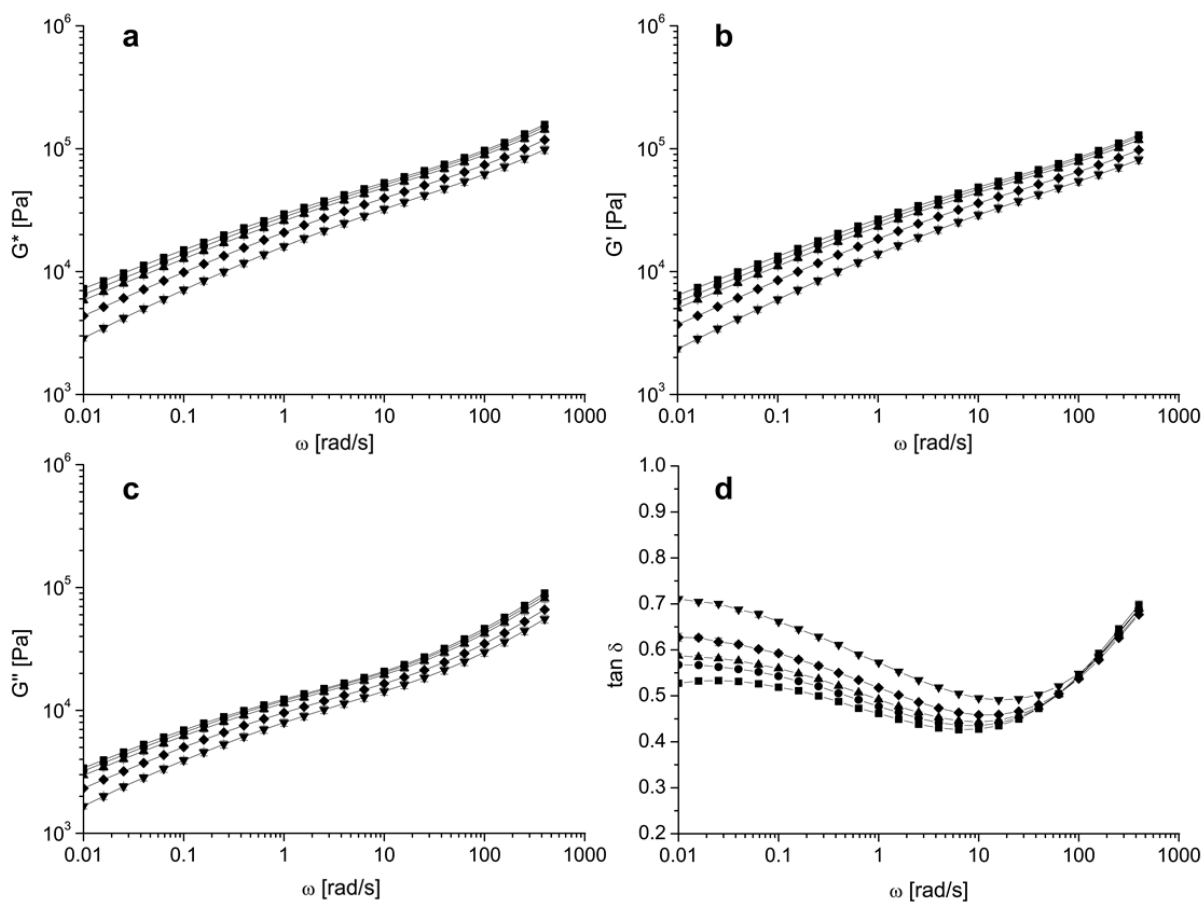


Fig. 25: Oscillation frequency sweep data of plain DuroTak® 87-4287 (—■—) and with ibuprofen concentrations of 1.0 % (—●—), 2.0 % (—▲—), 4.0 % (—◆—) and 8.0 % (—▼—), respectively, at 32 °C. The complex moduli G^* (a), the storage moduli G' (b), the loss moduli G'' (c), and the damping factors $\tan \delta$ (d) are plotted versus the angular frequency ω (means \pm SD; $n = 3$).

To get a deeper insight into the mechanical behavior of the PSA in dependence of the ibuprofen concentration, moduli and $\tan \delta$ values were normalized to API concentrations of 0 % for frequencies of 0.01, 0.1, 1, 10, and 100 rad/s at 21 °C (Fig. 26a–d) and 32 °C (Fig. 27a–d), respectively.

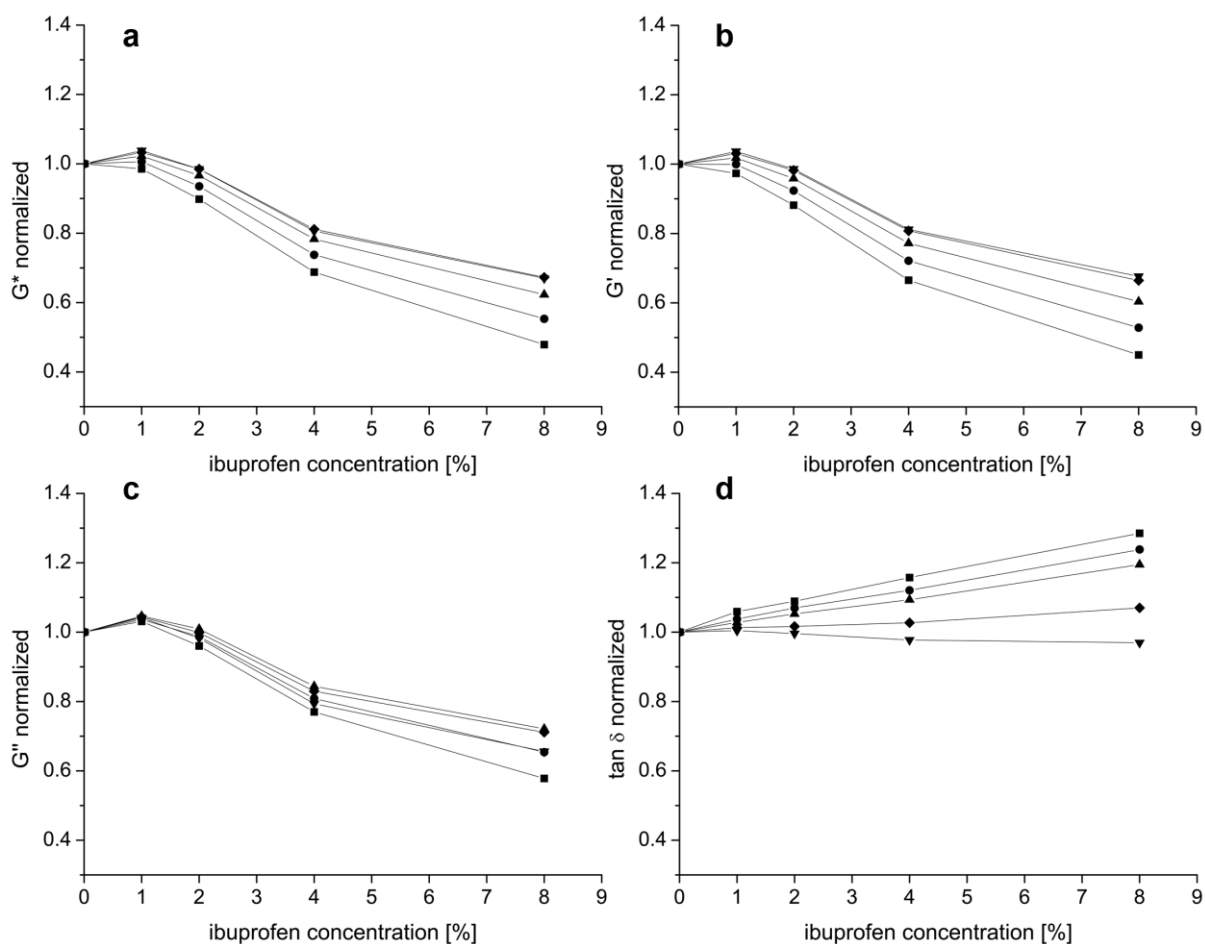


Fig. 26: Normalized plots of the complex moduli G^* (a), storage moduli G' (b), loss moduli G'' (c) and damping factors $\tan \delta$ (d) at 0.01 rad/s (—■—), 0.1 rad/s (—●—), 1 rad/s (—▲—), 10 rad/s (—◆—) and 100 rad/s (—▼—), respectively, versus the ibuprofen concentration at 21 °C (means; $n = 3$).

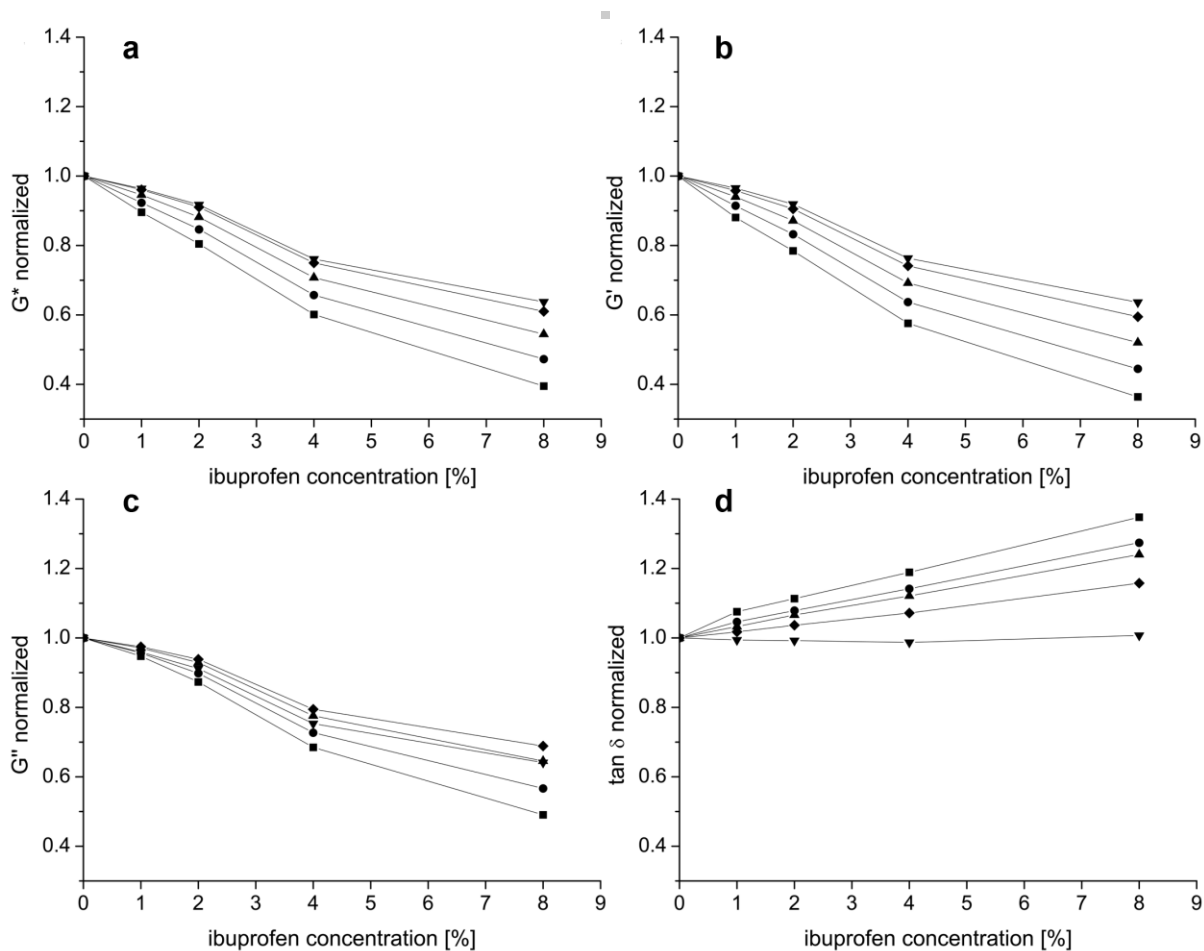


Fig. 27: Normalized plots of the complex moduli G^* (a), storage moduli G' (b), loss moduli G'' (c), and damping factors $\tan \delta$ (d) at 0.01 rad/s (—■—), 0.1 rad/s (—●—), 1 rad/s (—▲—), 10 rad/s (—◆—) and 100 rad/s (—▼—), respectively, versus the ibuprofen concentration at 32 °C (means; $n = 3$).

At 21 °C, an ibuprofen- and frequency-dependent tendency of decreasing G^* , G' and G'' values was observed (Fig. 26a–c). Obviously, the viscoelastic behavior of the PSA changes in dependence of the ibuprofen concentration. At the lowest frequency, the decrease of G^* , G' and G'' is most pronounced. At high frequencies, this decrease is less pronounced with highest values of G^* and G' at an ibuprofen concentration of 1 %. This is also true for G'' , but at all investigated frequencies.

To better understand the behavior of the moduli, the damping factor $\tan \delta$ should be taken into account. The $\tan \delta$ gives insight into the proportion of dissipated to stored energy, i.e. the proportion of viscous to elastic behavior. At lower frequencies, $\tan \delta$ values increased with increasing concentration of ibuprofen (Fig. 26d). The highest slope is apparent at $\omega = 0.01$ rad/s with a decrease at higher frequencies. At $\omega = 100$ rad/s, no change in $\tan \delta$ in dependence of the API concentration is detected.

From these results, it may be summarized that ibuprofen concentrations of up to 1 % cause an increase and higher ibuprofen concentrations a decrease in the mechanical strength of the PSA. An increased damping behavior can be observed at low frequencies.

At 32 °C, a similar ibuprofen- and frequency-dependent tendency of a more pronounced decrease of G^* , G' , and G'' values at lower frequencies and a less pronounced decrease at higher frequencies was observed (Fig. 27a–c). Interestingly, in contrast to the data derived at 21 °C, no maximum for the moduli is observed. The damping behavior showed the same tendency of an increase of $\tan \delta$ with increased drug concentration for lower frequencies and no change in $\tan \delta$ for higher frequencies (Fig. 27d). These results show that ibuprofen causes a decrease in the mechanical strength of the PSA at every investigated concentration. At lower frequencies, plastic deformation becomes more apparent indicated by an increased $\tan \delta$.

The softening of a PSA by a small molecule can be described as the effect of plasticizing. In the literature a plasticizer is defined as a low molecular weight compound that is added to polymers to improve their flexibility, to lower their T_g , to decrease their tensile strength, stiffness, and toughness, and to increase their elongation and ductility (35, 152–155, 178). The addition of low molecular weight compounds reduces the entanglements of the PSA and decreases the storage modulus G' (26,

178). Furthermore, the modulus is decreased with increasing amount of plasticizer at all frequencies (84). Plasticization can not only be caused by traditional plasticizers such as liquid paraffin (90, 178), triacetin (91, 92) and triethyl citrate (TEC) (94) but also by APIs such as ibuprofen (72), ketoprofen (152), nitroglycerin (21), nicotine (21), or chlorpheniramine maleate (155, 158). Based on the results obtained at 21 °C, it is concluded that concentrations of above 2 % ibuprofen have a plasticizing effect on DuroTak® 87-4287. In contrast, at 32 °C, ibuprofen has a plasticizing effect at every investigated concentration.

The effect of increased moduli at 1 % ibuprofen concentration at 21 °C could be explained by the phenomenon of antiplasticization. By incorporation of certain types of additives in polymers, the storage modulus and tensile strength of the films are increased, and the elongation is decreased. This effect is called antiplasticization, because except for the change in T_g , the opposite results are obtained with plasticization such as decreased storage modulus and tensile strength and increased elongation (35, 153). The anomaly of an increase in moduli and simultaneously reduction of the T_g is associated with an increase in γ -relaxation temperature (179).

Antiplasticization depends on physical and physicochemical interactions between the API and the polymer. On the one hand, time, temperature, stress, strain, and mechanical history affect the antiplasticization effect (180, 181). On the other hand, molecular weight, polarity, and concentration of the additive also have a significant influence (35, 160).

However, Anderson et al. (160) found that antiplasticization is based on the interaction of the polymer chain ends with the additive. It is not clear whether this mechanism can also be postulated for ibuprofen and DuroTak® 87-4287. Also, an interaction via hydrogen bonds with the alcohol side chains of the polymer is possible.

Known antiplasticizer polymer interactions were first observed by Jackson and Caldwell (153) and further studied by Anderson et al. (160) with traditional plasticizer polymer combinations. These interactions could also be observed for APIs as non-traditional plasticizers. Lee et al. (161) investigated phenacetin acetanilide and polyethylene terephthalate (PET), and Lin et al. (162) studied the influence of piroxicam on Eudragit® E. Based on the obtained results at 21 °C, it is concluded that a concentration of 1 % ibuprofen has an antiplasticizing effect on DuroTak® 87-4287. At 32 °C, no antiplasticizing effect by ibuprofen is apparent.

3.1.2.3. Temperature sweeps

In Fig. 28a–d, G^* , G' , G'' , and $\tan \delta$ are plotted in dependence of the temperature. The maximum of the $\tan \delta$ peak was used for determination of the T_g (DMTA) (Fig. 29). All moduli and T_g values were decreased by addition of ibuprofen at all concentrations.

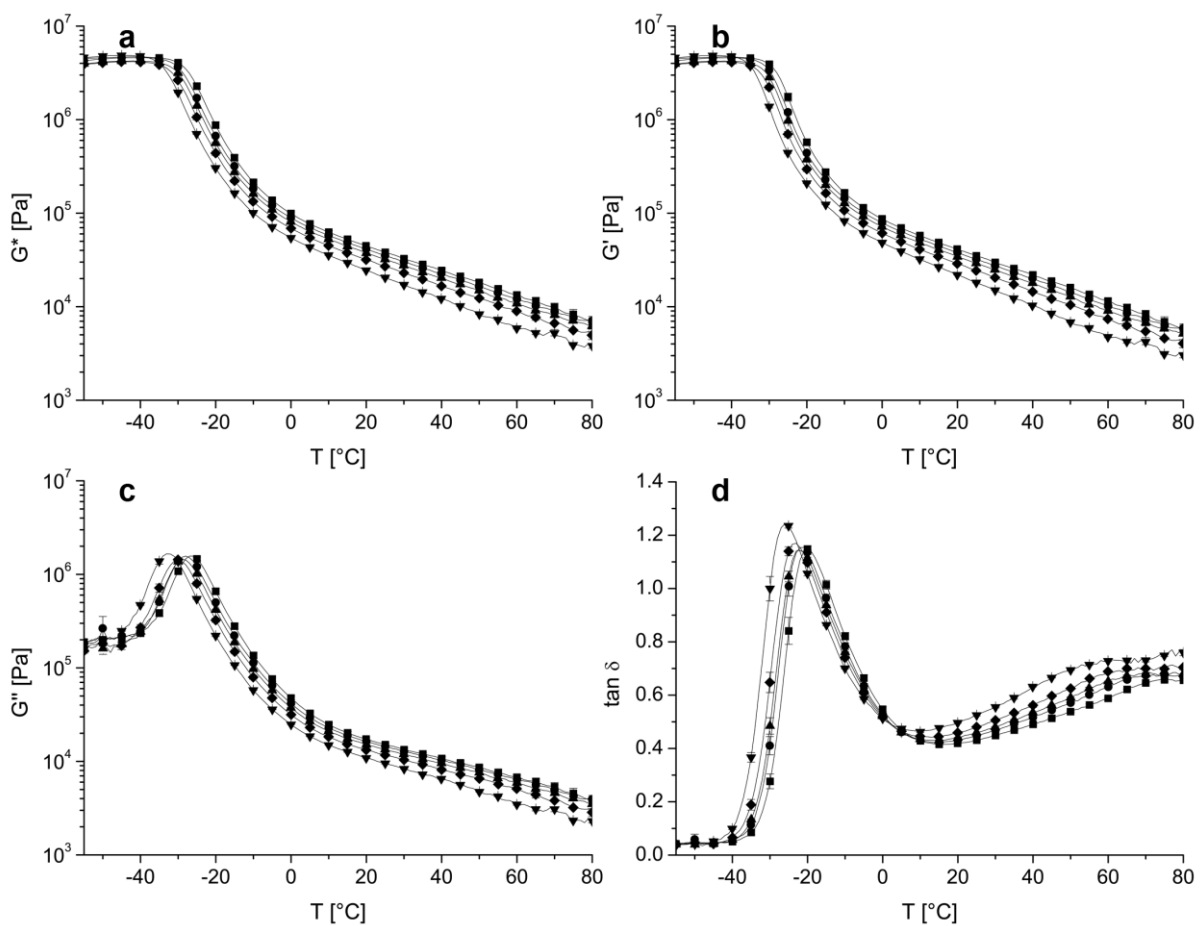


Fig. 28: Temperature sweep data of plain DuroTak® 87-4287 (—■—) and with ibuprofen concentrations of 1.0 % (—●—), 2.0 % (—▲—), 4.0 % (—◆—) and 8.0 % (—▼—), respectively, at 1 rad/s. Complex moduli G^* (a), storage moduli G' (b), loss moduli G'' (c), and damping factors $\tan \delta$ (d) plotted versus the temperature T (means \pm SD; $n = 3$).

The addition of low molecular weight compounds such as plasticizers reduces the entanglements of the polymer and lowers the plateau modulus of G' and the glass transition temperature of the systems (26, 178, 182).

At 21 °C, an increase of G^* , G' , and G'' at 1 % drug concentration by antiplasticization as observed with frequency sweeps at 21 °C could not be confirmed.

This may be explained by the fact that a strain of only 1 % was applied in the temperature sweep experiments in contrast to a 5 % strain used in the frequency sweep experiments. Furthermore, the PSA provides a mechanical deformation history due to the permanent deformation during measurement. This supports the hypothesis of Mascia and Margetts (183) and Soong et al. (181) that the antiplasticizing effect is a reversible physical crosslinking effect that depends on strain and mechanical history.

3.1.3. Differential Scanning Calorimetry (DSC)

The data obtained by DSC measurements (Fig. 29) demonstrate that the glass transition temperatures of blends of DuroTak® 87-4287 and ibuprofen decrease with the increasing percentage ibuprofen added to the formulations. Plasticization is a function of the T_g which depends on the ibuprofen concentration in DuroTak® 87-4287.

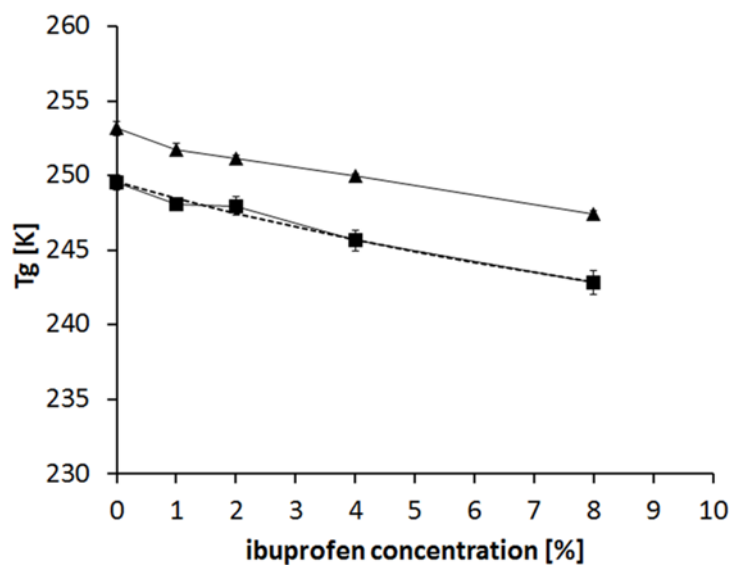


Fig. 29: Glass transition temperature of DuroTak® 87-4287 and ibuprofen at concentrations of 0 %, 1 %, 2 %, 4 %, and 8 %, respectively, measured with DSC (—■—) and DMTA (—▲—). Gordon-Taylor fit is displayed with $K = 5.2$ (---).

This effect has also been observed with excipients as well as APIs as plasticizers for polymers used as adhesives in transdermal patches (94, 155, 184–187).

A decrease of the T_g can be described by the Gordon-Taylor equation. In Fig. 29, the results of a theoretical mixture are given for a T_g of ibuprofen of -45.2 and the pure polymer of -23.6 °C.

The difference between the T_g values determined by DTMA and DSC is caused by the different methodologies to experimentally determine this parameter (35). With DTMA, the T_g is measured as a change in deformation behavior which is frequency-dependent. In contrast the determination of the T_g by DSC is based on a change in heat capacity. The exact relationship between these differently determined T_g values is still under investigation (151).

For the present study, the relation could be determined as follows:

$$T_g(\text{DSC})[\text{K}] = 0.96 \cdot T_g(\text{DMTA})[\text{K}] \quad \text{Eq. 2}$$

The single glass transition temperatures of the blends and the absence of the melting peak of ibuprofen at 77 °C support the results from microscopic investigations that ibuprofen is dissolved in the matrix at every investigated concentration.

3.1.4. Adhesion performance

To characterize the adhesion performance of the PSA formulations, tack and shear adhesion as the characteristic antipodal parameters for viscous and solid-like behavior were determined. In Fig. 30, an overview of the results of the probe tack test (a), rolling ball tack test (b) and shear adhesion (c) of the PSA formulations in dependence of the ibuprofen concentration is given. Adhesion data normalized to the drug-free PSA at 21 °C together with the theoretical curve profile according to Eq. 3 are displayed in Fig. 31.

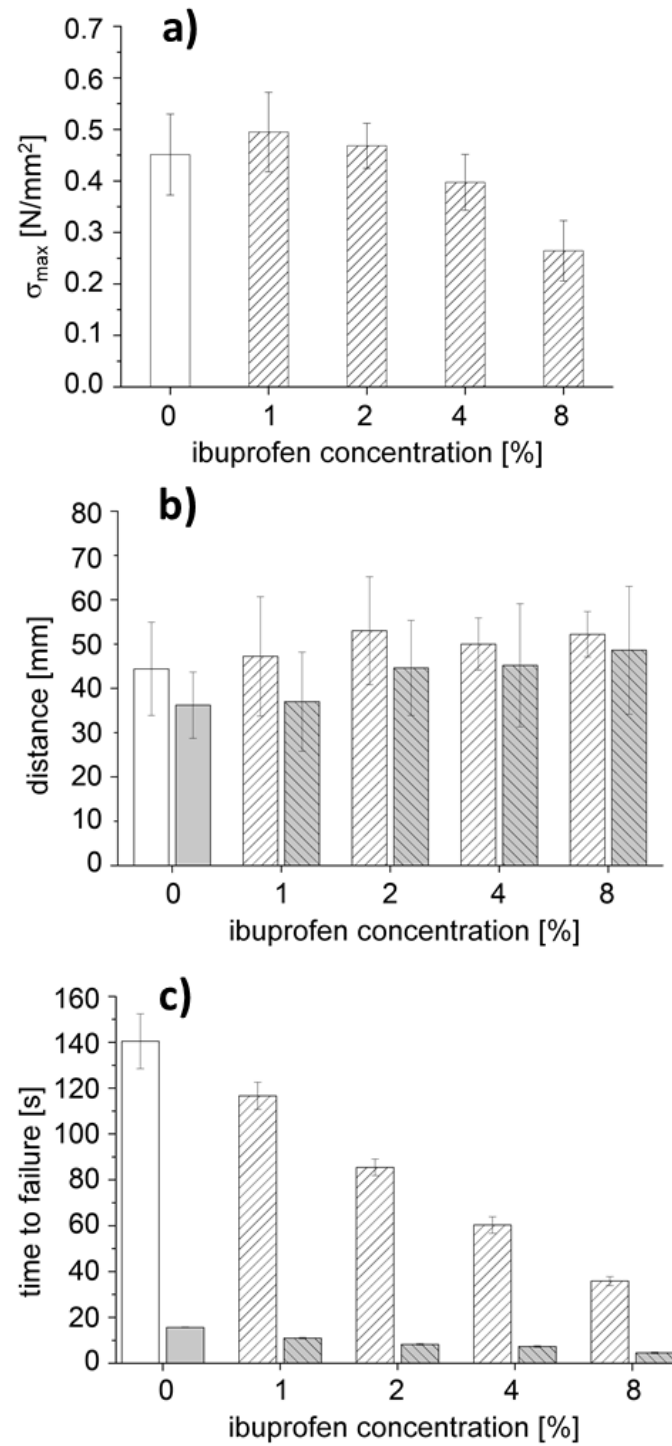


Fig. 30: Probe tack test (a), rolling ball tack test (b), shear adhesion (c) of DuroTak[®] 87-4287 at 21 °C and 32 °C (means \pm SD;

$n = 5$ for probe tack test and rolling ball tack test, $n = 3$ for shear adhesion).

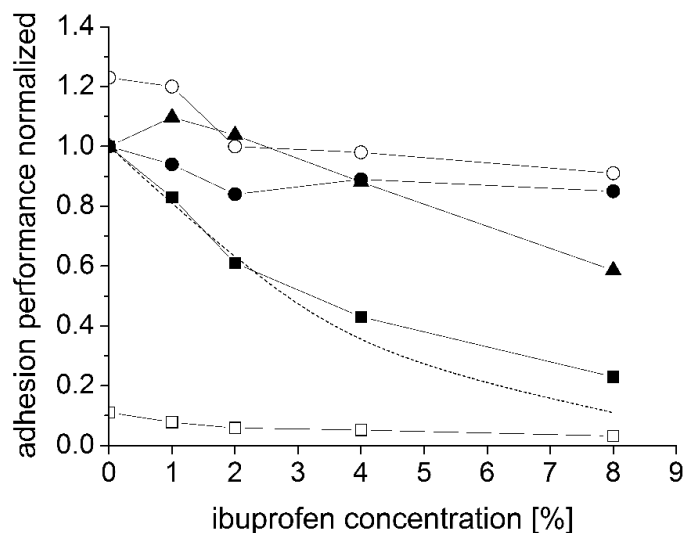


Fig. 31: Adhesion data normalized to the drug-free PSA at 21 °C of the probe tack test (—▲—), the rolling ball tack test (—●—) (—○—), the shear adhesion (—■—) (—□—) of DuroTak® 87-4287 in dependence of the drug concentration; closed symbols: 21 °C, open symbols: 32 °C (means; $n = 5$ for probe tack test and rolling ball tack test, $n = 3$ for shear adhesion). The dotted curve represents the theoretical profile according to Eq. 3.

3.1.4.1. Probe tack

Tack was determined as the maximum of the initial peak (σ_{max}) from stress strain curves (Figs. 30a and 31). The σ_{max} values were highest at 1 % ibuprofen concentration. With increasing drug concentration in the formulations, a decrease of the σ_{max} values was observed. Based on these results and those obtained by the frequency sweeps, it is assumed that ibuprofen at a concentration of 1 % interacts with the polymer by an improved resistance to debonding.

As discussed earlier, bonding can be correlated to lower frequencies and debonding to higher frequencies. For the probe tack test, bonding occurs within a dwell time of 1 s which corresponds to an angular frequency of 6.28 rad/s. Debonding takes place at a detachment speed of 5 mm/s and a

matrix thickness of 55 μm which correlates with an angular frequency higher than 100 rad/s. At the debonding step, tack is mainly dependent on cohesion and therefore on the elastic modulus.

As determined by frequency sweeps, G' is unaffected by antiplasticization at bonding frequencies, while it is increased at debonding frequencies (Fig. 26b). As a result, bonding is unaffected by ibuprofen, whereas debonding is increased. This indicates that tack is increased at a concentration of 1 % ibuprofen because of an increased resistance to debonding by antiplasticization.

At higher concentrations, ibuprofen has a plasticizing effect on the polymer, and all moduli are decreased. Thus, both bonding and debonding are affected. Bonding is increased by an improved wetting behavior, while debonding is decreased because G' is below a critical value at the debonding frequency, so that the PSA does not provide sufficient cohesion. Tack appears to be more influenced by a reduced cohesion than by an improved wetting behavior. Thus, a decrease in tack was observed at higher ibuprofen concentrations.

The phenomenon of an initial increase compared to the plain PSA and a final decrease in the tack by increasing concentrations of an API or excipient in PSAs has already been described before (91, 152, 186, 188). However, this observation has not yet been explained by the viscoelastic mechanism of plasticizing and antiplasticizing.

3.1.4.2. Rolling ball tack

The distance traveled by the ball is inversely proportional to the tackiness of the adhesive. A higher ball distance means lower tackiness. In Fig. 30b, it is shown that the distance traveled by the rolling ball increases with increasing ibuprofen concentration at 21 °C and 32 °C, respectively. Apparently, tack is increased at elevated temperature and decreased at higher ibuprofen concentrations (Fig. 31).

In contrast to the probe tack experiment, the anomaly of an increased tack at low drug concentrations could not be observed. On the one hand, the strain rate dependency for antiplasticization may be responsible for this observation. The strain rate i.e. the frequency of the rolling ball tack test is believed to be higher than that of the probe tack test. On the other hand, it should be noted that the data showed unsatisfactory reproducibility. To reduce the high standard deviation, larger steel balls were used to maximize the traveling distance. However, even with these steel balls, the standard deviation could not be noticeably reduced. It becomes clear that there is a trade-off between the simplicity of the experimental setup and the challenge in interpreting the data.

3.1.4.3. Shear adhesion

It was found that the shear adhesion significantly decreased with increasing concentrations of ibuprofen (Fig. 30c). At 21 °C, the time to failure is decreased from 140 s (drug-free PSA) to 30 s at a concentration of 8 % ibuprofen. A temperature increase in the drug-free PSA to skin temperature of 32 °C results in a decrease in the time to failure from 140 s to 15 s. If under these conditions, the drug concentration is increased up to 8 %, a final decrease in the time failure to 5 s is registered. These results are consistent with the data published by Minghetti et al., which revealed that the addition of miconazole nitrate to a methacrylic-based PSA significantly decreased shear adhesion values (189). Cilurzo et al. observed that potassium diclofenac and nicotine cause a reduction in the shear adhesion of a polyacrylate matrix to 9 % of the shear adhesion of the drug-free matrix (91).

The shear adhesion is controlled by zero shear viscosity η_0 which is related to molecular weight M_w , molecular weight between entanglements M_e , temperature T , glass transition temperature T_g , and the fitting parameters A and B by the following equation (37):

$$\log \eta_0 = 3.4 \log M_w - 2.4 \log M_e + \frac{A}{(T-T_g+70)} + B \quad \text{Eq. 3}$$

From Fig. 31, it is obvious that a good approximation results if a constant M_w and M_e changes in the order of $1/G'$ at $\omega = 1$ rad/s and T_g values from DTMA measurements are chosen.

The approach to choose $1/G'$ for M_e is based on the reciprocal relationship between the storage modulus and the M_e of a polymer (37). The frequency of 1 rad/s was chosen because it is in the same order of magnitude as the corresponding angular frequency ω derived by the deformation s/d and time to failure t via:

$$\dot{\gamma} = \frac{s}{d \cdot t} \hat{=} \omega \quad \text{Eq. 4}$$

Applied to our experimental conditions, the following angular frequency of 1.7 rad/s was calculated.

$$\dot{\gamma} = \frac{12 \text{ mm}}{0.05 \text{ mm} \cdot 140 \text{ s}} = 1.7 \text{ s}^{-1} \hat{=} 1.7 \text{ rad/s} \quad \text{Eq. 5}$$

At higher drug concentrations, the theoretical curve deviates from the measured data, because the frequency of 1.7 rad/s corresponds to the time to failure of the drug-free PSA. At higher drug concentrations, the time to failure decreases, and thus, the shear rate and corresponding frequency increases. At higher frequencies, a higher G' was observed and η_0 , or more precisely, the shear adhesion is expected to be higher than calculated.

From these results, it may be concluded that the shear adhesion of DuroTak® 87-4287 is decreased by addition of ibuprofen. Shear adhesion is mostly influenced by the temperature, while antiplasticization has only a marginal effect.

3.1.5. Suggested model of plasticization and antiplasticization

To illustrate the antiplasticizing effect, the model from Anderson et al. (160) was adopted and modified according to the results presented in this study (Fig. 32). If ibuprofen is added to DuroTak® 87-4287, the ibuprofen molecules are first attached to the polymer via hydrogen bonds.

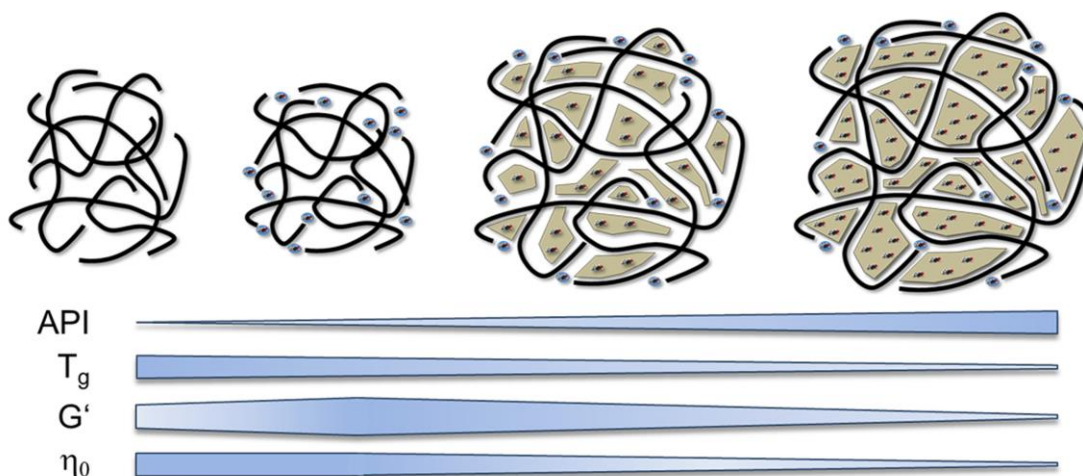


Fig. 32: Scheme of antiplasticizing and plasticizing effects of ibuprofen on the polymer structure of DuroTak® 87-4287 and change in the T_g , G' and η_0 in dependence on the API concentration.

This results in a more pronounced mechanical strength of the PSA within a certain frequency range. With tack tests performed at strain rates which correspond to this frequency range, higher tack values are obtained. The results from shear adhesion are less influenced by antiplasticization than by the T_g of the PSA. However, a certain influence of antiplasticization on the shear adhesion could be demonstrated. Temperature and strain below or above a certain threshold and mechanical history can cause a reduction in antiplasticization as observed by frequency sweeps at 32 °C and temperature sweeps (Fig. 25 and Fig. 28).

If larger quantities of ibuprofen are added, ibuprofen will accumulate in the free volume domains, and the average domain size increases. Moduli and therefore mechanical strength are reduced by the effect of plasticizing. In terms of adhesion properties, tack adhesion and shear adhesion decrease.

It is suggested that API/polymer blends may possess an antiplasticizing space which is characterized by time, temperature, stress, strain, molecular weight, and polarity of both compounds and additive concentration.

3.1.6. Conclusion

If a substance is added to a PSA, an unpredictable alteration of the mechanical properties can occur. Rheometry is a powerful tool to make predictions concerning the adhesion performance and the influence of the API or other additives on the viscoelastic behavior of the PSA. It was demonstrated that ibuprofen may act as plasticizer or antiplasticizer on DuroTak® 87-4287 (see Fig. 32). The plasticizing/antiplasticizing effect depends on the API concentration, temperature, strain, strain rate, and mechanical history. Thus, it is necessary to adjust the factors of the tests such that the condition for the intended application is simulated. It could be shown that the elastic modulus G' correlates well with the results obtained by probe tack measurements. Tack and G' were affected by plasticization and antiplasticization in dependence of ibuprofen concentration. Shear adhesion is mainly influenced by the T_g and the temperature. Antiplasticization contributes only marginally to the results of shear adhesion because of the low strain rate of the test.

In consequence, an alteration of the concentration of an API in a polymer by diffusion out of the polymer or migration into the polymer can lead to a change in the mechanical behavior due to plasticizing or antiplasticizing. Because the antiplasticizing space of an API/polymer blend can

certainly influence processing, stability and in vivo behavior a formulation containing the blend and therefore needs to be further investigated with regards to known API/polymer combinations.

3.2. Results and discussions of “Systematic investigation of the probe tack test”

In the second study, DuroTak® 387-2287, a solvent-based crosslinked acrylic PSA is investigated with the probe tack test by a DoE approach to evaluate all significant factors and possible interactions that may influence the test result.

3.2.1. DMA Measurements

The results of the frequency sweeps are displayed in Fig. 33. With increasing ibuprofen content, the modulus G^* decreases at all investigated frequencies whereas $\tan \delta$ values increase at lower frequencies. The onset of glass transition is shifted to higher frequencies with increasing ibuprofen content accompanied by a decrease of the $\tan \delta$ values at higher frequencies.

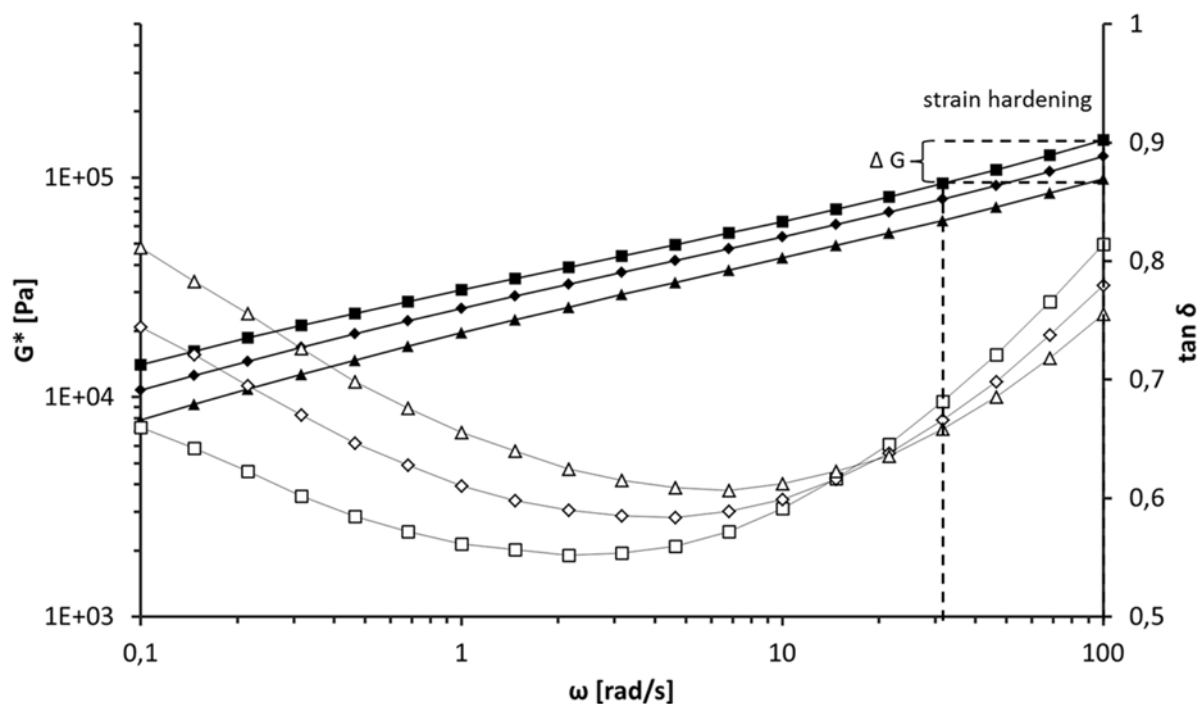


Fig. 33: Oscillation frequency sweep data of DuroTak® 387-2287. The complex moduli G^* with drug concentrations of 0 % (—■—), 6 % (—◆—) and 12 % (—▲—) and the damping factors $\tan \delta$ with drug concentrations of 0 % (—□—), 6 % (—◇—) and 12 % (—△—) are plotted versus the angular frequency ω .

3.2.2. ANOVA of the results of the probe tack test

The results of the probe tack test are displayed in Table 5. After backward reduction a highly significant reduced quadratic model with the highest polynomial order was developed from the results.

Table 5: Results of the probe tack test experiments (means, n = 5).

Standard	Run	Response σ_{\max} N/mm ²
8	1	8.33
3	2	8.88
5	3	8.17
26	4	5.53
6	5	4.33
24	6	6.76
12	7	9.53
18	8	7.71
17	9	8.14
23	10	3.64
30	11	8.24
14	12	5.80
34	13	6.76
31	14	3.08
19	15	5.32
15	16	8.08
7	17	8.51
33	18	6.50
16	19	7.36
11	20	8.95
28	21	10.71
13	22	6.32
9	23	8.24
25	24	5.92
20	25	6.42
4	26	8.24
1	27	5.90
29	28	10.49
22	29	10.98
10	30	9.17
27	31	8.50
32	32	6.34
2	33	10.99
21	34	11.03
36	35	9.55
35	36	7.38
37	37	8.02
38	38	7.47

The factors detachment speed (A), dwell time (B), contact force (C), adhesive matrix thickness (D), API content (E), and the interactions between the factors B and D (dwell time & adhesive matrix thickness), C and D (contact force & adhesive matrix thickness) as well as D and E (adhesive matrix thickness & API content) have a significant effect on σ_{max} (Table 6).

The adjusted R^2 of 0.9511 was in good agreement with the predicted R^2 of 0.9245. The variation of the data around the fitted model, known as the Lack of Fit (LOF), was found to be non-significant with $p = 0.6706$. A good signal-to-noise ratio was confirmed by an “Adequate Precision” of 35 (Table 6).

Table 6: Analysis of variance (ANOVA) of the reduced quadratic model.

Source	Sum of squares	df	Mean square	F-value	p-value		Adj. R ²	Pred. R ²	Adeq. Prec.
Model	137.73	9	15.30	81.0	< 0.0001	significant	0.9511	0.9245	35
Detachment speed (A)	29.37	1	29.40	155.4	< 0.0001	significant			
Dwell time (B)	16.25	1	16.40	86.0	< 0.0001	significant			
Contact force (C)	58.42	1	58.40	309.0	< 0.0001	significant			
Adhesive matrix thickness (D)	6.03	1	6.03	31.9	< 0.0001	significant			
API content (E)	7.94	1	7.94	42.0	< 0.0001	significant			
Interaction B-D	2.76	1	2.76	14.6	0.0007	significant			
Interaction C-D	1.09	1	1.09	5.8	0.0231	significant			
Interaction D-E	1.82	1	1.82	9.6	0.0044	significant			
Adhesive matrix thickness (D)²	3.29	1	3.29	17.4	0.0003	significant			
Residual	5.29	28	0.19						
Lack of Fit	3.54	20	0.18	0.8	0.6706	non-significant			
Pure Error	1.75	8	0.22						
Corrected Total	143.02	37							

3.2.3. Evaluation of the main effect plots

The main effect plots of the factors detachment speed (A), dwell time (B), contact force (C), adhesive matrix thickness (D) and API content (E) are displayed in Fig. 34.

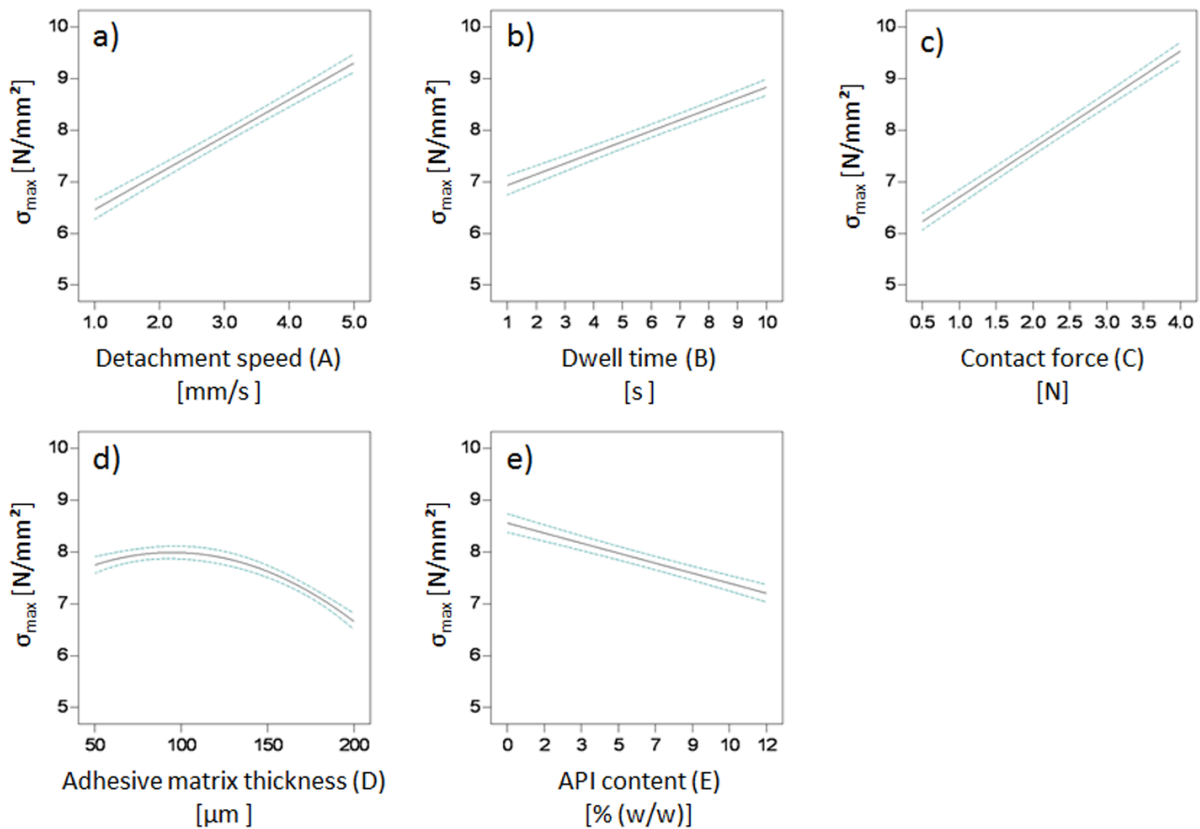


Fig. 34: Main effect plots of (a) Detachment speed (A), (b) Dwell time (B), (c) Contact force (C), (d) Adhesive matrix thickness (D), and (e) API content (E), generated with Design-Expert 8.0.6 software.

3.2.3.1. Factor A: Detachment Speed

It is obvious from Fig. 34a that the detachment speed has a significant effect on σ_{max} . It could be confirmed that an increase of detachment speed results in an increase of tack. This observation supports the results of studies performed by Satas (84). It is known that tack depends on the bonding

and debonding process between the probe and the adhesive and thus on the storage modulus G' (37). The larger G' the higher the tack, provided that the Dahlquist criterion of $G' < 10^5$ Pa is met (107). However, moduli of PSAs are not intrinsic material characteristics. They depend on the experimental parameters used, such as strain rate represented by the detachment speed (37). The detachment speed v is proportional to the strain rate $\dot{\gamma}$ which can be transformed into the respective frequency ω :

$$\frac{v}{h} = \dot{\gamma} \hat{=} \omega \quad \text{Eq. 6}$$

With the results of the rheological experiments it could be confirmed that the PSA undergoes a so called strain hardening (positive ΔG) at the debonding step with increasing detachment speed (Fig. 33).

3.2.3.2. Factor B: Dwell time

The dwell time has a positive effect on the response σ_{max} as shown in Fig. 34b. As found by Sherriff et al. (85), tack is also a function of wetting. Good wetting requires a sufficient fluidity of the adhesive on the one hand, and enough time to spread on the contact area on the other hand (37). Therefore, Dahlquist connected tack to the creep compliance $J(t)$ which is a function of time (190).

An alternative approach to explain the effect of the dwell time involves the apparent modulus E_a . Assuming, that the initial contact area between the adhesive and the probe at zero force is negligible, the contact area A_c is a function of the apparent modulus E_a , the contact force F_c and the fitting parameter β according to Tordjeman et al. (135) as follows:

$$A_c \approx \beta \frac{F_c}{E_a} \quad \text{Eq. 7}$$

The value of the fitting parameter β depends on the applied force and the apparent modulus. E_a represents the counteraction between the thickness h and the roughness $\langle a \rangle$ of the adhesive:

$$E_a = E \left(1 + \frac{\langle a \rangle^2}{2h^2} \right) \quad \text{Eq. 8}$$

According to Mezger (191), the tensile modulus E is directly proportional to the shear modulus G . As observed in Fig. 33, G measured as G^* in oscillatory shear decreases with decreasing frequencies (i.e. increasing dwell time). From these facts it may be concluded that, if the dwell time is prolonged, E_a decreases and the resulting contact area A_c increases.

The further explanation for the positive effect of the dwell time on σ_{max} is given by Creton et al. (107): A longer dwell time may increase the degree of relaxation of the adhesive at the start of the debonding phase. An adhesive with a relaxed polymer structure will show a higher tack than a non-relaxed adhesive.

In summary, it can be postulated that all three effects, namely creep compliance, apparent modulus and degree of relaxation contribute to an increase of tack with prolonged dwell time. These results confirm earlier studies also performed within the time frame of 1 to 10 s by Zosel (134), Satas (190) and Duncan et al. (109).

3.2.3.3. Factor C: Contact force

The applied contact force has a significant effect on the tack: With increasing contact force, σ_{max} increases (Fig. 34c). At high contact forces spreading and wetting are more pronounced resulting from the relationship between the contact area A_c and the contact force F_c (Eq. 7). These results confirm the observations by Satas (190) and Duncan (109).

3.2.3.4. Factor D: Adhesive matrix thickness

The obtained data of the probe tack test demonstrate that σ_{max} is related to the square of the adhesive matrix thickness, with lowest values at 200 μm and a maximum at around 100 μm (Fig. 34d).

There are four relevant parameters affected by the adhesive matrix thickness which influence the response σ_{max} : Strain rate, contact area, solvent residuals, and oriented polymer fraction.

With increasing film thickness h a decrease of the strain rate $\dot{\gamma}$ at the debonding stage will result according to Eq. 6. As already discussed in chapter 3.2.3.1, σ_{max} depends on strain rate and an increasing film thickness will cause a negative effect on the tack. This effect is most pronounced with thin films as the strain rate decreases non-linearly with increasing adhesive matrix thickness (Eq. 6, Fig. 35).

With increasing adhesive matrix thickness, an increase of the contact area A_c by a decrease of the apparent modulus E_a will occur according Eqs. 7 and 8. For viscoelastic polymers, it has additionally to be considered that the modulus E will decrease with decreasing strain rate $\dot{\gamma}$ according to the decrease of G^* in Fig. 33 and chapter 3.2.3.1. A higher contact area A_c will result in a higher σ_{max} (Fig. 35). This effect is more pronounced with thin films as the contact area A_c decreases non-linearly with decreasing adhesive matrix thickness h according to Eqs. 7 and 8.

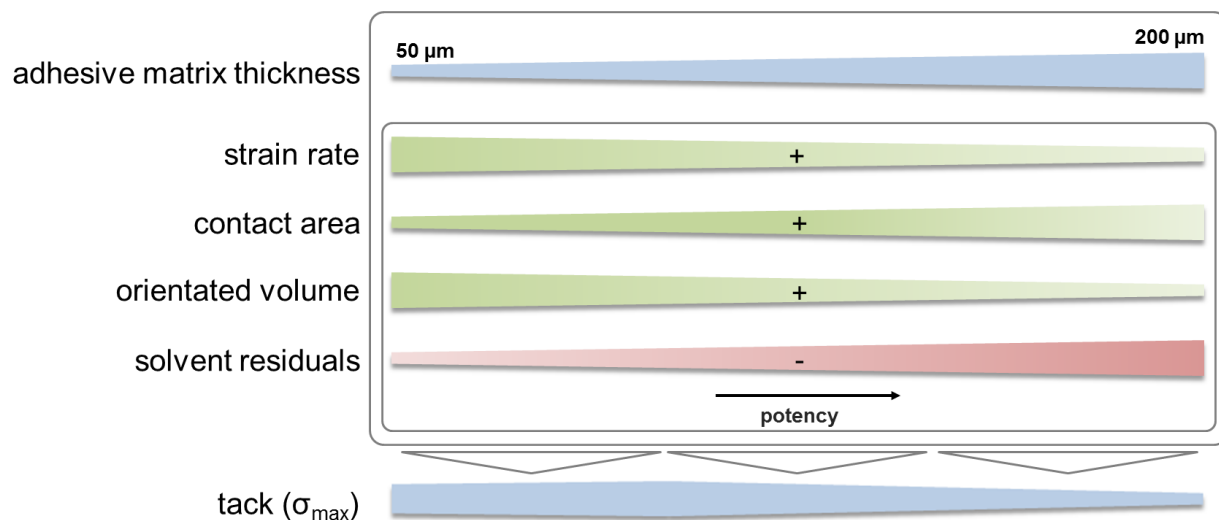


Fig. 35: Dependence of the tack σ_{max} on several relevant parameters which are affected by the adhesive matrix thickness. Parameters marked with (+) have an increasing effect on tack with increasing potency; parameters marked with (-) have a decreasing effect on tack with increasing potency.

The quality of the adhesive matrix is influenced by solvent residuals (37). It is known that the content of residual solvent is directly proportional to the adhesive matrix thickness. Thus, tack will decrease with increasing adhesive matrix thickness (Fig. 35). This effect is most pronounced with thick films as the drying rate is inversely proportional to the adhesive matrix thickness (37).

The ratio between polymer chains located at the interfaces, and those located in the bulk strongly decreases with increasing adhesive matrix thickness. It is well known, that surface effects such as orientation and organization of polymer chains may occur at polymer interfaces (138–142, 144, 192, 193). Schultz et al. (140) discovered that polymer chains with lewis base functionalities can interact with metal surfaces. These oriented structures exhibit glassy-like behavior with increased moduli (e.g. G , E) and thus, increased mechanical strength. The formal chemical name of DuroTak[®] 387-2287 is poly (2-ethylhexyl acrylate-co-vinyl acetate-co-2-hydroxyethyl acrylate-co-2,3-epoxypropyl

methacrylate) with a weight ratio of the components of 67:28:5:0.15 (38). The structure contains 5 % of 2-hydroxyethyl acrylate which can interact with the metal surface to build an oriented structure. With thick films this effect may be negligible due to the low fraction of oriented polymer chains compared to the total polymer volume. In contrast, the adhesion behavior of thin films is mainly determined by the orientation of the polymer chains (Fig. 36).

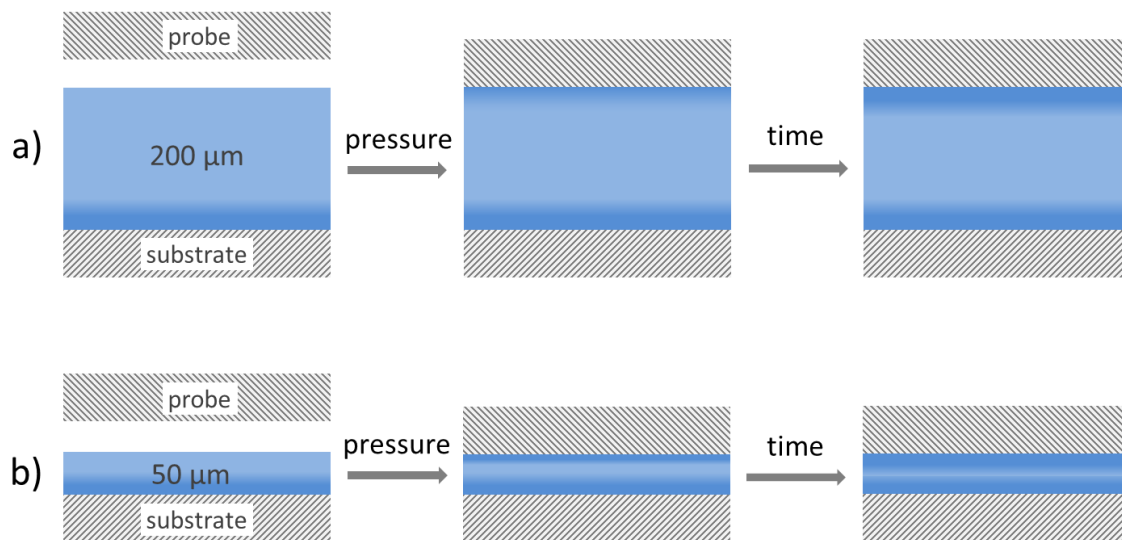


Fig. 36: Scheme of time-dependent polymer orientation (dark zones) at the interfaces between sample holder and probe for a thick (a) and a thin (b) adhesive matrix.

All the discussed parameters contribute to different extent each to the response σ_{max} , depending on the adhesive matrix thickness. The resulting effect is a relationship between σ_{max} and the square of the adhesive matrix thickness (Figs. 34d and 35). The general statement, that the adhesive matrix thickness has a positive effect on tack (37) could not be verified for the investigated system.

3.2.3.5. Factor E: API Content

The ibuprofen content has a negative effect on σ_{max} , with an increasing API content leading to a linear decrease of σ_{max} (Fig. 34e). A decrease of tack caused by an API has been observed earlier (186, 188), and explained by a plasticizing effect of the API.

The results of the probe tack test could also be confirmed by rheological measurements (Fig. 33). The shear modulus G^* decreases at all investigated frequencies with increasing amount of ibuprofen, which is a known evidence for plasticization (26, 84).

3.2.4. Interaction plots

The response surface plots of the interactions BD, CD and DE are displayed in Fig. 37.

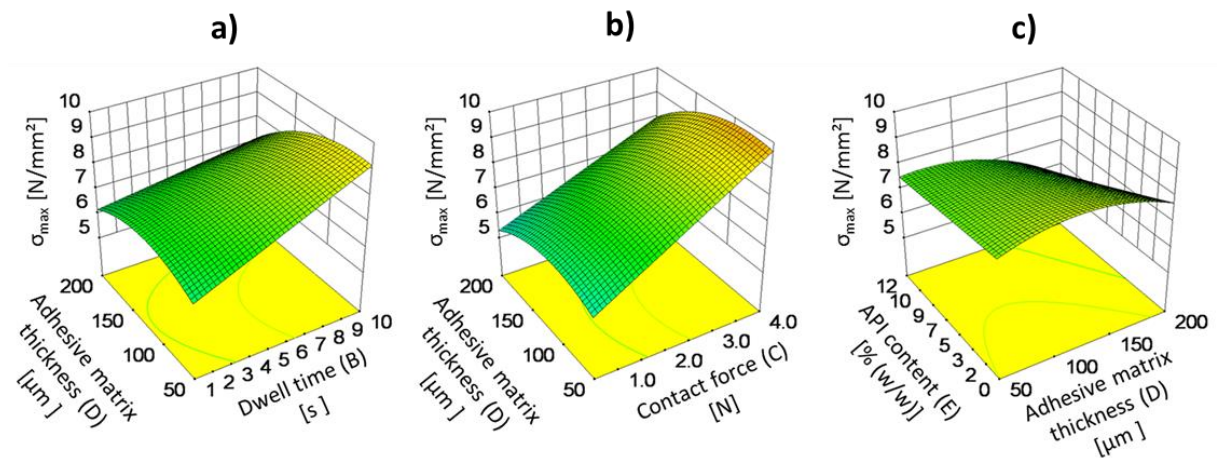


Fig. 37: Response surface plots of the probe tack test experiments with σ_{max} in dependence of (a) Dwell time (B) and adhesive matrix thickness (D), (b) Contact force (C) and adhesive matrix thickness (D), (c) Adhesive matrix thickness (D) and API content (E), generated with Design-Expert 8.0.6 software.

3.2.4.1. Interaction between Factors B and D

From the results of the ANOVA the two factors dwell time and adhesive matrix thickness were identified to interact (Table 6). The response surface plot in Fig. 37a shows an effect of the dwell time on σ_{max} that is dependent on the adhesive matrix thickness.

As shown earlier (Fig. 35), for thin adhesive matrices the most relevant parameters effecting σ_{max} are strain rate, contact area and oriented polymer volume. The strain rate is independent of the dwell time and will therefore not be considered as a relevant parameter.

The contact area A_c increases by decreasing the storage modulus (chapter 3.2.3.4). This effect occurs regardless of the adhesive matrix thickness. Therefore, this parameter may not be responsible for the more pronounced increase of σ_{max} observed with thin adhesive matrices in dependence of the dwell time (Fig. 37a).

Hence, the oriented polymer fraction (Fig. 36) is the only parameter which explains the interaction. A longer contact time with the metal surface causes a further orientation of the polymer, because orientation is a time-dependent process (140). As shown in Fig. 36, this orientation is more prominent in thin than in thick adhesive matrices as the fraction of oriented polymer chains in thin adhesive matrices is higher than in thick films. Thus, the mechanical strength of thin adhesive matrices is increased by orientation of the polymer chains, resulting in an increase of tack.

3.2.4.2. Interaction between Factors C and D

From the data displayed in Fig. 37b an interaction of the adhesive matrix thickness and the contact force becomes apparent. The contact force has a higher impact on σ_{max} at thin adhesive matrices than

at thick films. This result is somehow unexpected, because from Eqs. 7 and 8 it can be expected that the increase of the contact area A_c is more pronounced with thick films than with thin films.

As discussed before, the most important parameters influencing the tack of thin adhesive matrices are the contact area A_c and the oriented polymer fraction. Again, the mechanical strength of thin adhesive matrices appears to be higher than that of thicker films. If the quantity of adhesive bonds is increased, tack of the thinner films will increase in a stronger manner than tack of thicker films.

In addition, another parameter should be discussed here. Part of the energy applied by force to the adhesive matrix dissipates during deformation. During viscoelastic deformation all plastic deformation energy dissipates and as a consequence load transmission is decreased by damping. Therefore, for thicker adhesive matrices the applied force at the contact surface to the probe is reduced. In conclusion, with increasing contact force, the increase of tack of a thicker adhesive matrix is less pronounced than that of a thinner adhesive matrix due to its higher ability to dissipate energy via plastic deformation.

3.2.4.3. Interaction between Factors D and E

If ibuprofen is added to an adhesive matrix, a decrease of σ_{max} is observed as discussed in section 3.2.3.5. This behavior is consistent with previous studies (133) as its mechanism is related to plasticization. As only OFAT experiments were performed in those studies it has not been taken into account that there could also be an interaction of plasticization (e.g. API content) with other factors.

The results displayed in Fig. 37c reveal that there is a significant interaction between API content and adhesive matrix thickness. As expected, ibuprofen acts as plasticizer in thick adhesive matrices accompanied by a significant decrease of tack with increasing ibuprofen content. For thin adhesive

matrices the decrease of tack is less pronounced and non-significant at any investigated ibuprofen concentration. It may therefore be noted that the plasticizing effect decreases with decreasing adhesive matrix thickness.

The reason for this interaction can neither be explained by the different strain rates applied at debonding nor by any other information gathered from the rheological experiments. Therefore, one may conclude that tack should be decreased independent of the adhesive matrix thickness. However, with the performed rheological experiments no interfacial effects could have been investigated because the samples had to be at least 1200 μm thick to allow measurements with an appropriate resolution of the rheometer. This leads to the conclusion that orientation of polymer chains may also be responsible for the absence of a plasticizing effect of ibuprofen in thin adhesive matrices. A polymer with oriented chains can exhibit a pseudo-glassy behavior (138–140, 142) causing an increased robustness to plasticizing because above the glass transition temperature plasticizers have a less pronounced effect on the modulus G (178).

In summary, the interaction between the factors adhesive matrix thickness and API content may be explained by the oriented fraction of polymer chains at the interface and their resistance to plasticization.

3.2.5. Interpretation of the data

Generally, all observed effects can be traced back to the relationship between stress and strain:

$$\frac{F_{max}}{A_c} = \sigma_{max} = E \cdot \varepsilon \Leftrightarrow F_{max} = E \cdot \varepsilon \cdot A_c \quad \text{Eq. 9}$$

Where F_{max} is defined as the maximum force at break and ϵ is the strain; A_c is the contact area at the interface and can be related to the quantity of adhesion bonds; E is the tensile modulus and can be related to the quality of the adhesion bonds. It has to be considered that both A_c and E depend on the PSA properties as well as on the test conditions.

When contact is made at the bonding step, a contact area A_c is formed. A_c depends on wetting: The higher the wettability the higher A_c . Wetting is a function of the viscoelastic bulk properties of the adhesive as well as of the interfacial characteristics between substrate and adhesive. As described in chapter 3.2.3.2, A_c is proportional to the contact force and inversely proportional to the apparent modulus E_a (Eq. 7). E_a itself is proportional to E and inversely proportional to the adhesive matrix thickness h (Eq. 8). Therefore, good wetting requires a low E_a (i.e. a low E), a high contact force and a high adhesive matrix thickness.

At the debonding a high tensile modulus E results in high values of σ_{max} . As discussed previously, E is directly proportional to G and for viscoelastic polymers both moduli are strain rate-dependent. Furthermore, E is affected by physicochemical parameters such as plasticizing e.g. caused by solvent residuals or by an API. E also depends on physical factors such as oriented polymer fraction which itself is a function of time and adhesive matrix thickness.

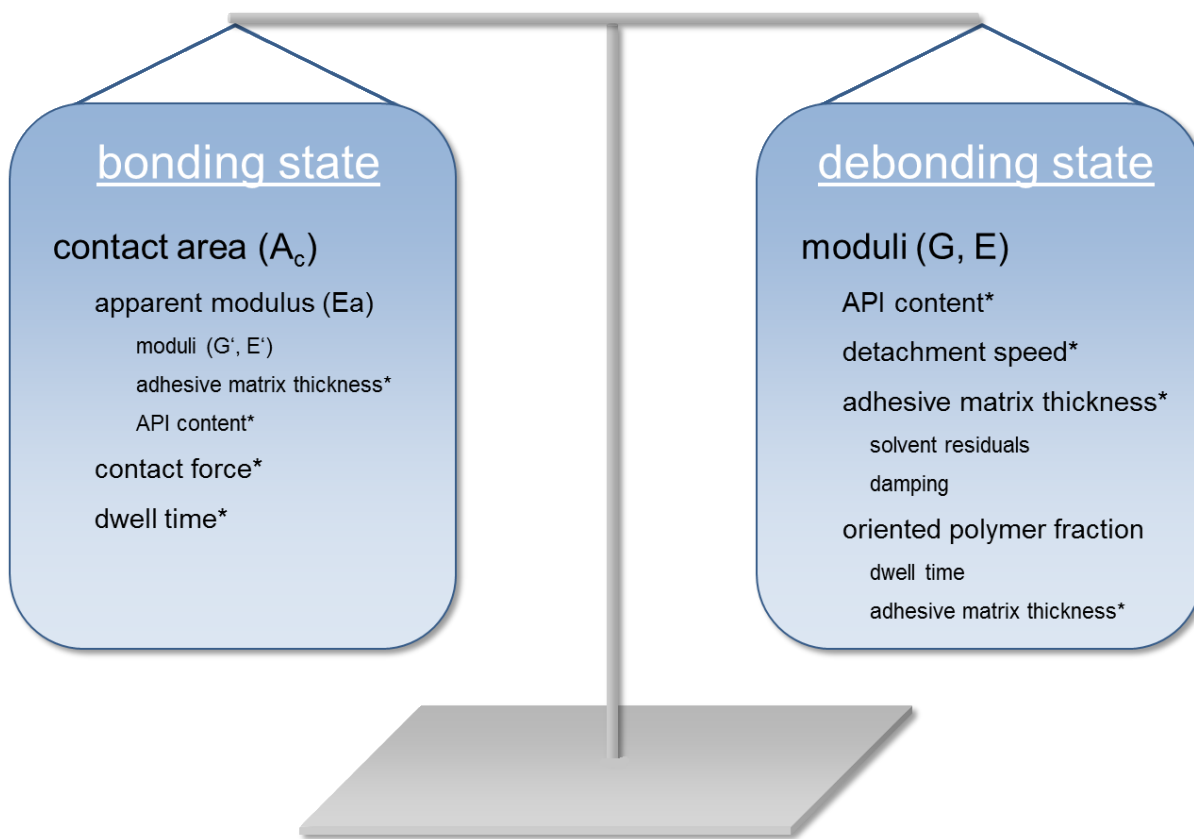


Fig. 38: Factors influencing the bonding and debonding state. Investigated factors are marked with a star.

It can be summarized that the factor contact force can be related to the bonding state and the factor detachment speed to the debonding state (Fig. 38). The factors dwell time, adhesive matrix thickness and API content are involved in an antagonistic way at the bonding and debonding state, respectively.

3.2.6. Conclusion

Although, the probe tack test has already been investigated extensively by several research groups, the performed experiments allowed the identification of significant factors and their interactions as well as their influence on tack. With a reasonable number of experiments the method of

experimental design for a measurement system analysis could clearly prove its superiority over the OFAT methodology which would not allow detecting interactions between the investigated factors.

All identified significant factors have to be monitored carefully with respect to their interactions. Furthermore, the general assumption that tack increases with an increase of adhesive matrix thickness needs to be reconsidered. It was found that tack increases with decreasing adhesive matrix thickness. An explanation for this observation was found to be the orientation of polymer chains. In terms of pressure sensitive adhesion this phenomenon should be investigated in more detail. For such experiments alternative methods such as atomic force microscopy or dielectric spectroscopy may be used.

The obtained results can also serve as a framework for future work with intelligent polymers where the orientation of polymer chains may be used to control the release rate of a drug.

3.3. Results and discussions of “Formulation development of a multiple polymer adhesive patch”⁴

The aim of the third study was to evaluate the statistical method of “Mixture Design” for the early stage development of a multiple polymer adhesive patch. For this purpose, blends of silicon adhesive, acrylic adhesive, oleyl alcohol as a surfactant and ibuprofen as a model drug were used.

⁴ This chapter has been published as shown in Table 10, p. 141.

Table 7: The responses of the design matrix and additional experiments (Ac = 100 % acrylic PSA, Si = 100 % silicone PSA, Ac_M = 80 % acrylic PSA + 20 % ibuprofen, Si_M = 80 % silicone PSA + 20 % ibuprofen, Opt = Optimization, Val = Validation run).

Run	Responses					
	Tack	Shear Adhesion	Crystal Growth	Extent of Creaming	Droplet Size	Droplet Distribution Range
	N/mm ²	min	%	%	µm	µm
1	0.20	3.9	5	6	3.8	5.0
2	0.40	24.1	10	4	5.0	2.5
3	0.28	9.2	0	15	5.0	2.5
4	0.33	3.1	90	11	27.5	45.0
5	0.31	7.8	90	11	40.0	70.0
6	0.17	3.3	100	25	23.8	27.5
7	0.32	12.3	0	27	12.5	5.0
8	0.18	1.4	10	14	6.3	7.5
9	0.42	30.2	0	7	8.8	7.5
10	0.28	6.4	25	24	12.5	15.0
11	0.26	7.1	10	20	7.5	5.0
12	0.29	9.7	0	16	5.0	5.0
13	0.18	1.5	50	27	10.0	16.0
14	0.31	5.9	30	21	10.0	10.0
15	0.35	9.4	90	9	40.0	70.0
16	0.31	6.7	15	20	11.3	7.5
Ac	0.45	17.2	0	n.a.	n.a.	n.a.
Si	0.55	56.9	0	n.a.	n.a.	n.a.
Ac _M	n.a.	n.a.	100	n.a.	n.a.	n.a.
Si _M	n.a.	n.a.	100	n.a.	n.a.	n.a.
Opt	0.36	18.4	2.5	n.a.	10.0	4.7
Val	0.38	17.8	0	22	11.4	4.3

Table 8: ANOVA of the results of tack, shear adhesion, crystal growth, extent of creaming, droplet size and droplet distribution range.

	Model				Pure Error		LOF			Adj. R ²	Pred. R ²	Adeq. Precision	Transformation
	Model	DF	Mean square	p-Value	DF	Mean square	DF	Mean square	p-Value				
Tack	RSQM[†]	7	0.011	< 0.0001	5	0.0004	3	0.0005	0.202	0.923	0.864	17	-
Shear adhesion	QM[†]	5	0.400	< 0.0001	5	0.0020	5	0.0014	0.644	0.988	0.973	51	Log
Crystal growth	RCM[‡]	8	2683.3	< 0.0001	5	33.33	2	7.85	0.798	0.982	0.972	26	-
Extent of creaming	RCM[‡]	7	119.1	< 0.0001	5	3.63	3	2.19	0.641	0.946	0.710	18	-
Droplet size	RCM[‡]	7	302.8	< 0.0001	5	2.03	3	6.83	0.112	0.973	0.775	27	-
Droplet distribution range	RCM[‡]	7	10.4	< 0.0001	5	0.31	3	0.52	0.283	0.923	0.741	14	Square root

*RSQM = Reduced Special Quartic Mixture, [†]QM = Quadratic Mixture, [‡]RCM = Reduced Cubic Mixture

3.3.1. Tack

For an adhesive of a transdermal patch it is important to adhere immediately when it is brought in contact with the skin. From the results displayed in Table 7, a “reduced special quartic mixture” (RSQM) model as the highest order polynomial was developed (Table 8). After reversed reduction of the model, the predicted R^2 of 0.864 was in good agreement with the adjusted R^2 of 0.922. The evaluation of the model by an ANOVA showed that the model with a p-value below 0.0001 was highly significant. Moreover, the variation of the data around the fitted model, the LOF, was found to be non-significant with $p = 0.2017$ and a good signal-to-noise ratio was confirmed by an “adequate precision” of 16. Following the scheme of Fig. 21, a “Box-Cox” Plot was utilized to evaluate the data for transformation. For the response tack the “Box-Cox” plot indicated that no transformation of the data was required. In the next step, the “normal probability plot of the studentized residuals” was investigated and showed normal distribution of the data confirmed by a linear relationship between the normal probability and the internally studentized residuals (Fig. 39a).

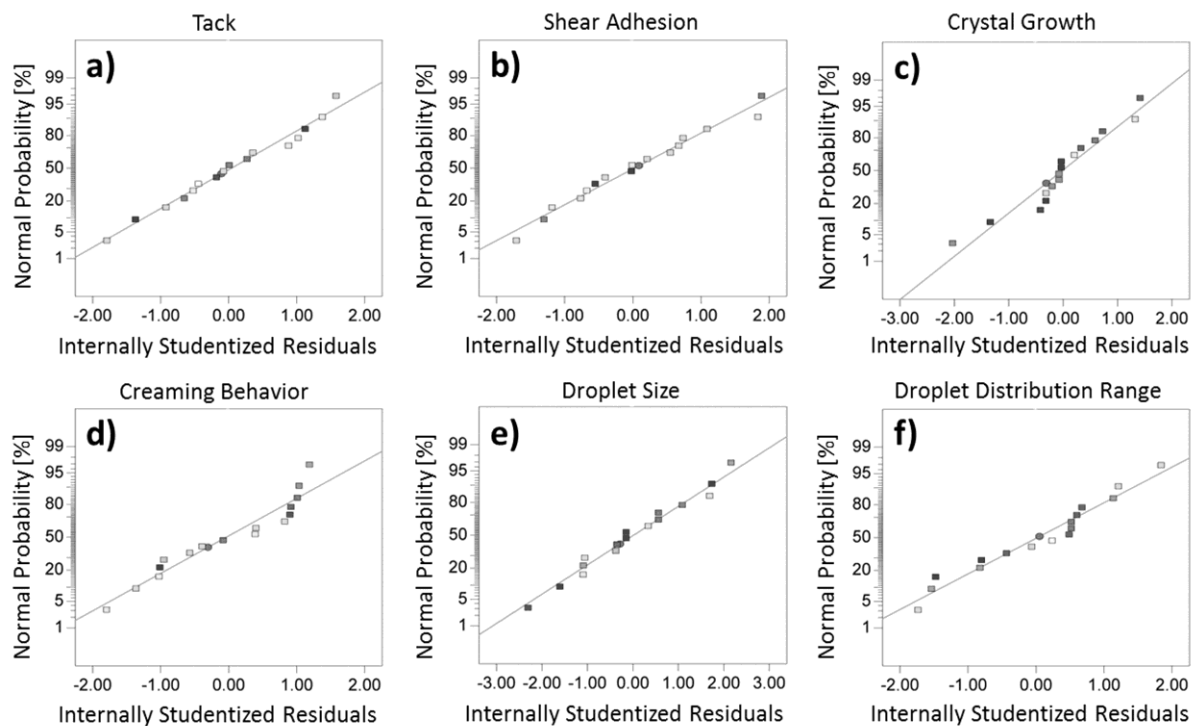


Fig. 39: Normal Plots of the studentized residuals for (a) Tack, (b) Shear adhesion, (c) Crystal growth, (d) Extent of creaming, (e) Droplet size, (f) Droplet distribution range, generated with Design-Expert 8.0.6 software.

Generally, a constant error may be revealed by observing patterns in an “internally studentized residuals versus predicted” plot. For the residuals of tack no constant error could be observed (Fig. 40a).

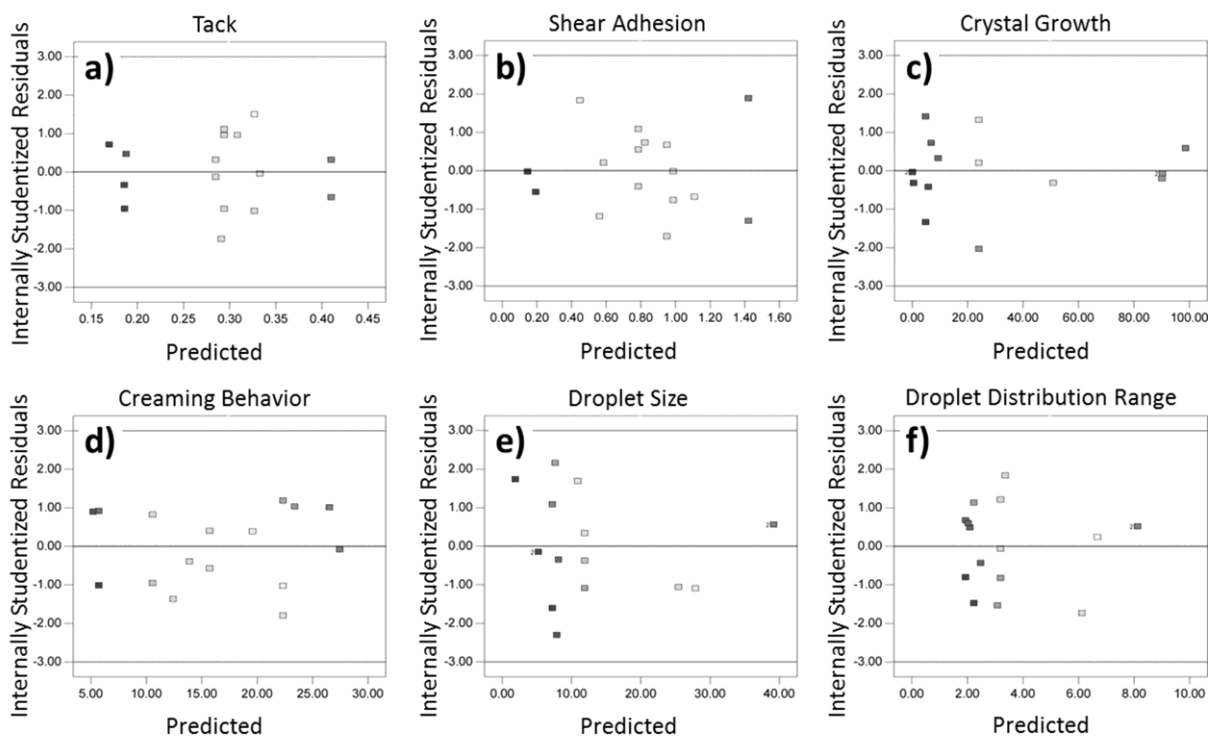


Fig. 40: Internally Studentized residuals versus predicted values for (a) Tack, (b) Shear adhesion, (c) Crystal growth, (d) Extent of creaming, (e) Droplet size, (f) Droplet distribution range, generated with Design-Expert 8.0.6 software.

From an “externally studentized residuals” plot, outliers or influential values may be identified. For tack, all residuals showed no influential values (Fig. 41a).

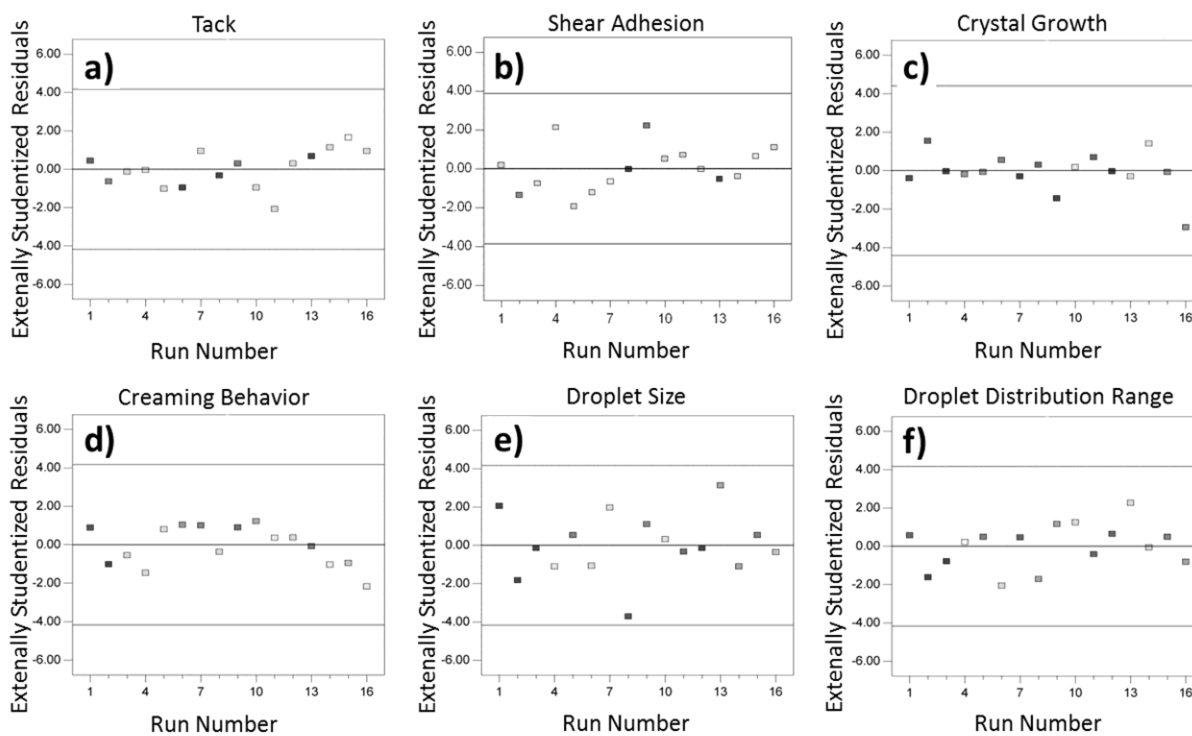


Fig. 41: Externally Studentized Residuals vs Run number for (a) Tack, (b) Shear adhesion, (c) Crystal growth, (d) Extent of creaming, (e) Droplet size, (f) Droplet distribution range, generated with Design-Expert 8.0.6 software.

Based on these results a model graph as contour plot was generated (Fig. 42a). From the contour plot it was observed that highest tack values of 0.40 N/mm^2 resulted from samples with 60 % amount of silicone adhesive (Fig. 42a).

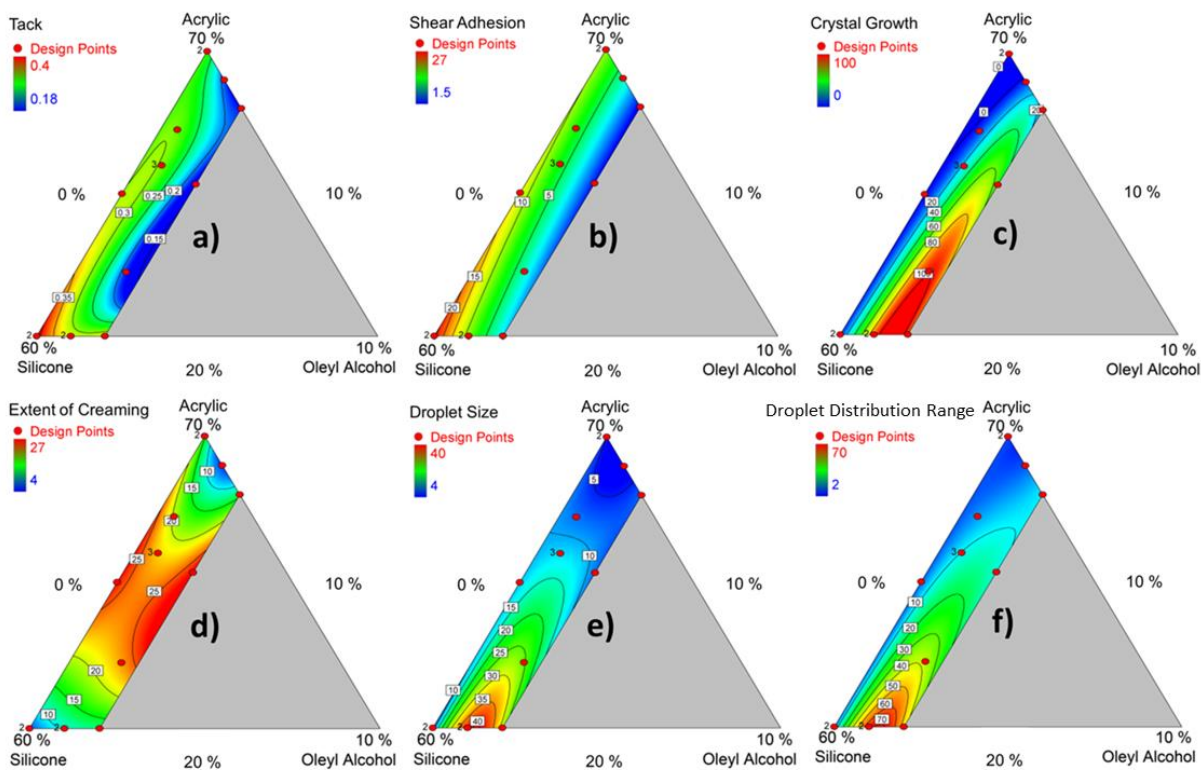


Fig. 42: Contour plots of the design space (a) Tack, (b) Shear adhesion, (c) Crystal growth, (d) Extent of creaming, (e) Droplet size, (f) Droplet distribution range, generated with Design-Expert 8.0.6 software.

Nevertheless, compared with measurements of 100 % silicone adhesive (S_i) the tack was decreased by 27 %. A comparison with a binary mixture of silicon adhesive and ibuprofen (S_{iM}) was not possible due to instant crystallization of the API in the matrix. With an increase of the amount of acrylic adhesive the decrease of tack was even more pronounced. The tack of mixtures containing 70 % acrylic adhesive was decreased by 42 % compared to 100 % acrylic adhesive (A_c). Again, a comparison

with a binary mixture of acrylic adhesive and ibuprofen (A_{cM}) was not possible because of crystallization of ibuprofen. From these observations it can be concluded that the decrease of tack is caused by ibuprofen as well as by the interaction of the two adhesives. A decrease of tack by the addition of small molecules is described in the literature (186, 188, 194). In particular, the decrease of tack by ibuprofen in an acrylic adhesive was previously investigated (133) and could be explained by a plasticizing effect of the API. The decrease of tack by interaction of the two adhesives may be explained by the macroscopic structure of the matrices. If an acrylic and a silicon adhesive are mixed together, they form a matrix with two phases (Fig. 43d). As for complex mixtures of crosslinked acrylic copolymers, silicone adhesives and interfacial active substances, the Bancroft rule as well as the HLB concept is not applicable. Stenert (195) assumes that the polymer with the smaller portion is forming the dispersed phase. If a force is applied vertically to the matrix and pulled away as it happens during the tack test, only the coherent phase can contribute to the resistance to this force. Compared to the plain adhesive matrix the resistance to the tack probe is reduced (Fig. 43b and e). Turning the focus on the addition of oleyl alcohol, a decrease of tack could be observed for all ratios with increasing amounts of oleyl alcohol (Fig. 42a). It is assumed that oleyl alcohol reduces the tack because of a plasticizing effect on the adhesive as observed in previous studies (196). Mixtures with increased amounts of silicone adhesive were less sensitive to the addition of oleyl alcohol than the acrylic adhesive.

3.3.2. Shear adhesion

Shear adhesion is critical for the long-term wear of transdermal patches. Low shear adhesion can result in sticking of the patch to the packaging material by cold flow of the adhesive. Furthermore, dark rings around the periphery of the patch caused by low shear adhesion are critical not only with

regard to the appearance (18). Moreover, dosing may be influenced by the altered area covered by the patch (105). The obtained shear adhesion values are displayed in Table 7. As recommended by the “Box-Cox” plot, a log transformation of the data was performed (Table 8). A highly significant “quadratic mixture” (QM) model with a p-value of 0.0001 was obtained from the data (Table 8). The predicted R^2 of 0.973 appeared to be very close to the adjusted R^2 of 0.988. The LOF test was non-significant and the “adequate precision” showed a very good signal-to-noise ratio. Diagnostics revealed normality of residuals (Fig. 39b) and no constant error in the “internally studentized residuals versus predicted” plot (Fig. 40b). Moreover, no outliers or influential values could be revealed by the “externally studentized residuals” plot (Fig. 41b). From the contour plot shown in Fig. 42b it was obvious that high silicon adhesive contents corresponded to high shear adhesion values. Compared to plain silicon adhesive, the shear adhesion value was reduced by 53 %. Also, with increasing amounts of acrylic adhesive a decrease of shear adhesion could be observed. For mixtures with increasing amounts of oleyl alcohol an exponential decrease was detected. These results showed that mixtures of a silicone and an acrylic adhesive, as well as the addition of ibuprofen or oleyl alcohol to these mixtures resulted in reduced shear adhesion values. Again, the macroscopic view may be helpful to understand the observed results. As discussed for tack, the matrix comprises a coherent and a dispersed phase (Fig. 43a and d).

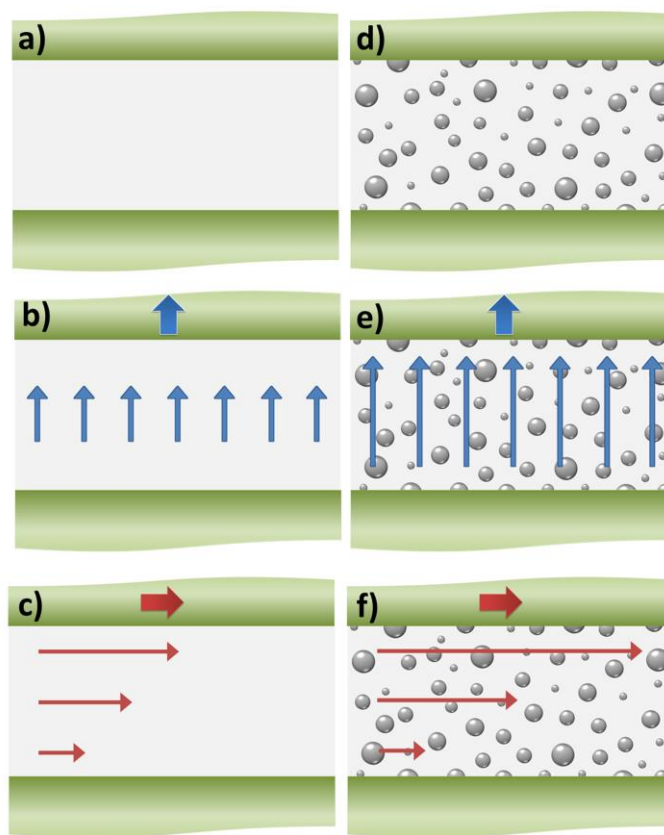


Fig. 43: Comparison of a one phase matrix (a, b, c) with a two phase matrix (d, e, f) with regard to their viscoelastic behavior during vertical (b, e) and horizontal (c, f) force application.

If the rheological model of stacked layers is applied (197), it can be assumed that the contact points of the layers of the coherent phase are reduced. This effect results in weaker attraction forces between the layers. If now a shear force is applied, higher shear rates will result compared to 100 % adhesive (Fig. 43c and f).

3.3.3. Crystal growth

For a drug like ibuprofen, which has to be applied at high doses, a high drug load with the drug being completely dissolved is desired to keep the patch as small as possible. The determination of crystal

growth after 24 h in oversaturated systems may serve as an estimate of the induction time of crystallization, which correlates with the drug concentration in the supersaturated system (198). Under the condition of a constant drug load, a decreased drug solubility of ibuprofen in the matrices is accompanied by an enhanced progress of crystallization. From the results of the ANOVA, a highly significant “reduced cubic mixture” (RCM) model was evolved after reversed reduction of the model terms to fit the response of crystal growth (Table 8). The model showed a predicted R^2 of 0.972 and an adjusted R^2 of 0.982. Both, the non-significant LOF test and an “adequate precision” of 26 confirmed the reliability of the model. The diagnostics indicated normality of the data and no constant error, outliers or influential values (Figs. 39c, 40c, and 41c). The crystal growth determined in binary mixtures of plain acrylic adhesive or silicone adhesive with ibuprofen was determined to be 100 % (Table 7). As already described in sections “Tack” and “Shear adhesion”, ibuprofen crystallized instantly during the drying step of the matrices. In contrast to these observations, ternary mixtures of acrylic adhesive, silicone adhesive and ibuprofen exhibited decreased crystal growth (Fig. 42c, Table 7). It is remarkable that the adhesives showed a synergistic effect on the reduction of crystallization. With quaternary mixtures containing oleyl alcohol, a low crystallization tendency was observed at increased acrylic adhesive contents with up to 5 % oleyl alcohol (Fig. 42c). In general, oleyl alcohol shows an enhancing effect on the induction of crystallization. Highest values were observed with lower levels of acrylic adhesive accompanied by high levels of oleyl alcohol. These effects will be discussed in detail together with the response “droplet size” in the section “droplet distribution range”.

3.3.4. Extent of creaming

The extent of creaming of the wet mixes gives information on their physical stability during processing. A low extent of creaming is desired to prevent phase segregation during manufacturing of the transdermal patch. The highly significant RCM model with a predicted R^2 of 0.710 and an adjusted R^2 of 0.946 was obtained by the ANOVA (Table 8). The validity of the model was confirmed by a non-significant LOF test and a good signal-to-noise ratio. Diagnostics showed normality and no irregular variation of the residuals (Figs. 39d, 40d, and 41d). The derived response surface displayed as contour plot showed a saddle-like structure, where lowest values for creaming were obtained at highest adhesive concentrations (Fig. 42d). The most pronounced phase separation was observed with equal proportions of the adhesives.

3.3.5. Droplet size

With regard to the performance and the appearance of the transdermal patch, a small droplet size is desired to prevent coalescence of the two phases and as shown later to achieve a reduced crystallization of ibuprofen. A RCM model was found to be highly significant for the droplet size (Table 8). The “LOF” test was non-significant, and the values showed a good “adequate precision”. The adjusted R^2 of 0.973 was found to be in reasonable agreement with the predicted R^2 of 0.775. The diagnostics showed good results (Figs. 39e, 40e, and 41e) and a contour plot was derived from the data (Fig. 42e). Smallest droplets were observed for ternary mixtures of silicone adhesive, acrylic adhesive and ibuprofen at any ratio as well as for quaternary mixtures with acrylic adhesive amounts above 60 % and oleyl alcohol at all investigated ratios (Fig. 42e). Largest droplets occurred at low amounts of acrylic adhesive and high amounts of oleyl alcohol with a maximum at 6 % oleyl alcohol. Interestingly, the maximum is located in the same region as observed for the crystal growth.

Crystallization inhibition in an emulsion is a known phenomenon, where two mechanisms contribute to this effect. First, heterogeneous crystallization starts with a nucleation which itself is triggered by an impurity (200). In a bulk liquid, the probability for incorporation of a nucleus is high. If the droplet size is decreased accompanied by an increase of the number of droplets, the probability to incorporate a nucleus into a single drop is reduced. Hence, heterogeneous crystallization is decreased in a two-phase system. Second, an increase in the interface by a reduction of the droplet size results in a positive interface free energy and thus in a destabilization of an arising nucleus (198). This effect results in an interfacial stabilization of supersaturated two-phase systems. For the investigated samples it was observed that a large droplet size corresponds to an increased crystallization of ibuprofen.

3.3.6. Droplet distribution range

To achieve a maximum stability of the two-phase matrices and to prevent coalescence by Ostwald ripening a narrow droplet distribution range is desired. Based on the results obtained by the “Box-Cox” plot a square root transformation of the data was performed. A RCM model with an adjusted R^2 of 0.923 and a predicted R^2 of 0.741 was derived by the ANOVA (Table 8). Furthermore, the ANOVA showed a high significance of the model, no LOF and a good signal-to-noise ratio. Diagnostics showed normality and no exceptional variation of the residuals (Figs. 39f, 40f, and 41f). As observed previously for the droplet size, the smallest droplet distribution ranges were observed for ternary mixtures of the adhesives containing ibuprofen as well as for mixtures with increased amounts of acrylic adhesive and oleyl alcohol. High droplet distribution ranges were obtained at low amounts of acrylic adhesive and high amounts of oleyl alcohol with a maximum at 6 % oleyl alcohol. The response surface of the droplet distribution range correlates well with the response surface of the droplet size.

3.3.7. Multi response optimization and validation

With a numerical optimization a combination of component levels that satisfy the requirements placed on each of the responses is searched. Although the mixture design was performed as a starting point for further experiments, a numerical optimization was carried out to validate the predictive accuracy of the models. The components of silicon adhesive, acrylic adhesive and oleyl alcohol were not adjusted to a specific set-point. For the responses tack and shear the requirement was set to maximum to achieve values close to those of the plain adhesives. Crystal growth, droplet size and droplet distribution range were selected to be minimized, whereas crystal growth was limited to a maximum of 10 %. The extent of creaming was not set to any limit because it is thought not to be controlled by formulation but by homogenization. The highest desirability was found to be 0.773 for a mixture of 31 % acrylic adhesive, 49 % silicone adhesive, 0 % oleyl alcohol and 20 % ibuprofen (Table 4). A validation sample with the recommended fractions derived from the multi response optimization was prepared and analyzed as described for the design runs. The responses were found to be in good agreement with the predicted values (Table 7).

3.3.8. Interpretation of the data

In summary, oleyl alcohol neither improves the miscibility of the polymers by reduction of the polymeric interface energy nor the solubility of ibuprofen in the mixtures. Therefore, the addition of oleyl alcohol should be reconsidered. In contrast to the mixtures at the periphery of the design space, wet mixes with equal fractions of polymer tend to be less stable. Furthermore, it could be shown that crystal growth of ibuprofen correlates well with droplet size and droplet distribution range of the multiple polymer adhesive systems, where lowest values for crystallization were found with mixtures containing small droplets.

3.3.9. Conclusion

It can be concluded that the presented data give information on the critical spots of the “mixture design” and where the design needs to be improved. One possibility of improvement may be an augmentation of the design to extended constraints of the adhesives and to different surfactants. Preferably, these surfactants should be polymers with polar and apolar functionalities that could interact with the immiscible polymers. As so called compatibilizers polyvinylpyrrolidone (PVP) or Soluplus® may be used (96). Moreover, process variables, such as mixing speed or viscosity of the wet mix as well as responses for performance indication, such as drug release may be added preferably in a combined design. The development of a design space for a transdermal patch via “mixture design” in the early stage of formulation development provides valuable information on the product as well as on the interactions of the components with an acceptable number of experiments.

3.4. Final discussion

It may be summarized that the development of a method to manufacture patches as well as patch samples for various analytical methods could successfully be established. With this method, samples with good and reproducible quality could be prepared, whereas the loss of material was kept to a minimum.

The results of the first study demonstrated clearly the relevance of rheometrical measurements for the development of transdermal patches. DMA/DMTA showed excellent reproducibility and could significantly detect the interaction between the API and the PSA with a comparatively low preparatory effort after the development of the method. Properties such as viscoelasticity, as well as its time and temperature dependence may be detected easily by rheometry compared to the standard test methods of the tape industry. As a result of the excellent reproducibility and the low limit of detection of DMA/DMTA, the phenomenon of antiplasticization could be detected. Because antiplasticization depends on many factors such as temperature, stress, strain, mechanical history, and API concentration the term “antiplasticizing space” was introduced. As it is likely that most polymer/API blends exhibit an antiplasticizing space it should also be considered for solid dispersions or coatings of other pharmaceutical dosage forms. The “antiplasticizing space” might be a critical factor of processing, stability as well as in-vivo behavior of API/polymer blends in transdermal and non-transdermal drug delivery. Moreover, the requirement of incorporation of viscoelastic data into the dossier for new drug product applications was recently included in the draft “Guideline on quality of transdermal patches” (11), which underlines the importance of DMA/DMTA for transdermal patch development.

Variation of an analytical result may be caused by alteration of the manufacturing process of the sample. However, it has to be emphasized that the variation of the result may also be caused by

changes in the sensitivity or linearity of the analytical method itself. Only if both processes are well understood, the cause of the variation may be identified. In the second study it was shown in an exemplary manner that analytical measurement systems can be thoroughly investigated by a QbD approach. The concept of the presented study is also of great interest in the field of analytical method development as recently a joint working group from the pharmaceutical industry published a comparable QbD approach for the evaluation of a chromatography method (201).

Orientation of polymer chains of the PSA as observed in this study might be of rather low importance for most transdermal patches but it might have the potential in innovative drug delivery systems. In particular, this phenomenon could be used to design intelligent drug controlling membranes, the permeability of which may be adjusted by temperature, pH, electrochemical potential or ionic concentration in the environment of the site of action or by an external trigger.

The data from the third study showed in an exemplary manner how the method of "Mixture Design" delivers detailed information on the product with minimal use of resources. By performing a reasonable number of experiments, the interaction of the components of the adhesive matrix as well as their influence on the performance of the transdermal patch could be investigated. Of particular interest is the fact that this method can be applied in the field of transdermal patch development as well as in other areas dealing with formulation development using a quality by design approach. The observed inhibition of crystallization of an API in a multiphase system such as an emulsion by decreasing the droplet size may also be used in other drug delivery systems. As an example solid dispersions are used to increase the solubility of poorly soluble APIs and have the advantage to be stable over a longer period of time. A further increase of API solubility might be achieved by combining solid dispersions with the observed effect of crystallization inhibition. A solid

microemulsion is expected to have improved solubility characteristics for an API compared to traditional solid dispersion systems.

Finally, it can be concluded that the challenge to develop and evaluate methods for transdermal patch development with higher quality and deeper understanding of the drug product could successfully be met.

4. References

4. References

- [1] Zaffaroni, A.
Drug-delivery system.
Patent US3854480 A (1974)
 - [2] Prausnitz, M.R., Langer, R.
Transdermal drug delivery.
Nat Biotechnol 26(11): 1261–1268 (2008)
 - [3] Wokovich, A.M., Prodduturi, S., Doub, W.H., Hussain, A.S., Buhse, L.F.
Transdermal drug delivery system (TDDS) adhesion as a critical safety, efficacy and quality attribute.
Eur J Pharm Biopharm 64(1): 1–8 (2006)
 - [4] Food and Drug Administration Center for Drug Evaluation and Research (CDER) Center for Biologics Evaluation and Research (CBER)
Approved Drug Products with Therapeutic Equivalence Evaluations.
34th ed., U.S. Department of Health and Human Services, Washington, D.C. (2014)
 - [5] Jacques, C.
Transdermal Patch Delivery Technologies Will Create New Blockbuster Drugs.
Assessed from: <http://www.luxresearchinc.com> (2014)
 - [6] Cilurzo, F., Gennari, C.G.M., Minghetti, P.
Adhesive properties: a critical issue in transdermal patch development.
Expert Opin Drug Deliv 9(1): 33–45 (2012)
 - [7] Gupta, H., Babu, R.J.
Transdermal Delivery: Product and Patent Update.
Recent Patents on Drug Delivery & Formulation 7(3): 184–205 (2013)
 - [8] Allhenn, D.
Innovative Arzneiformen.
1st ed., Wiss. Verl.-Ges., Stuttgart (2010)
 - [9] Naik, A., Kalia, Y.N., Guy, R.H.
Transdermal drug delivery: overcoming the skin's barrier function.
Pharm Sci Technol Today 3(9): 318–326 (2000)
 - [10] Council of Europe
European Pharmacopoeia.
7th ed., Council of Europe, Strasbourg (2010)
 - [11] Quality Working Party
Guideline on quality of transdermal patches.
Draft, European Medicines Agency, London (2012)
-

-
- [12] Michael Horstmann
Transdermal Therapeutic Systems: Current technologies of chemically and physically enhanced diffusive delivery.
Skin Forum 2011, Frankfurt/Main (2011)
- [13] Choy, Y., Prausnitz, M.
The Rule of Five for Non-Oral Routes of Drug Delivery: Ophthalmic, Inhalation and Transdermal.
Pharm Res 28(5): 943-948 (2011)
- [14] Wille, J.J.
Skin delivery systems: Transdermals, dermatologicals, and cosmetic actives.
1st ed., Blackwell Pub., Ames, Iowa (2006)
- [15] Gregoire, S., Ribaud, C., Benech, F., Meunier, J.R., Garrigues-Mazert, A., Guy, R.H.
Prediction of chemical absorption into and through the skin from cosmetic and dermatological formulations.
Br. J. Dermatol. 160(1): 80–91 (2009)
- [16] Cantor, A., Wirtanen, D.
Novel Acrylate Adhesives for Transdermal Drug Delivery.
Pharmaceutical Technology 02(01):28–38 (2002)
- [17] Sateesh Kandavilli, V.N.R.P.
Polymers in Transdermal Drug Delivery Systems.
Pharmaceutical Technology 02(05): 62–80 (2002)
- [18] Venkatraman, S., Gale, R.
Skin adhesives and skin adhesion: 1. Transdermal drug delivery systems.
Biomaterials 19(13): 1119–1136 (1998)
- [19] Brooke, L., Herrmann, C.
Cannabinoid Patch and Method for Cannabis Transdermal Delivery.
Patent US6113940 A (2000)
- [20] Van Buskirk GA et al.
Scale-up of adhesive transdermal drug delivery systems.
Pharm Res 14(7): 848–852 (1997)
- [21] Sharad K. Govil, L.J.W.
Adhesive mixture for transdermal delivery of highly plasticizing drugs - Patent application.
Patent 20090041832 (2009)
- [22] Potts, R.O., Guy, R.H.
Predicting Skin Permeability.
Pharm Res 9(5): 663-669 (1992)
-

-
- [23] Prausnitz, M.R., Mitragotri, S., Langer, R.
Current status and future potential of transdermal drug delivery.
Nat Rev Drug Discov 3(2): 115–124 (2004)
- [24] Güngör, S., Erdal, M.S., Özsoy, Y.
Plasticizers in Transdermal Drug Delivery Systems.
In: Recent Advances in Plasticizers, 1st ed. (Luqman M., ed): p. 91–112, InTech, Croatia (2012)
- [25] Takayasu, T., Kakubari, I., Shinkai, N., Kawakami, J., Nakajima, N., Uruno, A.
Patch.
Patent US6211425 B1 (2001)
- [26] Dillard, D.A., Pocius, A.V.
Adhesion Science and Engineering, Vol I: The Mechanics of Adhesion.
1st ed., New York, NY, Elsevier (2003)
- [27] Taub, M.B., Dauskardt, R.H.
Adhesion of pressure sensitive adhesives with applications in transdermal drug delivery.
Mater. Res. Soc. Symp. Proc. 662(Biomaterials for Drug Delivery and Tissue Engineering):
NN4.9/1-NN4.9/6 (2001)
- [28] Mayan, R.
Verbesserte Freisetzung von Ibuprofen aus Heißschmelzklebemassen durch Zusatz von
pharmazeutischen Hilfsstoffen.
Patent DE 19834496 A 1 (2000)
- [29] Foreman, P.B.
Acrylic Adhesives.
In: Technology of pressure-sensitive adhesives and products, 1st ed. (Benedek I., Feldstein
M.M., eds): p. 5-1 to 5-60, CRC Press - Taylor & Francis Group, Boca Raton, FL (2009)
- [30] Lambert, R., Lu, W., Liao, J.
Amphetamine transdermal compositions with acrylic block copolymer.
Patent US20140271865 A1 (2014)
- [31] Liao, J., Liu, P., Dinh, S.
Transdermal methylphenidate compositions with acrylic block copolymers.
Patent US20140276483 A1 (2014)
- [32] Ullmann, F., Elvers, B., Hawkins, S., Schulz, G.
Ullmann's encyclopedia of industrial chemistry.
5th ed., VCH, Cambridge (1992)
- [33] Haddock, T.H.
Pressure sensitive adhesive.
Patent EP 0 130 080 A1 (1985)
-

-
- [34] Pocius AV, Dillard DA, Chaudhury MK, editors
Adhesion science and engineering: The Mechanics of Adhesion.
1st ed., Amsterdam ;, Boston, Elsevier (2002)
- [35] Bonnet, M.
Kunststoffe in der Ingenieur Anwendung: Verstehen und zuverlässig auswählen.
1st ed., Vieweg + Teubner, Wiesbaden (2009)
- [36] Creton, C.
Pressure-Sensitive Adhesives: An Introductory Course.
MRS Bulletin June 2003: 434–439 (2003)
- [37] Benedek, I.
Pressure-sensitive adhesives and applications: Rheology of Pressure Sensitive Adhesives.
2nd ed., Dekker, New York, NY (2004)
- [38] Rote Liste Service GmbH
Rote Liste 2007: Arzneimittelverzeichnis für Deutschland (einschließlich EU-Zulassungen und bestimmter Medizinprodukte)
1st ed., Rote Liste Service, Frankfurt/Main (2007)
- [39] Lin, S.B., Durfee, L.D., Knott, A.A., Schalau II, G.K.
Silicone Pressure-Sensitive Adhesives.
In: Technology of pressure-sensitive adhesives and products, 1st ed. (Benedek I., Feldstein M.M., eds): p. 6-1 to 6-26, CRC Press - Taylor & Francis Group, Boca Raton, FL (2009)
- [40] Tan, H.S., Pfister, W.R.
Pressure-sensitive adhesives for transdermal drug delivery systems.
Pharm Sci Technol Today 2(2): 60–69 (1999)
- [41] Merrill, D.
Process for the production of a bodied silicone resin without the use of a catalyst.
Patent US4056492 A (1977)
- [42] Barnes, K., Gathman, S., Plante, D., Stark-Kasley, L.
Architectural coating compositions containing silicone resins.
Patent WO2006113183 A1 (2006)
- [43] Clark, H.
Room temperature curing silicone.
Patent US2934519 A (1960)
- [44] Metevia, V., Woodard, J.
Transdermal drug delivery device with amine-resistant silicone adhesive and method for making such a device.
Patent EP0180377 A2 (1986)
-

-
- [45] Woodard, J., Metevia, V.
Transdermal drug delivery devices with amine- resistant silicone adhesives.
Patent CA1253074 A1 (1989)
- [46] Briquet, F., Colas, A., Thomas, X.
Silikone in der Medizin.
Assessed from: <http://www.dowcorning.com> (2014)
- [47] Liu, Y., Paul, C., Ouyang, J., Foreman, P., Sridhar, L., Shah, S.
Silicone Acrylic Hybrid Polymer-Based Adhesives.
Patent US20120095159 A1 (2012)
- [48] Lauterback, T., Muller, W., Schacht, D., Wolff, H.
Silicone transdermal patch.
Patent US20030026830 A1 (2003)
- [49] Pfister, W., Wilson, J.
Silicone pressure sensitive adhesive compositons for transdermal drug delivery devices and related medical devices.
Patent US5232702 A (1993)
- [50] Pfister, W., Wilson, J.
Silicone pressure sensitive adhesive compositions for transdermal drug delivery devices and related medical devices.
Patent EP0524776 B1 (1995)
- [51] Kydonieus, A., Rossi, T., ARNOLD, C., Banga, A., SACHDEVA, V.
Transdermal hormone delivery.
Patent WO2013112806 A2 (2013)
- [52] Radloff, D., Wasner, M.
Skin-friendly plasters for the transdermal administration of non-steroidal antirheumatic agents.
Patent EP1120115 B1 (2007)
- [53] Wang, K., Osborne, J., Hunt, J., Nelson, M.
Polyisobutylene adhesives for transdermal devices.
Patent EP0525105 A1 (1993)
- [54] Wang, K., Osborne, J., Hunt, J., Nelson, M.
Drug delivery patches having mixture of high and low molecular weight polymers as adhesives which dissolve active agents, free of plasticizers and tackifiers.
Patent US5508038 A (1996)
- [55] Audett, J., Beste, R., Farinas, K., Putnam, W.
Polyisobutylene Adhesives Containing High Tg Tackifier for Transdermal Devices.
Patent WO1996022083 A1 (1996)
-

-
- [56] Enscore, D., Gale, R.
Matrix composition for transdermal therapeutic system.
Patent CA1217139 A1 (1987)
- [57] Jona, J., Audett, J., Singh, N.
Transdermal patch and method for administering 17-deacetyl norgestimate alone or in combination with an estrogen.
Patent US006071531A (2000)
- [58] Venkateshwaran, S., Fikstad, D., Ebert, C.
Pressure sensitive adhesive matrix patches for transdermal delivery of salts of pharmaceutical agents.
Patent US5985317 A (1999)
- [59] Robbins, W.
Transdermal therapeutic device and method with capsaicin and capsaicin analogs.
Patent WO1999030560 A1 (1999)
- [60] Santus, G., Kim, A., Francoeur, M., Bremer, U.
Transdermal patch.
Patent US5658587 A (1997)
- [61] Robbins, W.
Transdermal therapeutic device and method with capsaicin and capsaicin analogs.
Patent CA2314326 C (2008)
- [62] Enscore, D.
Non-sensitizing transdermal clonidine patch.
Patent WO2013072763 A2 (2013)
- [63] Enscore, D.
Transdermal propranolol patch for treatment of malignant melanoma.
Patent US20140294920 A1 (2014)
- [64] Bondi, J., Loper, A., Cohen, E.
Transdermal system for timolol.
Patent US4752478 A (1988)
- [65] Audett, J., Bailey, S.
Transdermal delivery of basic drugs using nonpolar adhesive systems and acidic solubilizing agents.
Patent US5879701 A (1999)
- [66] 3M
Drug Delivery Systems: Transdermal Components.
Assessed from: <http://solutions.3m.com> (2014)
-

-
- [67] Enscore, D.
Transdermal propranolol patch for treatment of malignant melanoma.
Patent WO2013072762 A2 (2013)
- [68] Yeh, S., Patel, N., Milstone, J.
Transdermal nicotine delivery system.
Patent US5230896 A (1993)
- [69] Cupo, F., Lebo, D., Lee, J., Ryoo, J., Toigo, O.
Transdermal antiemesis delivery system, method and composition therefor.
Patent WO2006028863 A1 (2006)
- [70] Chaudhuri, K.R.
Crystallisation within transdermal rotigotine patch: is there cause for concern?
Expert Opin Drug Deliv 5(11): 1169–1171 (2008)
- [71] Foreman, P.
Drug Solubility in Acrylic-Rubber Graft Copolymers: New Opportunities and Directions.
Annual Meeting Controlled Release Society, Copenhagen (2009)
- [72] Wu, C., McGinity, J.W.
Influence of ibuprofen as a solid-state plasticizer in Eudragit® RS 30 D on the physicochemical properties of coated beads.
AAPS PharmSciTech 2(4): 35–43 (2001)
- [73] Ranade, V.V.
Drug Delivery Systems. 6. Transdermal Drug Delivery.
J Clin Pharmacol 31(5): 401–418 (1991)
- [74] Mehdizadeh, A., Ghahremani, M.H., Rouini, M.R., Toliyat, T.
Effects of pressure sensitive adhesives and chemical permeation enhancers on the permeability of fentanyl through excised rat skin.
Acta Pharm 56(2): 219–229 (2006)
- [75] Passoni, G., Casetta, P., Stefanelli, P.
Adhesive transdermal formulations of diclofenac sodium.
Patent CA2471798 A1 (2003)
- [76] Govil, S., Rudnic, E., Sterner, D.
Transdermal nitroglycerin patch with penetration enhancers.
Patent US5262165 A (1993)
- [77] Scarbrough, C., Scarbrough, S., Shubbrook, J.
Transdermal delivery of metformin.
Patent US20120283332 A1 (2012)
- [78] Sharma, K., Roy, S., Roos, E.
Transdermal administration of buprenorphine.
Patent US5069909 A (1991)
-

-
- [79] Zeltman, J.
Transdermal patch and method for delivery of vitamin b12.
Patent EP2124907 A2 (2009)
- [80] Williams, A.C., Barry, B.W.
Penetration enhancers.
Breaking the Skin Barrier 56(5): 603–618 (2004)
- [81] Gale, R.
Methods for transdermal drug administration.
Patent US6348210 B1 (2002)
- [82] Kelly, B., Jacob, C.H., Costantino, C.
Micromechanisms of Tack of Soft Adhesives Based on Styrenic Block Copolymers.
Macromol Mater Eng 287(3): 163–179 (2002)
- [83] Tse, M.F.
Studies of triblock copolymer-tackifying resin interactions by viscoelasticity and adhesive performance.
J Adhes Sci Technol 3(1): 551–570 (1989)
- [84] Satas, D.
Handbook of pressure sensitive adhesive technology.
3rd ed., Satas & Associates, Warwick RI (1999)
- [85] Sherriff, M., Knibbs, R.W., Langley, P.G.
Mechanism for the action of tackifying resins in pressure-sensitive adhesives.
J Appl Polym Sci 17(11): 3423–3438 (1973)
- [86] Wypych, G.
Handbook of plasticizers.
2nd ed., ChemTec Pub., Toronto (2012)
- [87] Douroumis, D.
Hot-melt extrusion: Pharmaceutical applications.
1st ed., Wiley, Chichester, West Sussex (2012)
- [88] Burton, S., Tata, S.
Transdermal patch.
Patent US5948433 A (1999)
- [89] Wypych, G.
Handbook of plasticizers.
1st ed., ChemTec Pub., Toronto (2004)
- [90] Lin, S.-Y., Lee, C.-J., Lin, Y.-Y.
The Effect of Plasticizers on Compatibility, Mechanical Properties, and Adhesion Strength of Drug-Free Eudragit E Films.
Pharm Res 8(9): 1137–1143 (1991)
-

-
- [91] Cilurzo, F., Minghetti, P., Pagani, S., Casiraghi, A., Montanari, L.
Design and Characterization of an Adhesive Matrix Based on a Poly(Ethyl Acrylate, Methyl Methacrylate)
AAPS PharmSciTech 9(3): 748–754 (2008)
- [92] Elgindy, N., Samy, W.
Evaluation of the mechanical properties and drug release of crosslinked Eudragit films containing metronidazole.
Int J Pharm 376(1–2): 1–6 (2009)
- [93] Taghizadeh, S.M., Lahootifard, F.
Transdermal Excipients Effect on Adhesion Strength of a Pressure Sensitive Adhesive.
Iran Polym J (12 (3)): 243–248 (2003)
- [94] Aitken-Nichol, C., Zhang, F., McGinity, J.W.
Hot Melt Extrusion of Acrylic Films.
Pharm Res 13(5): 804–808 (1996)
- [95] Müller-Buschbaum, P., Ittner, T., Maurer, E., Körstgens, V., Petry, W.
Pressure-Sensitive Adhesive Blend Films for Low-Tack Applications.
Macromol Mater Eng 292(7): 825–834 (2007)
- [96] Nič, M., Jirát, J., Košata, B., Jenkins, A., McNaught, A.
IUPAC Compendium of Chemical Terminology.
1st ed., IUPAC, Research Triangle Park, NC (2009)
- [97] Everett, D.H.
Manual of Symbols and Terminology for Physicochemical Quantities and Units, Appendix II: Definitions, Terminology and Symbols in Colloid and Surface Chemistry.
Pure Appl Chem 31(4) (1972)
- [98] Zhao, H., Park, D.-W., Kim, S.-K., Lee, C.-H., Kim, D.-D.
The effects of pressure-sensitive adhesives and solubilizers on the skin permeation of testosterone from a matrix-type transdermal delivery system.
Drug Dev Ind Pharm 28(9): 1125–1131 (2002)
- [99] Ash, I., Ash, M.
Handbook of fillers, extenders, and diluents.
2nd ed., Synapse Information Resources, Endicott, NY (2007)
- [100] Gattefossé
Labrasol® Caprylocaproyl macrogol-8 glycerides EP.
Assessed from: <http://www.gattefosse.com/> (2014)
- [101] Nierle, J., Gaede, C.
Hybrid system for solubilizing pharmaceutically active substances in polymer matrices.
Patent WO2003080035 A1 (2003)
-

-
- [102] Haralambopoulos, C.
Adhesive matrix type transdermal patch and method of manufacturing same.
Patent US5965154 A (1999)
- [103] Fenton, J.
Maximizing Yield in Transdermal Manufacturing.
Assessed from: <http://www.drug-dev.com/> (2013)
- [104] Minghetti, P., Cilurzo, F., Casiraghi, A.
Measuring Adhesive Performance in Transdermal Delivery Systems.
American Journal of Drug Delivery 2(3) (2004)
- [105] Gutschke, E., Bracht, S., Nagel, S., Weitschies, W.
Adhesion testing of transdermal matrix patches with a probe tack test--in vitro and in vivo evaluation.
Eur J Pharm Biopharm 75(3): 399–404 (2010)
- [106] Pizzi, A., Mittal, K.L.
Handbook of adhesive technology.
2nd ed., M. Dekker, New York (2003)
- [107] Creton, C., Fabre, P.
Tack.
In: Adhesion Science and Engineering, Vol I: The Mechanics of Adhesion, D.A. Dillard and A.V. Pocius eds. Elsevier. pp. 535-576, 1st ed. (D.A. Dillard and A.V. Pocius, ed): p. 535–76, Elsevier, New York, NY (2003)
- [108] Creton, C.P.E., Editors, G.
Materials Science of Adhesives: How to Bond Things Together.
MRS Bulletin June 2003: 419–423 (2003)
- [109] Duncan, B., Abbott, S., Roberts, R.
Measurement Good Practice Guide No. 26: Adhesive Tack, National Physical Laboratory
Assessed from: <http://www.adhesivestoolkit.com> (2013)
- [110] Pressure Sensitive Tape Council
Test methods for pressure sensitive adhesive tapes: Peel Adhesion of Pressure Sensitive Tape.
15 ed., PSTC, Northbrook (2007)
- [111] Tsukatani, T., Hatano, Y., Mizumachi, H.
Bonding and Debonding Processes in Tack of Pressure-Sensitive Adhesives.
J Adhes 31(1): 59–71 (1989)
- [112] Scasso, A., Stefano, F.
Transdermal delivery device for the administration of fentanyl.
Patent WO2003097008 A2 (2003)
-

-
- [113] Serizawa, H.
Transdermal formulations of geranylgeranylacetone.
Patent US20130273138 A1 (2013)
- [114] Creton, C., Shull, K.R.
Probe Tack.
In: Applications of pressure-sensitive products, 1st ed. (Benedek I., Feldstein M.M., eds): p. 6-1 to 6-26, CRC Press - Taylor & Francis Group, Boca Raton (2009)
- [115] Kim, H., Lim, D., Park, Y.
Peel Resistance.
In: Applications of pressure-sensitive products, 1st ed. (Benedek I., Feldstein M.M., eds): p. 7-1 to 7-34, CRC Press - Taylor & Francis Group, Boca Raton (2009)
- [116] Derail, C., Allal, A., Marin, G., Tordjeman, P.
Relationship Between Viscoelastic and Peeling Properties of Model Adhesives. Part 2. The Interfacial Fracture Domains.
J Adhes 68(3-4): 203–228 (1998)
- [117] Kaelble, D.H.
Peel Adhesion: Influence of Surface Energies and Adhesive Rheology.
J Adhes 1(2): 102–123 (1969)
- [118] Pesika, N.S. et al.
Peel-Zone Model of Tape Peeling Based on the Gecko Adhesive System.
J Adhes 83(4): 383–401 (2007)
- [119] Renvoise, J., Burlot, D., Marin, G., Derail, C.
Adherence performances of pressure sensitive adhesives on a model viscoelastic synthetic film: A tool for the understanding of adhesion on the human skin.
Int J Pharm 368(1-2): 83–88 (2009)
- [120] Wokovich, A.M. et al.
Evaluation of substrates for 90 degrees peel adhesion - A collaborative study. I. Medical tapes.
J. Biomed. Mater. Res. Part B 87B(1): 105–113 (2008)
- [121] Pressure Sensitive Tape Council
Test methods for pressure sensitive adhesive tapes: Shear Adhesion of Pressure Sensitive Tape.
15 ed., PSTC, Northbrook (2007)
- [122] Antonov, S.V., Kulichikhin, V.G.
Shear Resistance.
In: Applications of pressure-sensitive products, 1st ed. (Benedek I., Feldstein M.M., eds): p. 8-1 to 8-18, CRC Press - Taylor & Francis Group, Boca Raton (2009)
-

-
- [123] Chang, E.P.
Viscoelastic Properties of Pressure-Sensitive Adhesives.
J Adhes 60(1-4): 233–248 (1997)
- [124] Zosel, A.
Shear Strength of Pressure Sensitive Adhesives and its Correlation to Mechanical Properties.
J Adhes 44(1-2): 1–16 (1994)
- [125] Herzog, B., Gardner, D.J., Lopez-Anido, R., Goodell, B.
Glass-transition temperature based on dynamic mechanical thermal analysis techniques as an indicator of the adhesive performance of vinyl ester resin.
J Appl Polym Sci 97(6): 2221–2229 (2005)
- [126] Menard, K.P.
Dynamic mechanical analysis: A practical introduction.
2nd ed., CRC Press - Taylor & Francis Group, Boca Raton, FL (2008)
- [127] Chang, E.P.
Viscoelastic Windows of Pressure-Sensitive Adhesives.
J Adhes 34(1-4): 189–200 (1991)
- [128] Dale, W.C., Paster, M.D., Haynes, J.K.
Mechanical Properties of Acrylic Pressure Sensitive Adhesives and Their Relationships to Industry Standard Testing.
J Adhes 31(1): 1–20 (1989)
- [129] Brummer, R., Hetzel, F., Kimmerl, C., Lenuck, V., Kenndoff, J.W., Knieler, R.
DMA zu Überwachung der Fertigung.
Adhäsion - kleben u. dichten 3(42): 26–29 (1998)
- [130] Derail, C., Marin, G.
Role of Viscoelastic Behavior of Pressure-Sensitive Adhesives in the Course of Bonding and Debonding Processes.
In: Applications of pressure-sensitive products, 1st ed. (Benedek I., Feldstein M.M., eds): p. 4-1 to 4-26, CRC Press - Taylor & Francis Group, Boca Raton (2009)
- [131] Chang, E.
Viscoelastic Properties and Windows of Pressure-Sensitive Adhesives.
In: Applications of pressure-sensitive products, 1st ed. (Benedek I., Feldstein M.M., eds): p. 5-1 to 5-22, CRC Press - Taylor & Francis Group, Boca Raton (2009)
- [132] Ho, K.Y., Dodou, K.
Rheological studies on pressure-sensitive silicone adhesives and drug-in-adhesive layers as a means to characterise adhesive performance.
Int J Pharm 333(1-2): 24–33 (2007)
-

-
- [133] Michaelis, M., Brummer, R., Leopold, C.S.
Plasticization and antiplasticization of an acrylic pressure sensitive adhesive by ibuprofen and their effect on the adhesion properties.
Eur J Pharm Biopharm 86(2): 234–243 (2014)
- [134] Zosel, A.
Adhesion and tack of polymers: Influence of mechanical properties and surface tensions.
Colloid Polym. Sci. 263(7): 541–553 (1985)
- [135] Tordjeman, P., Papon, E., Villenave, J.-J.
Squeeze elastic deformation and contact area of a rubber adhesive.
J Chem Phys 113(23): 10712–10716 (2000)
- [136] Gay, C., Leibler, L.
Theory of Tackiness.
Phys Rev Lett 82(5): 936 (1999)
- [137] Zosel, A.
The effect of bond formation on the tack of polymers.
J Adhes Sci Technol 11(11): 1447–1457 (1997)
- [138] Asloun, E.M., Nardin, M., Schultz, J.
Stress transfer in single-fibre composites: effect of adhesion, elastic modulus of fibre and matrix, and polymer chain mobility.
J Mater Sci 24(5): 1835-1844 (1989)
- [139] Lee, L.-H.
Molecular Bonding and Adhesion at Polymer-Metal Interphases.
J Adhes 46(1-4): 15–38 (1994)
- [140] Schultz, J.
Effect of Orientation and Organization of Polymers at Interfaces on Adhesive Strength.
J Adhes 37(1-3): 73–81 (1992)
- [141] Wu, S.
Polymer interface and adhesion.
8th ed., Dekker, New York (1982)
- [142] Habenicht, G.
Kleben.
6.th ed., Springer, Berlin Heidelberg (2009)
- [143] Dahlquist, C.A.
The Theory of Adhesion.
In: *Coatings technology handbook*, 3rd ed. (Tracton A.A., ed): p. 5-1 to 5-9, CRC Press - Taylor & Francis Group, Boca Raton (2006)
-

-
- [144] Ma, W., Vodungbo, B., Nilles, K., Theato, P., Lüning, J.
Surface and bulk ordering in thin films of a symmetrical diblock copolymer.
J Polym Sci B Polym Phys 51(17): 1282–1287 (2013)
- [145] Hefer, A.W.
Adhesion in Bitumen-Aggregate Systems and Quantification of the Effects of Water on the Adhesive Bond.
Dissertation, Texas, Texas A&M University (2004)
- [146] R. Brummer, F.H.C.H.
Correlation of Polymer Properties with Dynamic Mechanical Measurements.
Appl Rheol 7: 173–178 (1997)
- [147] Foreman, P., Eaton, P., Shah, S.
Rubber-Acrylic Hybrid Pressure Sensitive Adhesives, National Starch and Chemical Company.
Assessed from: <http://www.pstc.org> (2013)
- [148] Coughlin, C.S., Mauritz, K.A., Storey, R.F.
A general free volume based theory for the diffusion of large molecules in amorphous polymers above Tg. 4. Polymer-penetrant interactions.
Macromolecules 24(7): 1526–1534 (1991)
- [149] Palzer, S., Zürcher, U.
Kinetik unerwünschter Agglomerationsprozesse bei der Lagerung und Verarbeitung amorpher Lebensmittelpulver.
Chemie Ingenieur Technik 76(10): 1594–1599 (2004)
- [150] Wilkes, C.E., Summers, J.W., Daniels, C.A., Berard, M.T.
PVC handbook.
1st ed., Hanser, Munich, Cincinnati (2005)
- [151] Stark, W.
Investigation of the curing behaviour of carbon fibre epoxy prepreg by Dynamic Mechanical Analysis DMA.
Polym Test 32(2): 231–239 (2013)
- [152] Crowley, M.M. et al.
The influence of guaifenesin and ketoprofen on the properties of hot-melt extruded polyethylene oxide films.
Eur J Pharm Sci 22(5): 409–418 (2004)
- [153] Jackson, W.J., Caldwell, J.R.
Antiplasticization. III. Characteristics and properties of antiplasticizable polymers.
J Appl Polym Sci 11(2): 227–244 (1967)
- [154] Mitchell, B.S.
An introduction to materials engineering and science: For chemical and materials engineers.
1st ed., John Wiley, Hoboken (NJ) (2004)
-

-
- [155] Wu, C., McGinity, J.W.
Non-traditional plasticization of polymeric films.
Int J Pharm 177(1): 15–27 (1999)
- [156] Arzhakov, M.S., Arzhakov, S.A., Gustov, V.V., Kevdina, I.B., Shantarovich, V.P.
Physical and Mechanical Behavior of Polymer Glasses. V. Structural Plasticization.
Int J Polym Mater 47(2-3): 149–167 (2000)
- [157] Siepmann, F., Le Brun, V., Siepmann, J.
Drugs acting as plasticizers in polymeric systems: A quantitative treatment.
J Control Release 115(3): 298–306 (2006)
- [158] Jenquin, M.R., Liebowitz, S.M., Sarabia, R.E., McGinity, J.W.
Physical and chemical factors influencing the release of drugs from acrylic resin films.
J Pharm Sci 79(9): 811–816 (1990)
- [159] Jackson, W.J., Caldwell, J.R.
Antiplasticization. II. Characteristics of antiplasticizers.
J Appl Polym Sci 11(2): 211–226 (1967)
- [160] Anderson, S.L., Grulke, E.A., DeLassus, P.T., Smith, P.B., Kocher, C.W., Landes, B.G.
A Model for Antiplasticization in Polystyrene.
Macromolecules 28(8): 2944–2954 (1995)
- [161] Lee, J.S., Leisen, J., Choudhury, R.P., Kriegel, R.M., Beckham, H.W., Koros, W.J.
Antiplasticization-based enhancement of poly(ethylene terephthalate) barrier properties.
Polymer 53(1): 213–222 (2012)
- [162] Lin, S.-Y., Lee, C.-J., Lin, Y.-Y.
Drug-polymer interaction affecting the mechanical properties, adhesion strength and release kinetics of piroxicam-loaded Eudragit E films plasticized with different plasticizers.
J Control Release 33(3): 375–381 (1995)
- [163] Anderson, M.J., Whitcomb, P.J.
DOE simplified: Practical tools for effective experimentation.
2nd ed., CRC Press - Taylor & Francis Group, Boca Raton, Fla (2007)
- [164] Kleppmann, W.
Versuchsplanung: Produkte und Prozesse optimieren.
8th ed., Hanser, Munich (2013)
- [165] Siebertz, K., Bebbler, D.T.v., Hochkirchen, T.
Statistische Versuchsplanung: Design of Experiments (DOE)
1st ed., Springer, Heidelberg, Dordrecht (2010)
- [166] Yu, L.X.
Pharmaceutical quality by design: product and process development, understanding, and control.
Pharm Res 25(4): 781–791 (2008)
-

-
- [167] International Conference on Harmonisation of Technical Requirements for Registration of Pharmaceuticals for Human Use (ICH)
Guidance for Industry Q8(R2) Pharmaceutical Development.
2nd ed., U.S. Department of Health and Human Services, Washington, D.C (2009)
- [168] Burghaus, R., Mogk, G., Mrziglod, T., Hübl, P.
Method and system for the automatic design of experiments.
Patent US7079965 B2 (2006)
- [169] Keller, P.A.
Six sigma demystified.
2nd ed., McGraw-Hill, New York (2011)
- [170] Keller, P.A.
Statistical process control demystified.
1st ed., McGraw-Hill, New York (2011)
- [171] Cornell, J.
Experiments with mixtures: designs, models, and the analysis of mixture data.
3rd ed., Wiley, New York (2002)
- [172] Anderson, M.J., Whitcomb, P.J.
RSM simplified: Optimizing processes using response surface methods for design of experiments.
1st ed., CRC Press - Taylor & Francis Group, Boca Raton, Fla (2005)
- [173] Belavendram, N.
Quality by design.
1st ed., Prentice Hall, London, New York (1995)
- [174] Vikström, E., Björk, R., Rydén, P.
Methods and apparatus for automated predictive design space estimation.
Patent US20130218529 A1 (2013)
- [175] Wikström, E., Sundström, H., Nordahl, T.
Methods and apparatus for automated predictive design space estimation.
Patent US8412356 B2 (2013)
- [176] Göndör, V., Koczor, Z.
Improvement of the Measurement System Analysis Using Experimental Design, Budapest, Hungary, Óbuda University (2010)
- [177] Lampert, A., Seiberth, J., Haefeli, W.E., Seidling, H.M.
A systematic review of medication administration errors with transdermal patches.
Expert Opin Drug Saf 13(8): 1101–1114 (2014)
- [178] George Wypych, editor
Handbook of plasticizers.
1st ed., Norwich, William Andrew Publishing (2004)
-

-
- [179] Xiao, C. et al.
Positronium Annihilation Lifetime and Dynamic Mechanical Studies of γ -Relaxation in BPA-PC and TMBPA-PC Plasticized by TOP.
Macromolecules 32(23): 7913–7920 (1999)
- [180] Mascia, L.
Antiplasticization of poly (vinyl chloride) in relation to thermal ageing and non-linear viscoelastic behaviour.
Polymer 19(3): 325–328 (1978)
- [181] Soong, S.Y., Cohen, R.E., Boyce, M.C., Chen, W.
The effects of thermomechanical history and strain rate on antiplasticization of PVC.
Polymer 49(6): 1440–1443 (2008)
- [182] Bing, Y., Chris, M., Eli, M.P.
Explanation of tackifier effect on the viscoelastic properties of polyolefin-based pressure sensitive adhesives.
J Appl Polym Sci 99(5): 2408–2413 (2006)
- [183] Mascia, L., Margetts, G.
Viscoelasticity and plasticity aspects of antiplasticization phenomena: Strain rate and temperature effects.
J of Macromolecular Sc, Part B 26(2): 237–256 (1987)
- [184] Lunter, D.J., Daniels, R.
New film forming emulsions containing Eudragit® NE and/or RS 30D for sustained dermal delivery of nonivamide.
Eur J Pharm Biopharm 82(2): 291–298 (2012)
- [185] Michelle, R.J., Stephen, M.L., Rafael, E.S., James, W.M.
Physical and chemical factors influencing the release of drugs from acrylic resin films.
J. Pharm. Sci. 79(9): 811–816 (1990)
- [186] Taghizadeh, S.M., Soroushnia, A., Mirzadeh, H., Barikani, M.
Preparation and In Vitro Evaluation of a New Fentanyl Patch Based on Acrylic/Silicone Pressure-Sensitive Adhesive Blends.
Drug Dev Ind Pharm 35(4): 487–498 (2009)
- [187] Trenor, S.R., Suggs, A.E., Love, B.J.
Influence of penetration enhancers on the thermomechanical properties and peel strength of a poly(isobutylene) pressure sensitive adhesive.
J Mater Sci Lett 21(17): 1321–1323 (2002)
- [188] Gullick, D.R., Pugh, W.J., Ingram, M.J., Cox, P.A., Moss, G.P.
Formulation and characterization of a captopril ethyl ester drug-in-adhesive-type patch for percutaneous absorption.
Drug Dev Ind Pharm 36(8): 926–932 (2010)
-

-
- [189] Minghetti, P., Cilurzo, F., Casiraghi, A., Montanari, L.
The effect of thickness and water content on the adhesive properties of methacrylic patches.
Acta Technologiae et Legis Medicamenti 11(2): 81–92 (2000)
- [190] Satas, D.
Handbook of pressure sensitive adhesive technology.
2nd ed., Van Nostrand Reinhold, New York (1989)
- [191] Mezger, T.
The Rheology Handbook: For Users of Rotational and Oscillatory Rheometers.
2nd ed., Vincentz Network, Hannover (2006)
- [192] Chalykh, A.E., Shcherbina, A.A.
Transition Zones in Adhesive Joints.
In: Applications of pressure-sensitive products, 1st ed. (Benedek I., Feldstein M.M., eds): p. 3-1 to 3-32, CRC Press - Taylor & Francis Group, Boca Raton (2009)
- [193] Tracton AA, editor
Coatings Technology Handbook.
3rd ed., CRC Press - Taylor & Francis Group, Boca Raton (2005)
- [194] Govil, S., Weimann, L.
Adhesive mixture for transdermal delivery of highly plasticizing drugs.
Patent US20020150613 A1 (2002)
- [195] Stenert, M.
Entwicklung binärer und ternärer Polymerblends auf der Basis von Polymethylmethacrylat, Poly(n-butylacrylat), Polystyrol und deren Diblockcopolymeren.
Dissertation, Universität GH Essen, Essen, (2000)
- [196] Hille, T.
Transdermal absorption of active substances from subcooled melts.
Patent US 6344211 B1 (2002)
- [197] Mezger, T.
Das Rheologie-Handbuch: Für Anwender von Rotations- und Oszillations-Rheometern.
2nd ed., Vincentz Network, Hannover (2006)
- [198] Yoreo, J.J. de, Vekilov, P.G.
Principles of Crystal Nucleation and Growth.
In: Biomineralization: Principles of crystal nucleation and growth (Dove P., Yoreo J. de, Weiner S., eds): p. 57–93, Mineralogical Society of America, Washington, DC (2003)
- [199] Sonoda, K., Furuzono, T., Walsh, D., Sato, K., Tanaka, J.
Influence of emulsion on crystal growth of hydroxyapatite.
Solid State Ionics 151(1–4): 321–327 (2002)
-

- [200] McClements, D.J.
Crystals and crystallization in oil-in-water emulsions: Implications for emulsion-based delivery systems.
Adv Colloid Interface Sci 174(174): 1–30 (2012)
- [201] Barnett, K. et al.
Using Quality by Design to Develop Robust Chromatographic Methods.
Pharmaceutical Technology 14(11): 48–64 (2014)
-

5. Appendix

5.1 Appendix – Curriculum Vitae

Entfällt aus datenschutzrechtlichen Gründen.

5.2 Appendix – Publication List

Publications

Michaelis M., Brummer R., Leopold C.S.

Plasticization and antiplasticization of an acrylic pressure sensitive adhesive by ibuprofen and their effect on the adhesion properties.

Eur J Pharm Biopharm 86, 234-243 (2014)

Michaelis M., Leopold C.S.

Mixture Design Approach for Early Stage Formulation Development of a Transdermal Delivery System.

Drug Dev Ind Pharm (2014), DOI: 10.3109/03639045.2014.971029

Michaelis M., Leopold C.S.

A Measurement System Analysis with Design of Experiments: Investigation of the Adhesion Performance of a Pressure Sensitive Adhesive with the Probe Tack Test.

[submitted]

Table 9: Journal articles with authors contributions and reference chapters.

Journal articles						
Title	Journal	Authors	Contribution	Percentage	Reference Chapters	
Plasticization and antiplasticization of an acrylic pressure sensitive adhesive by ibuprofen and their effect on the adhesion properties.	European Journal of Pharmaceutics and Biopharmaceutics [published]	Michaelis M., Brummer R., Leopold C.S.	Project plan, experiments, data analysis, publication Supervisor Supervisor	100 %	2.1, 3.1	
Mixture Design Approach for Early Stage Formulation Development of a Transdermal Delivery System.	Drug Development and Industrial Pharmacy [published]	Michaelis M., Leopold C.S.	Project plan, experiments, data analysis, publication Supervisor	100 %	2.2, 3.2	
A Measurement System Analysis with Design of Experiments: Investigation of the Adhesion Performance of a Pressure Sensitive Adhesive with the Probe Tack Test.	Journal of Pharmaceutical and Biomedical Analysis [submitted]	Michaelis M.,	Project plan, experiments, data analysis, publication	100 %	2.3, 3.3	

Poster

Michaelis M., Leopold C.S.

Presentations

The Probe Tack Test: A Design of Experiments Approach.

8th World Meeting on Pharmaceutics, Biopharmaceutics and Pharmaceutical
Technology of the APV 2012, Istanbul, Turkey

Michaelis M., Leopold C.S.

Rheological and Adhesion Properties of a Crosslinked Acrylic Pressure
Sensitive Adhesive used for Transdermal Patches containing Ibuprofen.
GDCh Forum 2011, Bremen, Germany

Michaelis M., Leopold C.S.

Influence of Ibuprofen Content on the Adhesion Properties and Rheological
Behavior of an Acrylic Pressure Sensitive Adhesive.
Skin Forum 12th Annual Meeting 2011, Frankfurt/M, Germany
Winner of the poster prize

Michaelis M., Leopold C.S.

Influence of Ibuprofen Content on Adhesion Properties of an Acrylic Pressure
Sensitive Adhesive
AAPS Annual Meeting & Exposition 2010, New Orleans, USA

Oral Presentations

Michaelis M., Leopold C.S.

Is there a Sticky Sweet Spot? Mixture Design of a Pressure Sensitive Adhesive Emulsion Formulation.

4th European User Meeting on Design of Experiments 2012, Vienna, Austria.

Michaelis M., Leopold C.S.

Dynamisch Mechanische Thermoanalyse von wirkstoffbeladenen Haftklebstoffen.

Rheology Meeting 2011, Hamburg, Germany.








Michaelis M., Leopold C.S.



Influence of Ibuprofen Content on the Rheological and Thermal Behavior of an Acrylic Pressure Sensitive Adhesive.

DPhG Annual Conference 2010, Braunschweig, Germany.

5.3 Appendix – Hazardous Materials

Table 10: Hazardous materials and GHS labeling.

Substance	Supplier	Danger symbol	Hazard statements	Precautionary statements
Ibuprofen	BASF, Germany	  	H302, H361d, H411	P301, P312
Isopropanol	Kraemer & Martin, Germany	 	H225, H319, H336	P210, P233, P303+P361+P353 P305+P351+P338 P403+P235
Ethylacetat	BCD, Germany	 	H319, H225, H336, EUH066	P210, P233, P303+P361+P353 P305+P351+P338 P403+P235

Substance	Supplier	Danger symbol	Hazard statements	Precautionary statements
DURO-TAK 387-2287	Henkel, GB		H319, H225, H336, H351, EUH066	P210, P261, P280, P308 + P313, P370 + P378
DURO-TAK 87-4287	Henkel, GB		H319, H225, H336, H351, EUH066	P210, P261, P280, P308 + P313, P370 + P378

6. Eidesstattliche Versicherung

Hiermit versichere ich an Eides statt, die vorliegende Arbeit selbstständig und ohne fremde Hilfe sowie nur mit den angegebenen Hilfsmitteln und Quellen erstellt zu haben. Ich versichere zudem, keinen weiteren Promotionsversuch an einer anderen Einrichtung unternommen zu haben.

Hamburg, den

Marc Michaelis
